Journal of
Medicinal Chemistry

Article

Discovery of Pyrido[2,3-b]indole Derivatives with Gram-negative Activity Targeting Both DNA Gyrase and Topoisomerase IV

Yimin Hu, Houguang Shi, Mingwei Zhou, Qingcheng Ren, Wei Zhu, Weixing Zhang, Zhiwei Zhang, Chengang Zhou, Yongqiang Liu, Xiao Ding, Hong C Shen, S. Frank Yan, Fabian Dey, Waikwong Wu, Guanglei Zhai, Zheng Zhou, Zhiheng Xu, Ying Ji, Hua Lv, Tianyi Jiang, Wen Wang, Yunhua Xu, Maarten Vercruysse, Xiangyu Yao, Yi Mao, Xiaomin Yu, Kenneth Bradley, and Xuefei Tan

J. Med. Chem., **Just Accepted Manuscript** • DOI: 10.1021/acs.jmedchem.0c00768 • Publication Date (Web): 04 Aug 2020

Just Accepted

is published by the American Chemical Society. 1155 Sixteenth Street N.W., Washington, DC 20036

Discovery of Pyrido[2,3-b]indole Derivatives with Gram-negative Activity Targeting Both DNA Gyrase and Topoisomerase IV

Yimin Hu,[†] Houguang Shi,[†] Mingwei Zhou,[†] Qingcheng Ren,[‡] Wei Zhu,[†] Weixing Zhang,[†] Zhiwei Zhang,[†] Chengang Zhou,[†] Yongqiang Liu,[†] Xiao Ding,[†] Hong C. Shen,[†] S. Frank Yan,[ǁ] Fabian Dey,[&] Waikwong Wu,[ǂ] Guanglei Zhai,[ǂ] Zheng Zhou,[ǂ] Zhiheng Xu,[ǂ] Ying Ji,[Δ] Hua Lv,[§] Tianyi Jiang,[§] Wen Wang,[#] Yunhua Xu,[#] Maarten Vercruysse,[⊥] Xiangyu Yao,[¶] Yi Mao,[¶] Xiaomin Yu,[¶] Kenneth Bradley,[⊥] and Xuefei Tan*[, †]

Department of [†]Medicinal Chemistry, [ǁ]CADD, [ǂ]Lead Discovery, [Δ]pCMC, [§]Pharmaceutical Sciences, [¶]Discovery Infectious Diseases, Roche Innovation Center Shanghai, Roche Pharma Research and Early Development, Building 5, 720 Cailun Road, Shanghai, 201203 China,

Department of [&]CADD, [⊥]Discovery Infectious Diseases, Roche Innovation Center Basel, Roche Pharma Research and Early Development, Grenzacherstrasse 124, CH-4070 Basel, Switzerland

[#]MicuRx Pharmaceuticals, Inc. (Shanghai)

Floor 3, Building B, 1976 Middle Gaoke Road, Shanghai, 201210 China

[‡]WuXi AppTec (Wuhan) Co., Ltd.

No. 666 Gaoxin Road, Wuhan East Lake High-tech Development Zone, Hubei, 430075 China

Abstract: The rise of multi-drug resistant (MDR) Gram-negative (GN) pathogens and the decline of available antibiotics that can effectively treat these severe infections is a major threat to modern medicine. Developing novel antibiotics against MDR GN is particularly difficult as compounds have to permeate the GN double membrane, which has very different physicochemical properties, and have to

circumvent a plethora of resistance mechanisms such as multiple efflux pumps and target modifications. The bacterial type II topoisomerases DNA gyrase ($GyrA_2B_2$) and Topoisomerase IV ($ParC_2E_2$) are highly conserved targets across all bacterial species and validated in the clinic by the fluoroquinolones. Dual inhibitors targeting the ATPase domains (GyrB/ParE) of type II topoisomerases can overcome target-based fluoroquinolone resistance. However, few ATPase inhibitors are active against GN pathogens. In this study, we demonstrated a successful strategy to convert a 2-carboxamide substituted azaindole chemical scaffold with only Gram-positive (GP) activity into a novel series with also potent activity against a range of MDR GN pathogens. By systematically fine-tuning the many physicochemical properties, we identified lead compounds such as **17r** with a balanced profile showing potent GN activity, high aqueous solubility, and desirable PK features. Moreover, we showed the bactericidal efficacy of **17r** using a neutropenic mouse thigh infection model.

Keywords: Gyrase, Topoisomerase, Gram-negative, Pyrido[2,3-b]indole

Introduction

The rapid increase in bacterial resistance against all antibiotics in the clinic is an urgent global health problem. The most severe bacterial infections are increasingly escaping first-line and even last-resort antibiotics treatments. These life-threatening multi-drug resistant (MDR) infections are mainly caused by the so-called ESKAPE pathogens, i.e., *Enterococcus faecium*, *Staphylococcus aureus*, *Klebsiella pneumoniae*, *Acinetobacter baumannii*, *Pseudomonas aeruginosa*, and *Enterobacter* species.[1,2] The last four fall into the category of Gram-negative (GN) bacteria, which are particularly challenging to treat, as compounds with intracellular targets have to pass through both the negatively charged outer membrane and hydrophobic inner membrane.[3,4] The distinct physicochemical properties required of a compound to cross both barriers make targeting GN bacteria more challenging than Gram-positive (GP) bacteria, which lack an outer membrane. Also, many adaptive resistance mechanisms developed by the bacteria such as efflux pumps, inactivation of enzymes, mutation, or biofilm further

complicate such a challenge. As a result, no new class of antibiotic with GN activity has reached the market in the last 40 years.[5-7]

The bacterial type IIA topoisomerases, i.e., DNA gyrase and topoisomerase IV, are well-known antibacterial targets. These essential enzymes solve critical DNA-topology changes during replication, transcription, and recombination. Specifically, DNA gyrase introduces negative supercoils into DNA and relaxes positive supercoils that accumulate during replication and transcription. Topoisomerase IV also removes positive supercoils as well as decatenates the replicated sister chromosomes. DNA gyrase is a heterotetramer composed of two A (GyrA) and two B subunits (GyrB). The two GyrB subunits hydrolyze two ATP molecules, which drive the catalytic function, i.e., binding, cleavage, and relegation of the DNA segments. Similarly, Topoisomerase IV consists of two C subunits (ParC) and two E subunits (ParE). The ParE subunits hydrolyze ATP driving the enzymatic activity.[8] Dual targeting of both GyrB and ParE subunits is possible as both ATP binding sites are very similar and results in very low spontaneous resistance frequencies. Also, because both enzymes are highly conserved across GP and GN bacteria, a dual GyrB/ParE ATPase inhibitor can have broad-spectrum activity.[9]

Fluoroquinolones (FQ) are one of the most commonly prescribed broad-spectrum antibiotics that target both DNA gyrase and Topoisomerase IV. However, due to its overuse and misuse for decades FQ resistance in hospitals has increased significantly.[10] The resistance mechanisms include both target-based mutations and non-target based such as plasmid-mediated resistance and efflux, which are difficult to overcome even by the newer generation FQ in the clinic.[11] FQ antibiotics target the catalytic sites in the GyrA/ParC subunits and stabilize the cleaved DNA-enzyme complex, which results in lethal double-stranded DNA breaks. Targeting alternative binding sites such as GyrB/ParE ATPase domains, which is distinct from the FQ mode-of-action (MoA), enables new antibacterial agents to overcome target-based FQ resistance and to achieve broad-spectrum activity. Novobiocin previously established the clinical proof of concept of this new MoA in the 1950s. It was, however, the first and only marketed drug of this new class. The use of Novobiocin declined rapidly due to the later development of more effective antibiotics. It was eventually withdrawn from the market due to the rise of resistance development and potential safety concerns.[12]

Over the last fifty years, industry and academia continued to work on finding novel scaffolds targeting the GyrB/ParE ATP binding site. Along with the continuously improved technical understanding of the molecular details of the MoA and factors driving resistance development against antibiotics, numerous chemical scaffolds were identified showing gradual improvements in physicochemical properties, safety, and antibacterial coverage compared to Novabiocin.[13-15] However, the spectrum of these GyrB/ParE dual inhibitors has been mainly limited to a GP spectrum, with only a few common respiratory GN pathogens such as *Haemophilus influenzae*.

A breakthrough scaffold targeting the GyrB/ParE ATPase site having GN activity was discovered eventually by Trius Therapeutics. Their novel tricyclic pyrimido[4,5-b]indole series, derived from a pyrrolopyrimidine scaffold, showed for the first time antibacterial activity effectively covering also GN pathogens such as *P. aeruginosa*, *A. baumannii*, and *K. pneumoniae* (represented by **GP6** in **Figure 1**).[16-18] The enhanced GN activity of this series is attributed to its rigidity, orientation of a critical amino group, and ability to adopt both neutral and charged states, all of which helps to penetrate the GN double membranes.[13] This series showed dual activity against both GyrB and ParE ATP binding site, resulting in very low resistance frequencies. Additionally, Soo Yei Ho et al. recently showed that a GyrB/ParE scaffold with only GP activity could be modified to yield broad-spectrum activity by carefully modulating the physicochemical property of zwitterionic compounds (represented by **ETC44** in **Figure 1**).[19]

In this study, we report our efforts in discovering pyrido[2,3-b]indole derivatives as a novel class of dual GyrB/ParE inhibitors with promising GN bacteria activities and *in vivo* bactericidal efficacy in a neutropenic mouse thigh infection model.

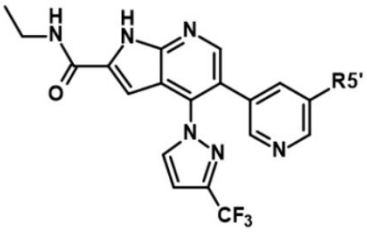

	AZ10 (R5'=CO_2H)	AZ17 (R5'=CN)
GyrB *Ki*	5 nM	23 nM
ParE *Ki*	5 nM	10 nM
MIC *S. aureus*	>25 mM	3.13 mM
MIC *E. coli*	inactive	inactive
LogD	-0.99	2.62

GP-positive only compounds, AZ10 and AZ17

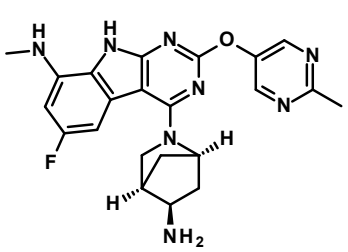

Trius GP6
GyrB Ki <1 nM ParE Ki <1 nM
MICs *E. coli* ATCC25922 0.344 μg/mL
***K. pneumoniae* ATCC 700603 1.358 μg/mL**
***A. baumannii* ATCC 19606 0.678 μg/mL**
***P. aeruginosa* ATCC 27853 0.679 μg/mL**

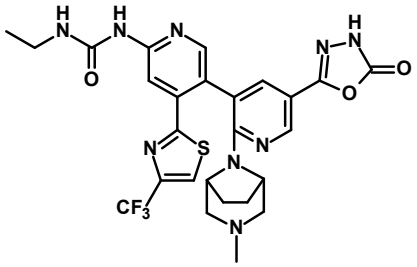

ETC44
GyrB IC_{50} 2 nM ParE IC_{50} 3 nM
MICs *E. coli* 0.57 μg/mL
***K. pneumoniae* ARC 1865 16 μg/ml**
***A. baumannii* ARC3495 0.5 μg/ml**
***P. aeruginosa* PAO1 1.14 μg/mL**

Figure 1. A few GyrB/ParE dual-inhibitor scaffolds. a) AZ GN-positive only azaindole ureas, **AZ10** and **AZ17**; b) Trius' GN-active tricyclic pyrimido[4,5-b]indole, **GP6**; and c) ETC's GN-active zwitterionic pyridine urea, **ETC44**.

RESULTS AND DISCUSSIONS

It has become increasingly apparent that in-house compound libraries of pharmaceutical companies are not well suited for the identification of antibacterial starting points due to their different physicochemical properties compared to most marketed antibiotics.[20,21] Therefore, we decided not to rely on a high-throughput screening campaign but to utilize the rich published collection of various potent DNA Gyrase/Topoisomerase IV GP antibiotics as medicinal chemistry starting points for the development of antibiotics against GN bacteria. A literature survey identified an azaindole scaffold (represented by **AZ10** and **AZ17** in **Figure 1**) previously discovered by AstraZeneca (AZ).[22] This class of compounds possesses a balanced dual enzymatic potency against both GyrB and ParE enzymes in GP bacteria. This feature could also be retained when improving the antibacterial activity against GN bacterial pathogens. Meanwhile, the overlay of the ATP binding sites of ParE crystalized with azaindole **AZ10** (PDB code: 4EMV) active against GP bacteria (*S. pneumoniae*), and GyrB crystalized with tricyclic pyrimido[4,5-b]indole **GP1** (PDB code: 4KFG) active against GN bacteria (*E. coli*) showed a good structural alignment of the key ligand pharmacophores (**Figure 2**). Notably, first, in both cores, the bi-dentate hydrogen bond interaction in donor-donor-acceptor pattern with strongly conserved

aspartic acid (Asp78 in *S. pneumoniae* ParE, Asp73 in *E. coli* GyrB) and a tightly bound water molecule were present. Comparing the scaffolds in the alignment (**Figure 2**) reveals a small shift. This shift is likely due to steric reasons of the substitution at 2-position in **GP1**, pushing the compound further away from the Glu-Arg salt bridge. Nonetheless, the **AZ10** azaindole 5-position pyridine ring overlaps well with the pyrimidine ring of **GP1**, both forming cation-π stacking interactions with the neighboring arginine side chain (Arg 76 in *E. coli* GyrB and Arg 81 in *S. pneumoniae* ParE, respectively). While the meta carboxylate substituted R5'-pyridine of **AZ10** forms a direct, **GP1** engages in a water-mediated H-bond to Arg 136. A more pronounced difference can be observed in the more hydrophobic part of the pocket where the 2-carboxamide of the azaindole occupies the latter only partially compared to the **GP1** tricyclic core. Lastly, the substitution along the R4-vector, the position held by an amine-containing unsaturated ring disclosed by Trius, is filled by a substituted pyrazole. While the latter mostly engages with the floor of the pocket, the former also forms an H-bond with Asn 46.

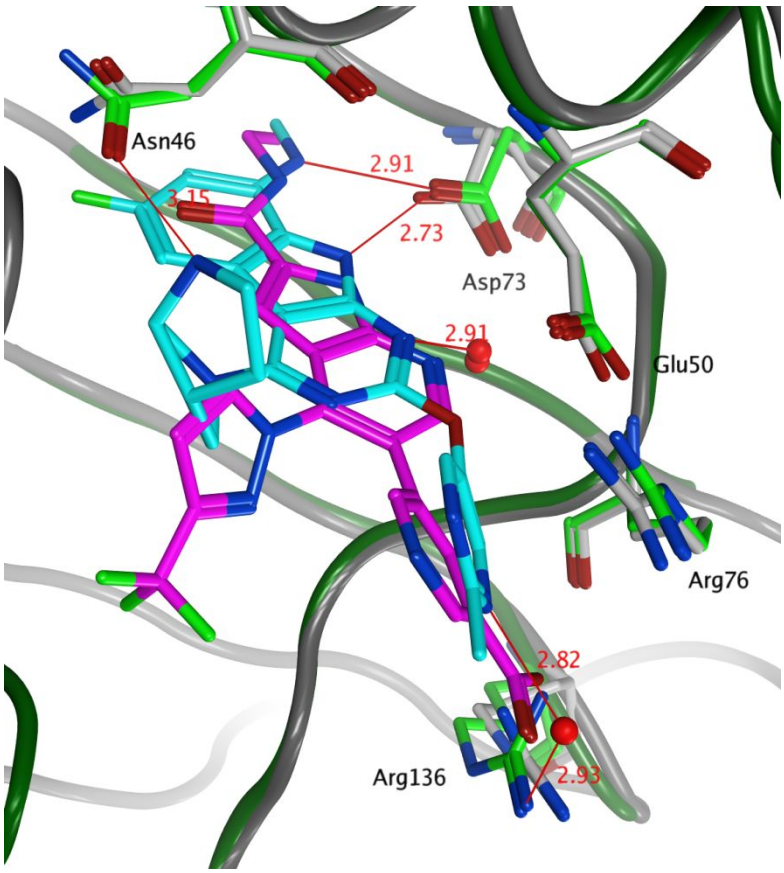

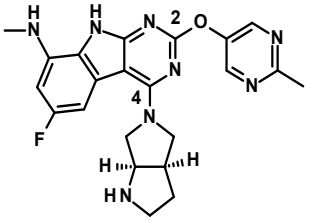

Trius GP1

Figure 2. Overlay of X-ray crystal structures of ATP binding sites of GyrB with bound **GP1** (PDB code: 4KFG, protein shown with green ribbon and carbons, ligand with cyan carbons) and ParE with bound **AZ10** (PDB code: 4EMV, protein shown with grey ribbon and carbons, ligand with magenta carbons). Hydrogen bonding interactions as red lines and residue labels shown for structure 4KFG. Further residues and water molecules omitted for clarity.

We decided to first introduce further rigidity into the azaindole scaffold, a strategy that had been shown in several cases to be successful in obtaining anti-GN activity.[23] After a few attempts, we were successful in replacing the latter by a fused ethyl aniline, which not only lowered the strain in the high energy bioactive conformation (H-bond donors facing each other) of the azaindole analog **(AZ10)**[22] but also generated a rigid scaffold that could still maintain the same hydrogen-bonding network with the protein and the structural water (**Figure 3**). As such, a new type of tricyclic pyrido[2,3-b]indole analogs exemplified by **10a-d** were synthesized (**Table 1**). A 6-fluorine substitution was incorporated in the tricyclic core based on modeling, to optimally fill the hydrophobic pocket and form additional van der Waals interactions.

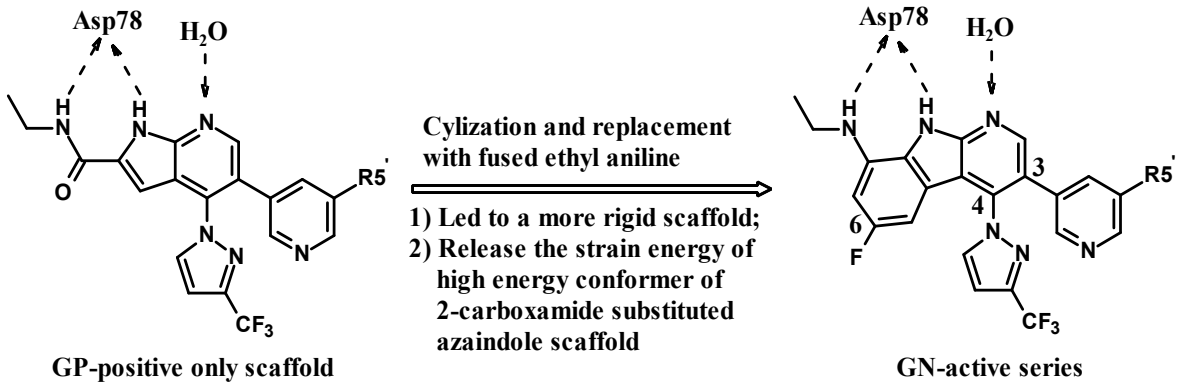

Figure 3. Design of novel tricyclic pyrido[2,3-b]indole scaffold.

To our delight, these analogs showed superior enzymatic potency in both GyrB and ParE biochemical assays (**10b-d**, GyrB *Ki* < 1 nM, ParE *Ki* < 5 nM). The carboxylic acid analog **10a** is the least active compound with GyrB *Ki* = 45 nM and ParE *Ki* = 118 nM, respectively. Furthermore, despite the high lipophilicity (predicted LogD > 3), these analogs were not only potent against GP bacteria

(represented by *S. aureus* ATCC 29213, MIC < 0.25 μg/mL), but also considerably active against GN bacteria such as *E. coli* ATCC 25922 (**10b-d**, MICs ~ 0.5 μg/mL). However, we noticed that a hybrid molecule composed of an R4 non-aryl ring substitution, such as 3-amino proline analog was completely inactive (data not shown). Both pyridine 5'-carboxamide **10b** and 5'-nitrile analog **10d** also demonstrated a good potential for broad-spectrum antibacterial coverage as indicated in **Table 2**, and to our delight, displayed activity against GN MDR strains. In a small panel of selected GN bacteria intended for an initial assessment of GN bacteria coverage, compounds **10b** and **10d** showed MICs < 6 μg/mL, with consistently better potencies against *E. coli* and *A. baumannii* pathogens, but less active against *K. pneumoniae* and *P. aeruginosa* species. Except for A. *baumannii* ATCC 51432 (**10d** only), there was no significant potency shift between the GN bacteria wild-type and MDR stains indicating structural features and physicochemical properties favorable for GN double membrane permeation and devoid of strong efflux. Encouraged by these findings, we then explored the structure-activity relationship (SAR) of substitution at the 3-position of the pyrido[2,3-b]indole scaffold (**Table 1**).

Based on the analysis of our new analogs and the X-ray co-crystal structure of **AZ10** (PDB code: 4EMV), it was reasonable to assume that the R3-pyridine ring formed cation-π stacking interactions with Arg 81 (Arg 76 in *E. coli* GyrB), and a suitable substitution on the 5'-position of the pyridine ring could potentially interact with the adjacent amino acid Arg 140 (Arg 136 in *E. coli* GyrB). Both amino acids had been reported before as being critical for good enzymatic activity. Thus, additional substituents capable of forming optimal hydrogen-bonding interaction with Arg 81 and/or Arg 140 were evaluated. **Table 1** shows binding affinities of these analogs against both GyrB and ParE enzymes as well as their antibacterial activities in both GP bacteria (*S. aureus* ATCC 29213) and GN bacteria (e.g., *E. coli* ATCC 25922). The majority of substitutions were well tolerated, as indicated by their potent *Ki* values of either GyrB or ParE. The least potent compound **10k** (GyrB *Ki* = 53 nM and ParE *Ki* = 239.5 nM) still showed good GP activity (MIC = 0.5 μg/mL) in *S. aureus* ATCC 29213 and weak GN activity (MIC = 8 μg/mL) in *E. coli* ATCC 25922. Similar to the carboxylic acid analog **10a**, strongly acidic and basic compounds like **10g**, **10k**, **10n**, and **10p** were much less active in *E. coli* ATCC 25922 (MICs ≥ 8 μg/mL). Interestingly, the basic analog **10l** (pKa = 8.62) was the exception with *E.*

coli ATCC 25922 MIC = 1 μg/mL. A potential reason for the latter could be related to the strong compound accumulation propensity that free amino groups can induce.[24] Compared with **10b** and **10d**, more recent analogs **10h**, **10i**, and **10t** demonstrated 2-fold improvement of potency against *E. coli* ATCC 25922 (MICs = 0.25 μg/mL). Additionally, the R3 group optimization led to not only new compounds with improved anti-GN bacterial activity in *E. coli* ATCC 25922 but also an improved GN bacteria coverage (**Table 2**, pyrimidine **10h** and pyrazolo[1,5-a]pyrimidine **10t**, MICs ≤ 2 μg/mL).

Table 1. Enzymatic (Ki) and antibacterial potency (MIC) and physicochemical property of pyrido[2,3-b]indole derivatives, **10a-u**.

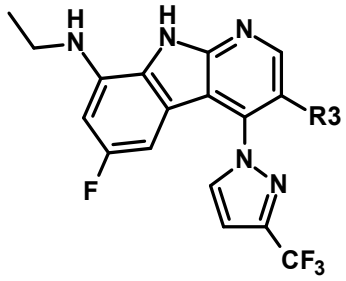

Cmpd	R3	GyrB *Ki*[a] (nM)	ParE *Ki*[a] (nM)	MIC[b] *S. aureus* ATCC 29213 (μg/mL)	MIC[b] *E. coli* ATCC 25922 (μg/mL)	pKa[c]	mlogD$_{7.4}$[d]
10a		45	118	1	>16	3.57	1.9
10b		1.3	<1	<0.016	0.5		3.25
10c		<1	4.3	<0.25	0.5		3.42
10d		<1	<1	<0.016	0.5		3.63
10e		nd	nd	<0.125	2	8.15[e]	3.05
10f		nd	nd	<0.125	0.5		3.41
10g		3.71	<1	0.5	8	10.2[e,f]	2.28

10h		< 1	< 1	<0.016	0.25		3.48
10i		<1	32	<0.016	0.25	4.84[f]	3.44
10j		1.13	68.6	<0.25	1		3.64
10k		53	239.5	0.5	8	8.85[e,f]	2.8
10l		7.1	22.4	<0.25	1	8.62[f]	2.94
10m		<1	11.2	<0.016	0.5		3.56
10n		nd	nd	0.25	>8	3.51	2.02
10o		nd	nd	<0.125	1		3.1
10p		nd	nd	0.444	>11.4	4.78	1.93
10q		nd	nd	<0.056	0.71		3.66
10r		nd	nd	<0.056	0.73	7.59[e]	3.38
10s		nd	nd	<0.057	2.83	9.85[ef]	3.62
10t		1.23	4.74	0.031	0.25		3.54
10u		71	31	<0.125	1	5.44[e]	2.54

[a]*Ki*: inhibition constant; [b]MIC: minimum inhibitory concentration; [c]pKa: acid dissociation constant, measured in a photometric titration assay; [d]mlog$D_{7.4}$: machine learning prediction of intrinsic distribution coefficient between octanol and aqueous buffer (pH 7.4) based on in-house training set data, which measured in a CAMDIS assay;[25] [e]predicted from MoKa (version 2); [f]ionization constant of the conjugate acid

Table 2. Antibacterial GN broad-spectrum coverage of selected compounds **10, 15,** and **17**.

Cmpd	MIC[a]	MIC	MIC	MIC

	E. coli strains (μg/mL)			*K. pneumoniae* strains (μg/mL)			*A. baumannii* strains (μg/mL)			*P. aeruginosa* strains (μg/mL)		
	ATCC 25922[b]	ATCC 35218[b]	ATCC BAA-2340[c]	ATCC 10031[b]	ATCC 700603[b]	ATCC BAA-2146[c]	ATCC 19606[b]	ATCC 51432[b]	ATCC BAA-747[c]	PAO-1[b]	ATCC 27853[b]	ATCC BAA-2113[c]
10b	0.5	0.76	0.76	0.09	0.76	3.02	0.76	3.02	3.02	2	0.76	0.76
10d	0.5	1.45	2.91	0.73	1.45	5.82	0.73	>23.3	1.45	2	5.82	1.45
10h	0.25	0.34	1.38	0.09	0.69	1.38	0.17	1.38	0.69	2	1.38	0.34
10i	0.25	2.85	2.85	0.178	1.42	5.7	1.42	5.7	2.85	2	2.85	1.42
10m	0.5	1.47	1.47	0.183	1.47	>23.5	073	>23.5	>23.5	4	>23.5	1.47
10t	0.25	0.75	0.75	0.38	0.75	1.5	0.38	1.5	0.75	2	1.5	0.75
15r	<0.25	1	2	<0.03	4	8	1	1	0.5	2	na	2
17r	0.31	3.13	12.5	<0.02	6.26	12.5	0.78	0.78	0.39	1.3	1.56	1.56
17x	0.81	5.56	2.78	0.09	22.2	22.2	5.56	5.56	2.78	10	11.1	11.1

[a]MIC: minimum inhibitory concentration; [b]representative GN wide-type bacteria strains; [c]representative GN MDR bacterial strain.

Among these newly identified R3 modifications, further modification on the pyrimidine ring of **10h** seemed attractive. The 2'-position of the pyrimidine was envisioned as a prominent site for derivatization because this vector is pointing toward the solvent-exposed area, therefore presumably, various groups could be accommodated without a loss of good inhibitory activity. Also, variation in this region was highly feasible due to many building blocks commercially available. **Table 3** lists the SAR of a selection of 2'-position modified R3-pyrimidine analogs. As expected, the majority of compounds maintained strong binding affinities to both enzymes, with ParE binding activity more strongly affected by these modifications. A protein overlay between GyrB and ParE, however, did not provide any reason for the observed potency difference. Except for compound **12g**, all analogs had potent GP activity in *S. aureus* ATCC 29213 (MIC ≤ 0.25 μg/mL), likely due to their favorable inner membrane permeability. In terms of GN activity against *E. coli* ATCC 25922, for the neutral analogs, except **12k**, analogs **12a-d**, **12h-j**, and **12v** all showed comparable antibiotic potency to compound **10h.** Additionally, introduction of small polar groups such as alcohols, amides, or aniline amino groups, likely improved the analogs' ability to better penetrate outer membranes of *E. coli* ATCC 25922 as indicated by the smaller potency shift from GP to GN stains (1~4-fold compared to 16-fold potency shift for analog **10h** between *S. aureus* ATCC 29213 and *E. coli* ATCC 25922). The comparable antibacterial potency was also maintained for the two weakly basic compounds **12p** and **12q** in *E. coli*

ATCC 25922. Concerning charged molecules, the basic secondary amino compounds (**12l-n** and **12r-u**) had weaker anti-GN activity, which could be due to poor penetration through the inner membrane, as indicated by the decreased *S. aureus* ATCC 29213 potency when compared to compound **10h**. The GN activity varied for the few acid analogs (**12e-g**, **12o**, and **12w**). As these acids had similar pKa values and identical GP activity against *S. aureus* ATCC 29213, it is reasonable to assume the particular charged form of these compounds could have different GN outer membrane permeability profiles.

Compound **10h** suffered from high microsomal instability. Although the 2'-positon of pyrimidine is not the predicted site of metabolism from Metasite (version 6.0.1), to our surprise, the majority of new analogs listed in **Table 3** yielded improved microsomal stability. Among those, three analogs **12j**, **12p**, and **12v** achieved relatively high metabolic stability in mouse microsomal assay.

Due to the high lipophilicity (predicted LogD 3.48), compound **10h** also had very low aqueous solubility (LYSA < 0.2 μg/mL). For the newly synthesized analogs (**12e, 12f, 12s, 12t,** and **12w**), all of which contained a charged group, marginal to good improvement of solubility profiles (LYSA 8~133 μg/mL) were observed. The acidic analog **12f** displayed better solubility with an LYSA of 67 μg/mL, and it also exhibited potent anti-GN activity with *E. coli* ATCC 25922 MIC = 0.375 μg/mL.

Table 3. Pyrido[2,3-b]indole GyrB/ParE dual inhibitors, **10h** and **12a-x**.

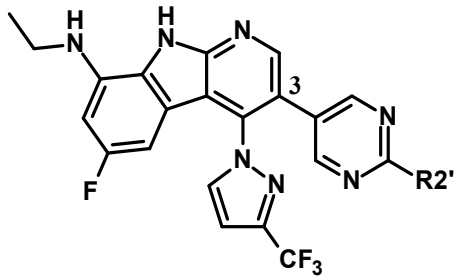

Cmpd	R2'	GyrB *Ki*[a] (nM)	ParE *Ki*[a] (nM)	MIC[b] *S. aureus* ATCC	MIC[b] *E.coli* ATCC	LM[c] (mL/min/mg)	LYSA[d] (μg/mL)	pKa[e]

				29213 (μg/mL)	**25922 (μg/mL)**			
10h	-H	<1	<1	<0.016	0.25	76.1	<0.2	
12a	-CH_3	<1	11.3	<0.016	0.5			
12b(S)		<1	<1	<0.25	0.5	52.8	<0.2	
12c(R)		<1	<1	<0.25	0.5	57.2	<1	
12d		<1	9.7	<0.25	1	58.7	<1	
12e	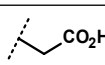	1.1	2.6	<0.016	1	44.0	9	3.83
12f		<1	21.1	<0.016	0.375	43.8	67	3.8
12g		<1	<1	4	16			3.90
12h		<1	<1	<0.25	<0.25	55.5	<0.2	
12i		nd	nd	<0.25	<0.25			
12j	-OCH_3	<1	29.1	<0.016	0.5	20.2	<1	
12k	-OCH_2CH_3	<1	40.4	<0.016	2	37.0	<0.3	
12l	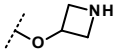	1	62.1	0.063	1			8.62[f]
12m		<1	2.3	0.063	1	62.2	<1	9.06[f]
12n	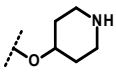	2.6	3	0.063	1			9.34[f]
12o	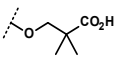	<1	5.6	<0.016	2	43.5	<1	4.71
12p	-NH_2	<1	<1	0.063	1	25.9	7.6	4.39[f]
12q	-$NHCH_3$	<1	7.0	<0.016	0.25	53.1	<1	2.78[f,g]
12r	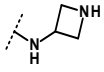	<1	7.8	<0.25	4			9.35[f]
12s		8.4	22	0.25	2	60.1	8.3	9.55[f]
12t	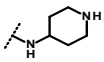	<1	<1	0.063	1	57.9	7.6	9.52[f]
12u		<1	8.7	0.031	1	61.4	<1	8.6[f]

12v		<1	49.3	<0.016	1	24.2	<1	
12w	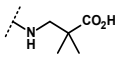	<1	2.9	<0.016	4		133	5.25
12x[h]		2	24	<0.016	0.75	22.9	148	3.8

[a]*Ki*: inhibition constant; [b]MIC: minimum inhibitory concentration; [c]LM: scaled intrinsic clearance of compound in mouse liver microsomes; [d]LYSA: solubility determined by lyophilization solubility assay (LYSA) at pH 6.5; [e]predicted from MoKa (version 2); [f]ionization constant of conjugate acid; [g]pKa: acid dissociation constant, measured in a photometric titration assay; [h]**12x** is a methyl aniline analog of compound **12f** (also see **Figure 5**).

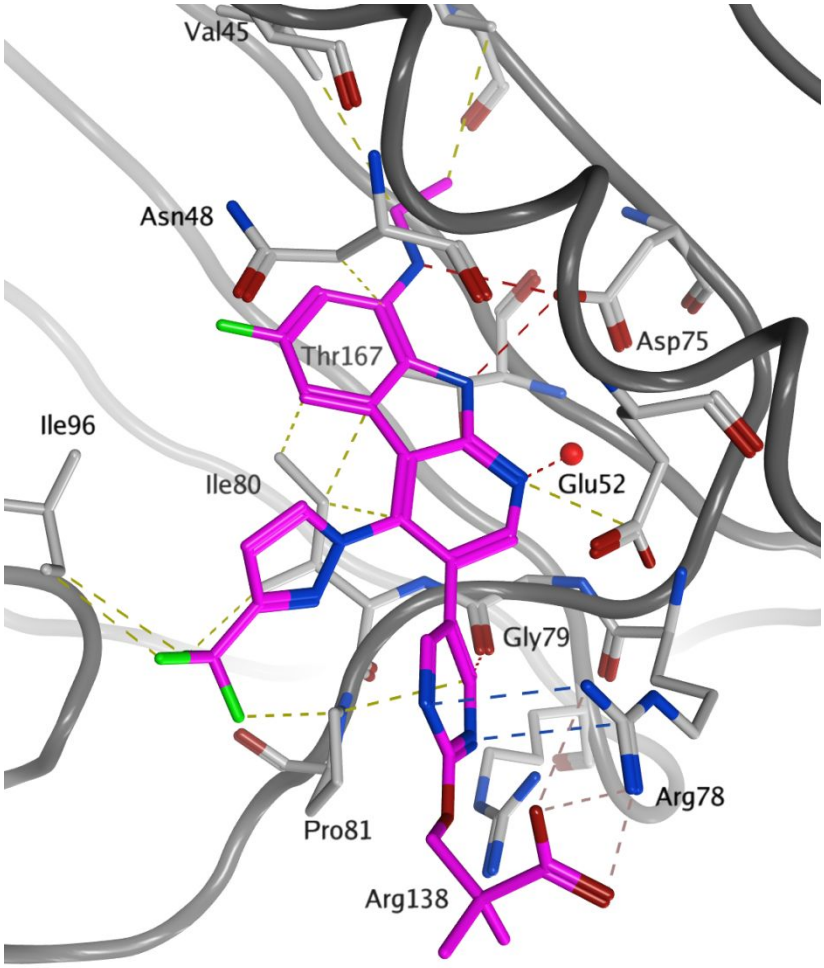

Figure 4. X-ray structure of *P. aeruginosa* GyrB in complex with compound **12o** (PDB code: 6M1S). Key protein residues shown as sticks with grey and ligand with magenta carbons. All water molecules

except for structural water are hidden for clarity. Interactions are shown as color-coded dashed lines (H-bonds in red, vdW in yellow, cation-π stacking in blue and salt bridge in light pink).

The X-ray co-crystal structure of compound **12o** (PDB code: 6M1S) in complex with *P. aeruginosa* GyrB protein is shown in **Figure 4**. As expected, there is a strong hydrogen-bonding network formed between the ligand and amino acid Asp 75 and the structural water molecule. The tricyclic pyrido[2,3-b]indole scaffold adopts a hydrogen-bond donor-donor-acceptor pattern that is the same as that seen for the Trius tricyclic scaffold. Compared to the original azaindole scaffold, there is a minor dihedral angle change between the tricyclic ring and the R3-pyridine. The cation-π stacking interaction between Arg 78 and the pyridine ring was maintained. Meanwhile, the 2'-oxypropanoic acid-containing substituent formed a salt bridge interaction with Arg 78. Albeit the inherent flexibility of the latter substituent, it is well defined in the electron density, which is partially stabilized by the adjoining molecule of the next asymmetric unit (not shown). As mentioned before, both Arg 78 and Arg 138 are important for good enzymatic activity. Whereas no direct interaction with Arg 138 was observed, there is room for a water molecule to form a bridged H-bond interaction between the latter and one of the pyrimidine nitrogens similar to the **GP1** structure. In addition, an H-bond of the polarized C4' pyrimidine hydrogen to the backbone carbonyl oxygen of Gly 79 is observed. Due to the steric demand of the phenyl ring of the pyrido[2,3-b]indole and the R3 pyrimidine substituent, the R4 3'-CF_3 pyrazole substitution adopted a marginally bigger out of plane twist (58 ^{o}C in **12o** vs. 53.1 ^{o}C in **AZ10**). The 3'-CF_3 group sits on top of the hydrophobic groove formed by amino acids Pro 81 and Ile 80 and 96. The 4' and 5'-position of the pyrazole ring point toward a solvent-exposed area opposite which two conserved amino acids (Asn 48 and Asp 51, omitted for clarity, see **Figure 5**) are located. These residues can be utilized to improve binding affinity further. Overlay with the Trius X-ray co-crystal structure (**GP1**, PDB code: 4KFG) revealed a shift of the scaffold partially due to the ethyl vs. methyl difference. The limited room available in the back of the pocket results in the former being pushing slightly towards the opening of the pocket, i.e., along the Asp 75 acceptor and water donor while maintaining these key interactions. However, once a methyl aniline analog such as **12x** was used, the

two tricyclic cores overlaid more closely (**Figure 5**). Nonetheless, a small shift of the cores is still apparent, which is - as discussed for the AZ analog before - due to the change from the R2- to the R3-position substitution. The latter yielding shorter interaction distances for the H-bonds due to tighter packing of the core with the protein. Conversely, the Trius compound has a closer π-π stacking to Arg 78 (76 in *E. coli* GyrB) than the R3-pyrimidine ring and trying to replace R4-pyrazole with non-aryl groups such as Trius R4 proprietary amines failed to give better antibacterial potency indicating different SAR in this region. Nonetheless, it was apparent that one could take advantage of two additional conserved amino acids Asn 48 and Asp 51 for R4 group optimization.

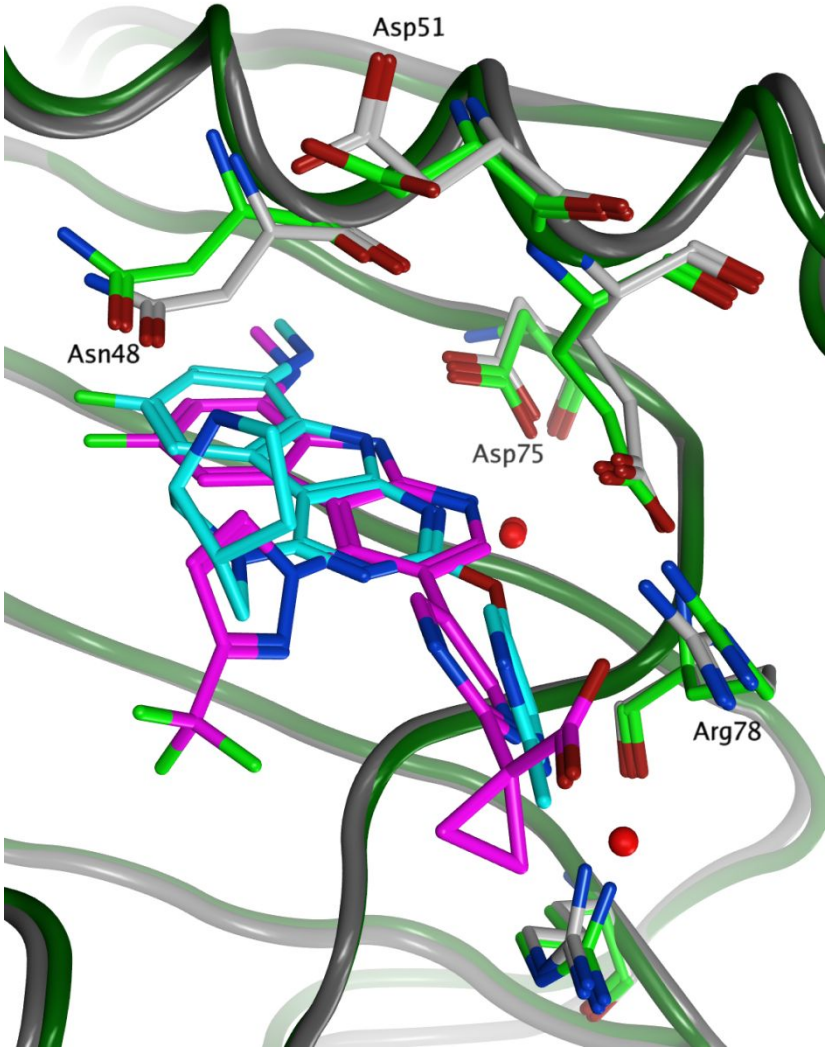

Figure 5. X-ray co-crystal structures overlay between **GP1** (PDB code: 4KFG, protein shown with green ribbon and carbons, ligand with cyan carbons) and compound **12x** (PDB code: 6M1J, protein shown with grey ribbon and carbons, ligand with magenta carbons). Further residues and water molecules omitted for clarity.

Therefore, having explored the R3 area and its impact on physicochemical properties, we then focused on the R4 group refinement. **Table 4** lists several R4 variations keeping the R3 pyridine-3-carbonitrile group fixed. Due to a balanced physicochemical property, the pyrazole 3'-CF_3 substitution not only had an excellent fit in the hydrophobic pocket (*Ki* < 1 nM), but also showed a MIC of 0.5 μg/mL against *E. coli* ATCC 25922. A change to 3'-CF_2 (**15i**) resulted in 2-fold of activity decrease. Furthermore, an effort to explore alternative hydrophobic substitutions such as Me (**15e**), Et (**15f**), isopropyl (**15g**), and *tert*-butyl (**15h**) all decreased anti-GN activities (4~16 folds). The pyrazole 3'-CN substitution (**15a**), however, showed a surprisingly 2-fold improvement in anti-GN potency (*E. coli* ATCC 25922 MIC = 0.125 μg/mL) and an 8-fold of GP to GN potency shift. The few polar substituents like carboxylic acid (**15b**) and amine (**15d**) were completely inactive (MICs > 16 μg/mL), which might be due to both the incompatibility with the hydrophobic floor of the pocket and the less favored physicochemical properties at R4. A few heterocycle alternatives to the pyrazole were explored as well. Although an acceptable anti-GP potency was observed (*S. aureus* ATCC 29213 MIC = 0.063 μg/mL), the phenyl 3'-CF_3 (**15j**) showed much decreased anti-GN activity (MIC > 16 μg/m) in *E. coli* ATCC 25922, and the imidazole 4'-CF_3 (**15k**) was even inactive. For the two other replacements, pyrazole 4'-CF_3 (**15l**) and thiazole 3'-CF_3 (**15m**), their MICs were maintained or slightly decreased. It is evident that specific heterocyclic rings at R4 position are ideal for GN activity, although the precise reason remained elusive.

Table 4. Pyrido[2,3-b]indole GyrB/ParE dual inhibitors, **10d** and **15a-m**.

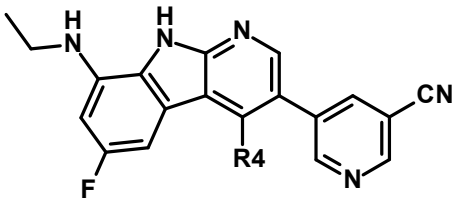

Cmpd	R3	GyrB *Ki*[a] (nM)	ParE *Ki*[a] (nM)	MIC[b] *S. aureus* ATCC 29213 (μg/mL)	MIC[b] *E. coli* ATCC 25922 (μg/mL)	LYSA[c] (μg/mL)	pKa[d]
10d		<1	<1	<0.016	0.5	<0.3	
15a		1	< 1	<0.016	0.125	<1	
15b		nd	nd	>16	>16		4.08
15c		< 1	65.5	0.125	8		2.02[e]
15d		nd	nd	2	16		8.09
15e		< 1	25.7	<0.25	2	<1	
15f		<1	<1	<0.25	1	<0.3	
15g		< 1	28.4	<0.25	>16	<0.7	
15h		1.02	157.4	<0.25	>16	<0.3	
15i		4.7	59.8	<0.25	1	<1	
15j		nd	nd	0.063	>16		
15k		nd	nd	0.25	>16		
15l		<1	1.1	<0.016	1	<1	
15m		8.3	156	<0.016	0.5	<1	

[a]*Ki*: inhibition constant; [b]MIC: minimum inhibitory concentration; [c]LYSA: solubility determined by lyophilization solubility assay (LYSA) at pH 6.5; [d]pKa: ionization constant predicted from MoKa (version 2); [e]conjugate acid.

With pyrazole as the preferred heterocycle, we then evaluated the possibility to substitute the latter further. As indicated in **Table 5**, among the compound prepared, the 3',4'-bis-substituted free amino compound **15r** maintained excellent anti-GN activity (*E. coli* 25922 MIC = 0.25 μg/mL). However, an attempt to further rigidify this molecule by ring cyclization gave decreased antibacterial potency as shown by analog **15u** (*E. coli* ATCC 25922 MIC = 1 μg/mL). Meanwhile, it was also noticed that the impact on potency for the CF_3 substitution on the R4 bicyclic core was not as significant as on the 3'-mono-substituted pyrazole ring (e.g., **15u** vs. **15x**). The aqueous solubility of two amino analogs **15r** and **15x** achieved LYSA = 90 μg/mL and 34 μg/mL, respectively. We attributed such good solubility improvement to the molecules' effective disruption of the intermolecular π-π stacking interaction that is partially responsible for the low solubility of this series of analogs.

Table 5. Pyrido[2,3-b]indole GyrB/ParE dual inhibitors, **10d** and **15n-z**.

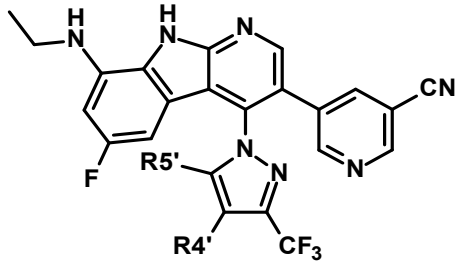

Cmpd	R4' / R5'	MIC[a] *E. coli* ATCC 25922 (μg/mL)	pKa[b]	LM[c] (mL/min/mg)	LYSA[d] (μg/mL)
10d		0.5		61.8	<0.3

15n		>16	3.55		
15o		2		nd	nd
15p		>16			
15q		4		nd	nd
15r		<0.25	8.08[e]	47.0	90
15s		8			
15t		>16			
15u		1	6.57[e]	73.2	<0.3
15v		2	9.44	nd	<1
15w		4	8.27	nd	nd
15x		2	7.62[e]	70.3	34
15y		2	8.33	20.2	nd
15z		4	8.11	52.1	200

[a]MIC: minimum inhibitory concentration; [b]pKa: ionization constant predicted from MoKa (version 2); measured in a photometric titration assay; [c]LM: scaled intrinsic clearance of compound in mouse liver microsomes; [d]LYSA: solubility determined by lyophilization solubility assay (LYSA) at pH 6.5; [e]conjugate acid dissociation constant, measured in a photometric titration assay.

The subsequent combination of several newly identified R4 groups and promising R3 modifications, such as the 2-methoxypyrimidine led to the syntheses of analogs **17r, 17u,** and **17x**. To our delight, not only did the mono amino compound **17r** maintain the same good potency (*E. coli* ATCC 25922 MIC = 0.312 μg/mL), but the bicyclic compound **17x** improved its activity (*E. coli* ATCC 25922 MIC = 0.812 μg/mL) and with a good solubility of LYSA = 350 μg/mL, the highest solubility among the whole series.

The good anti-GN activity, acceptable aqueous solubility, and metabolic stability of compounds **15r**, **17r**, and **17x** then supported their further evaluation *in vivo*.

Table 6. Comparison between pyrido[2,3-b]indole GyrB/ParE dual inhibitors, **15** and **17**.

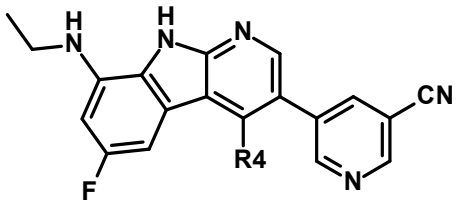

15

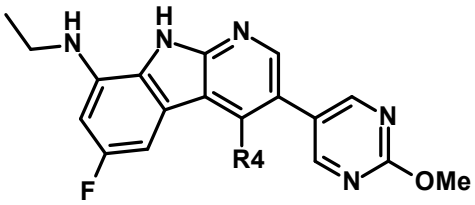

17

Cmpd	R4	MIC[a] *E. coli* ATCC 25922 (μg/mL)	LYSA[b] (μg/mL)	fu[c]	Cl[d] in liver microsome[d] (mL/min/kg)	Cl[d] in hepatocyte (mL/min/kg)
15r		<0.25	90	1.2	47.0	48.6
15u		1	<0.3	1.2	73.2	nd
15x	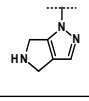	2	34	4.4	70.3	74.6
17r		0.312	15	2.7	<20.2	45.3
17u		1	4	1.6	77.4	nd
17x		0.8	350	11	21.8	53.9

a MIC: minimum inhibitory concentration; [b]LYSA: solubility determined by lyophilization solubility assay (LYSA) at pH 6.5; [c]fu: percentage of compound free fraction in a plasma protein binding assay; [d]Cl: scaled mouse intrinsic clearance of compound.

Table 7 shows mouse SDPK IV study results of compounds **15r**, **17r**, and **17x**. All three basic compounds showed medium *in vivo* clearances (Cl_{iv}), which correlate well with the *in vitro* hepatic clearances. The half-lives are short, around 1~2 hr, and the area under the curve (AUC) falls into the range of 320~340 μg*hr/mL. These compounds demonstrated a medium to high volume of distribution

with the plasma protein binding in the range of 89~99%. Although not displaying optimal PK profiles, these compounds nonetheless proceeded into an animal efficacy study for the initial PK/PD relationship exploration.

A neutropenic mouse thigh infection model with *E. coli* ATCC 25922 was used to evaluate the *in vivo* efficacy of compounds. Exemplified by compound **17r**, **Figure 6** shows the corresponding log unit of CFU reductions under different dose regimens. A good dose-response was observed for compound **17r**, and at 45 mpk *b.i.d.*, the bactericidal efficacy that corresponds to one log unit of CFU reduction (vs. vehicle) was achieved. Free AUC/MIC mostly predicts the PK/PD relationship of other Topoisomerase antibiotics like FQ. Even though no detailed PKPD study was performed, fAUC/MIC was still used as PK index in this project at the early screening stage. So, in the mouse thigh infection model, **17r** showed bactericidal efficacy at fAUC/MIC ≥ 6, which also accounts for a total of fAUC ~ 30 μg*hr/mL (See SI).

Although the *in vivo* efficacy in mice infected with *E. coli* ATCC 25922 was successfully demonstrated, the lower activity of compound **17r** against other GN pathogens was insufficient for additional *in vivo* efficacy profiling (**Table 2**). Additional chemistry efforts to further improve this chemical series' GN broad-spectrum activity and physicochemical properties targeting other infection models such as pneumonia and urinary tract infection (UTI) will be reported in due course.

Table 7. Single-dose intravenous pharmacokinetics of representative compounds in the mouse.

Cmpd	Cmax_D[a] (kg*ng/mL/mg)	AUC_{iv}_D[b] (hr*kg*ng/mL/mg)	Cl_{iv}[c] (mL/min/kg)	$t_{1/2}$[d] (hr)	V_{ss}[e] (L/kg)
15r	305	324	50	1.8	5.8
17r	494	341	48	1.6	3.6
17x	792	327	51	0.8	1.6

[a]C_{max}_D: dose-normalized maximal concentration; [b]AUC_{iv}_D: dose-normalized area under the curve; [c]Cl_{iv}: plasma clearance; [d]$t_{1/2}$: half-live of compound in plasma; [e]V_{ss}: volume of distribution at the steady-state.

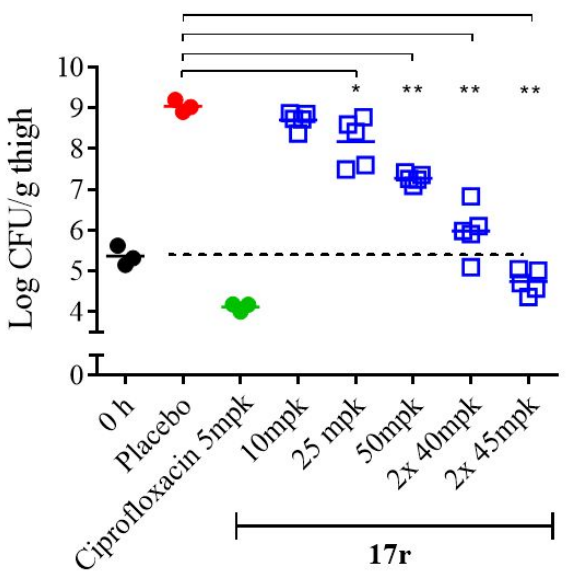

Figure 6: *In vivo* efficacy in neutropenic mouse thigh model. The plot shows the log unit CFU levels in *E. coli* ATCC 25922 after twelve hours of infection with the treatment of either placebo (black dots), ciprofloxacin control (green dots), or compound **17r** (blue squares). The line for each animal group represents the mean, mpk is mg/kg, 2x is two doses with three hours interval. Statistical significance (Dunnett's multiple comparison test) vs. placebo, one asterisk represents adjusted P values 0.01-0.05 and two asterisks P <0.001.

CHEMISTRY

All the final compounds were synthesized via the key pyrido[2,3-b]indole tricyclic intermediate **7**, of which the preparation is illustrated in **Scheme 1**. 2,4-Difluoro-1-nitro-benzene was reacted with ethyl amine in EtOH via nucleophilic aromatic substitution to afford nitroaniline **2**, which was then deprotonated by NaH and reacted with di-*tert*-butyl carbonate to give the Boc-protected nitroaniline **3**. The nitro group of the aniline **3** was reduced by H_2 with palladium on carbon, to afford aniline **4**. Subsequent Buchwald-Hartwig cross-coupling reaction of the aniline **4** with 2,3,5-trichloropyridine was carried out in the presence of palladium acetate, cesium carbonate, and BINAP to yield compound **5**. The tricyclic pyrido[2,3-b]indole **6** was obtained by cyclization of **5** via an intramolecular direct arylation using $Pd_2(dba)_3$ catalyst and Xantphos ligand. Finally, the bi-chloro substituted tricyclic

intermediate **7** was obtained from MCPBA oxidation of the tricyclic pyridine followed by $POCl_3$ chlorination.

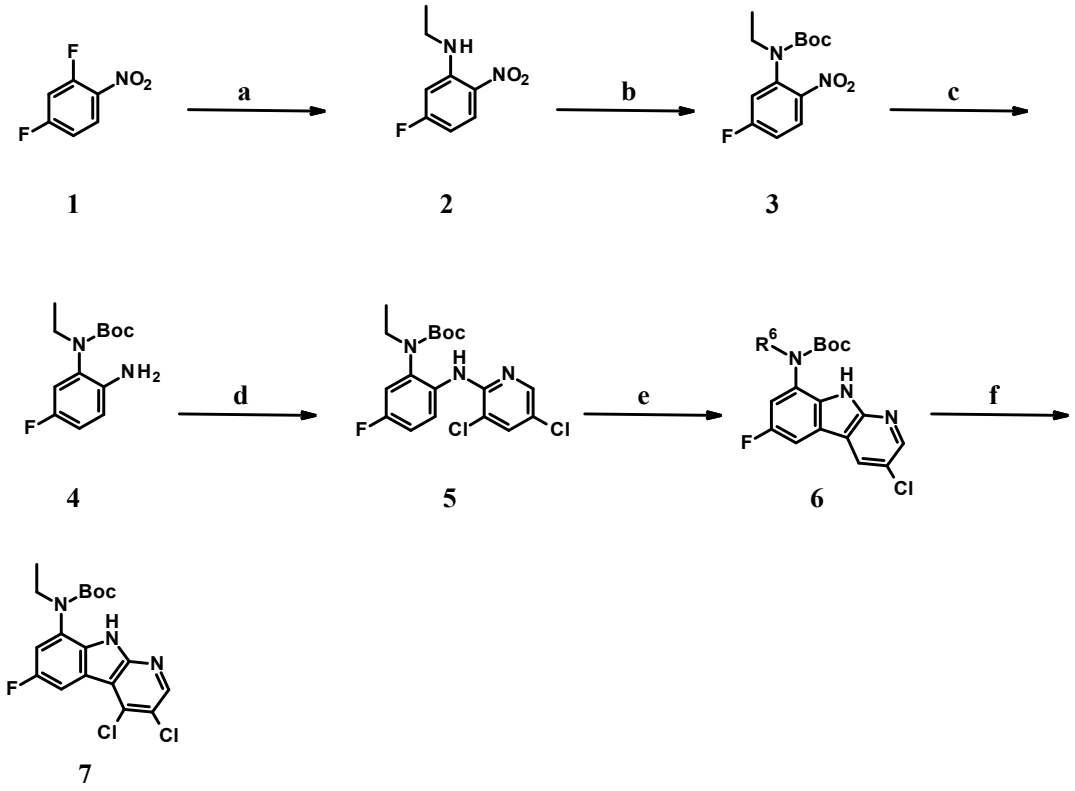

Scheme 1. Synthesis of key intermediate **7**. a) $EtNH_2$, EtOH, 0 °C, 3 hr, 63% yield; b) NaH, Boc_2O, THF, 0 °C then rt, 16 hr, 86% yield; c) H_2 50 psi, Pd/C, MeOH, rt, 18 hr, 92% yield; d) 2,3,5-trichloropyridine, $Pd(OAc)_2$ BINAP, Cs_2CO_3, 1,4-dioxane, 120 °C, 16 hr, 74% yield; e) $Pd_2(dba)_3$, X-Phos, DBU, DMA/o-xylene, 130 °C, 4 hr, 51% yield; f) m-CPBA, DCM, 30 °C; 12 hr, then $POCl_3$, DMF, -5 °C to 0 °C, 1 hr, 42% yield.

The general preparation of final compounds **10a-u** and **12a-w** is depicted in **Scheme 2**. The key intermediate **7** was first reacted with 3-(trifluoromethyl)-1H-pyrazole through base promoted nucleophilic aromatic substitution to give compound **8**. For the syntheses of compounds **10a-u**, compound **8** was reacted with various boronic acids or esters under palladium catalyzed Suzuki coupling reaction condition to give compounds **9**. In some cases, additional chemical transformations were carried out before the Boc-protecting group was removed by trifluoroacetic acid treatment to give the final compounds **10a-u**. For the syntheses of pyrimidine compounds **12a-w**, intermediate **8** was

reacted with a variety of pyrimidine R3' substituted boronic acids or esters under Suzuki coupling condition to afford compounds **11**; similarly, when necessary, appropriate chemical transformations were applied before the Boc-protecting group was removed by the treatment of trifluoroacetic acid to afford the final compounds **12a-w**.

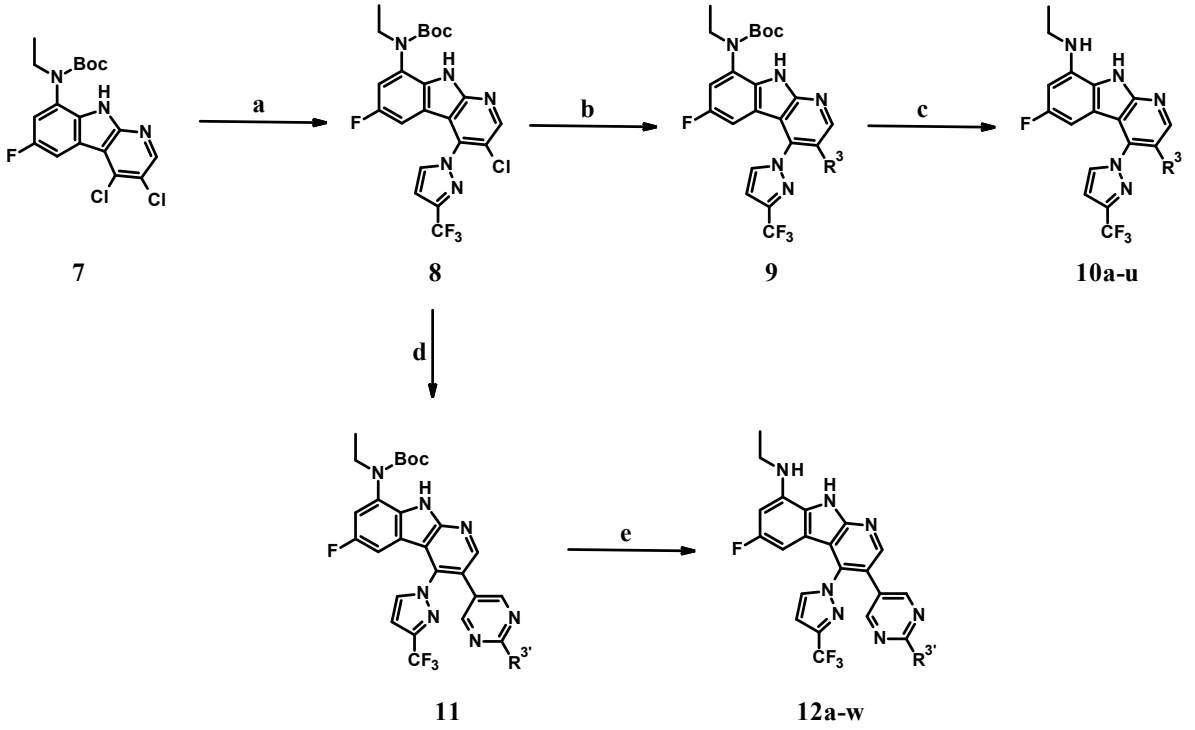

Scheme 2. Examplar synthesis of compounds **10a-u** and **12a-w**. a) 3-(trifluoromethyl)pyrazole, K_2CO_3, DMSO, 120 °C, 12 hr, 86% yield; b) **9d**, 3-cyanopyridine-5-boronic acid pinacol ester, Pd_2db_3, X-Phos, K_3PO_4, 1,4-dioxane/H_2O, 100 °C, 12 hr, 66% yield; c) **10d**, TFA, DCM, rt, 2 hr, 81% yield; d) **11j**, (2-methoxypyrimidin-5-yl)boronic acid, Pd_2db_3, XPhos, K_3PO_4, 1,4-dioxane/H_2O, 100 °C, 12 hr, 64% yield; e) **12j**, TFA, DCM, rt, 1 hr, 40% yield.

Finally, the general synthesis for the preparation of final compounds **15a-z**, **17r, 17u,** and **17x** is depicted in **Scheme 3**. Similar to the **Scheme 2**, the intermediate **7** was first reacted with a variety of derivatized pyrazole reagents under either base promoted aromatic nucleophilic substitution or Buchwald-Hartwig cross-coupling reactions to afford compounds **13a-z**. Subsequent Suzuki coupling reaction with 5-(4,4,5,5-tetramethyl-1,3,2-dioxaborolan-2-yl)pyridine-3-carbonitrile then yielded compounds **14a-z**. Whenever needed, additional chemical transformations were carried out before the

Boc-protecting group was removed to give final compounds **15a-z**. Meanwhile, intermediates **13r**, **13u**, and **13x** were reacted with 2-methoxy-5-(4,4,5,5-tetramethyl-1,3,2-dioxaborolan-2-yl)pyrimidine individually via Suzuki coupling reactions to give compounds **16r**, **16u**, and **16x**. After the removal of Boc-protecting group, final compounds **17r**, **17u**, and **17x** were then obtained.

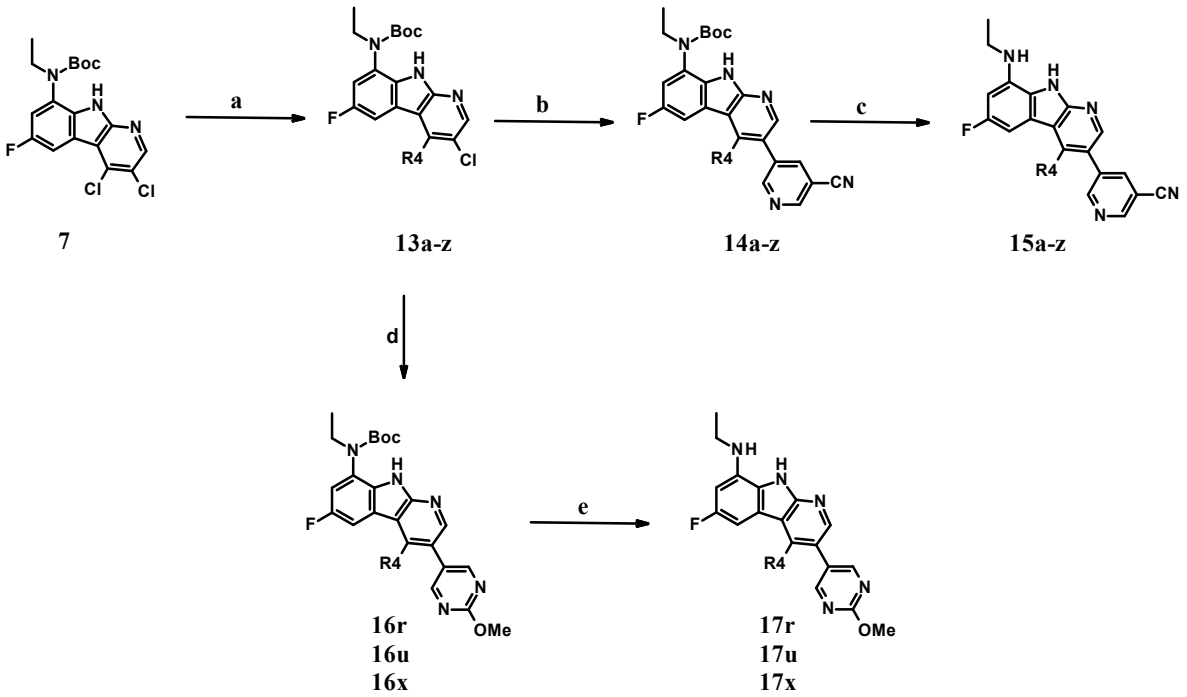

Scheme 3. Examplar synthesis of **15a-z** and **17r**, **17u**, and **17x**. a) **13r**, ethyl 3-(trifluoromethyl)-1H-pyrazole-4-carboxylate, K_2CO_3, DMSO, 120 °C, 33% yield; b) **14r**, 5-(4,4,5,5-tetramethyl-1,3,2-dioxaborolan-2-yl)nicotinonitrile, CsF, $Pd_2(dba)_3$, X-phos; 1,4-dioxane/H_2O, 110 °C, 12 hr, 89% yield; NH_4Cl, HOBt, PyBOP, DIPEA, DMF, 30 °C, 1 hr, 96% yield; BH_3-THF, 80 °C, 0.5 hr, 27% yield; c) **15r**, TFA, DCM, rt, 1 hr, 75% yield; d) **16x**, *tert*-butyl 4,6-dihydro-1H-pyrrolo[3,4-c]pyrazole-5-carboxylate, K_2CO_3, DMSO, 120 °C, 12 hr, 93% yield; 2-methoxy-5-(4,4,5,5-tetramethyl-1,3,2-dioxaborolan-2-yl)pyrimidine, K_3PO_4, cataCXium A-Pd-G2, THF-H_2O, 70 °C, 12 hr, 93% yield; e) **17x**, TFA, DCM, 30 °C, 1 hr, 57% yield.

CONCLUSION

Due to the rapid increase of bacterial resistance to marketed antibiotics, novel antibacterial agents are needed urgently. In particular, medicines that can treat MDR GN infections because these infections are associated with the highest mortality rates and have limited treatment options. Dual

ATPase inhibitors targeting DNA gyrase GyrB subunit and Topoisomerase IV ParE subunit have the potential to be broad-spectrum antibiotics due to the high level of protein conservation across pathogenic bacterial species and overcome target-based FQ resistance. Using an information-driven approach, we converted the 2-carboxamide substituted azaindole scaffold with only GP activity into a novel chemical series that is also very potent against the ESKAPE GN pathogens. Expanding the activity spectrum was mainly achieved by increasing the original AZ scaffold's rigidity via a unique ring cyclization strategy. A systematic exploration of the physicochemical properties associated with GN antibacterial activity enabled us to identify the lead molecule **17r**, which has a balanced profile of GN activity, aqueous solubility, and SDPK properties. Moreover, we showed the dose-dependent cidal efficacy of **17r** in a neutropenic mouse thigh infection model. To further develop this series, the compounds need to show improved broad-spectrum *in vitro* coverage of GP and GN clinical isolates and in vivo efficacy in multiple infection models (pneumonia and UTI). A novel class of GyrB/ParE dual inhibitors that can cure the most difficult-to-treat resistant infections in the clinic[26] would address an urgent medical need considering the ever-increasing resistance toward existing antibiotics.

EXPERIMENTAL SECTION

General Methods for Chemistry. Reactions involving air-sensitive reagents were carried out under an atmosphere of nitrogen or argon. The microwave assisted reactions were carried out in a Biotage Initiator Sixty. Solvents and reagents were obtained from commercial sources and were used without further purification unless otherwise noted. All reactions were monitored by thin-layer chromatography (TLC) on Merck silica gel 60 F254 TLC glass plates (visualized by UV fluorescence at λ = 254 nm) or analytical LC-MS. All intermediates and final compounds were purified by either silica gel flash chromatography or preparative HPLC (prep-HPLC) using one of the following instruments: (i) Biotage SP1 system and the Quad 12/25 cartridge module; (ii) ISCO Combi-flash chromatography instrument. Silica gel brand and pore size: (a) KP-SIL 60 Å, particle size 40–60 μm; (b) CAS registry no., silica gel, 63231-67-4, particle size 47–60 μm silica gel; (c) ZCX from Qingdao Haiyang Chemical Co., Ltd., pore 200–300 or 300–400; (iii) prep-HPLC on a reverse-phase column

using a Waters XBridge OBD Phenyl (30 mm x 100 mm, 5 μm) or OBD RP18 (30 mm x 100 mm, 5 μm) column under acidic conditions (A, 0.1% formic acid in H_2O; B, 0.1% formic acid in acetonitrile) or basic conditions (A, 0.01% ammonia in H_2O; B, acetonitrile). For SFC chiral separation, either intermediates or final compounds were separated using a chiral column (Daicel Chiralpak IC, 30 mm x 250 mm, 5 μm) on a Mettler Teledo SFC-Multigram system (solvent system of 95% CO_2 and 5% IPA (0.5% Et_3N in IPA), backpressure of 100 bar, UV detection at 254 nm). Optical rotation was measured using a Rudolph Autopol V automatic polarimeter at a wavelength of 589 nm. The purity of final compounds as measured by LC-MS was ≥95%. LC-MS spectra were obtained using UPLC coupled with single quadrupole mass detector (Waters Acquity UPLC-3100 Mass Detector, Waters Acquity UPLC-SQ Detector, Waters Acquity UPLC-SQ Detector). Standard LC-MS conditions were as follows. Columns: Waters Acquity BEH C18, 2.1 mm × 50 mm x 1.7 μm and Waters Acquity CSH C18 column, 2.1 mm × 50 mm x 1.7 μm. Flow rate: 0.8 mL/min. Gradient: 5-95% eluent B over 3 min under mobile phase conditions: 1) acidic condition: A, 0.1% formic acid in H_2O; B, 0.1% formic acid in acetonitrile; or 2) basic condition: A, 0.05% $NH_3 \cdot H_2O$ in H_2O; B, acetonitrile. Mass spectra (MS): Generally only ions which indicate the parent mass are reported, and unless otherwise stated the mass ion quoted is the positive mass ion $(M+H)^+$. NMR spectra were obtained using Bruker Avance 400 MHz spectrometer, operating at 400.13 MHz (^1H) and 100.62 MHz (^{13}C). High-resolution mass spectra (HRMS) were obtained on Xevo G2-XS-QTOF mass spectrameter equipped with an electrospray ionization source. All of the reported yields are for isolated products and not optimized.

Synthetic procedure for the synthesis of *tert*-butyl N-(3,4-dichloro-6-fluoro-9H-pyrido[2,3-b]indol-8-yl)-N-ethyl-carbamate (7).

N-Ethyl-5-fluoro-2-nitro-aniline (2). Ethylamine solution (234.26 g, 1.56 mmol, 30% in EtOH) was added dropwise to 2,4-difluoronitrobenzene (80 g, 0.503 mol) at 0 °C over 15 min. After completion of the addition, the reaction mixture was stirred at 0 °C for 3 h. The solution was diluted with EtOH (500 mL) and poured into 2.5 L of ice-water. The resulting precipitates were collected by filtration and dried

in vacuo to afford the title compound (143 g, 63% yield) as a yellow solid. MS obsd (ESI+) [$(M+H)^+$] 185.0.

***tert*-Butyl N-ethyl-N-(5-fluoro-2-nitro-phenyl)carbamate (3).** To a suspension of sodium hydride (32.58 g, 814.48 mmol, 60 % dispersion in mineral oil) in dry THF (800 mL) was added N-ethyl-5-fluoro-2-nitro-aniline (30 g, 162.9 mmol) portion wise at 0 °C. The solution was stirred at 0 °C for 1 h. Then the solution of di-*tert*-butyl dicarbonate (30 g, 162.9 mmol) in THF (200 mL) was added dropwise and the reaction continued for another 15 h at 15 °C. The reaction mixture was poured into 350 mL of ice-water and extracted with EtOAc (500 mL) two times. Combined organics were dried over anhy. Na_2SO_4, filtered, and concentrated *in vacuo*. The crude product was purified by flash chromatography (silica gel, 1-5% ethyl acetate in petroleum ether) to afford the title compound (40 g, 86.4% yield) as a yellow solid. MS obsd (ESI+) [$([M-100]+H)^+$] 185.1.

***tert*-Butyl N-(2-amino-5-fluoro-phenyl)-N-ethyl-carbamate (4).** To a solution of *tert*-butyl N-ethyl-N-(5-fluoro-2-nitro-phenyl)carbamate (120 g, 422.1 mmol) in MeOH (1 L) was added palladium on carbon (8 g, 50 wt. % loading) under N_2, then the suspension was degassed under vacuum and purged with H_2 several times. The reaction mixture was stirred at 15 °C for 18 h under H_2 atmosphere (50 psi). The remaining palladium catalyst was removed by filtration and the filtrate was concentrated *in vacuo* to afford the title compound (98.2 g, 91.5% yield) as a white solid. MS obsd (ESI+) [$([M-100]+H)^+$] 155.1.

***tert*-Butyl N-[2-[(3,5-dichloro-2-pyridyl)amino]-5-fluoro-phenyl]-N-ethyl-carbamate (5).** To a solution of *tert*-butyl N-(2-amino-5-fluoro-phenyl)-N-ethyl-carbamate (60 g, 235.94 mmol) and 2,3,5-trichloropyridine (45.2 g, 247.74 mmol) in 1,4-dioxane (800 mL) was added cesium carbonate (153.74 g, 471.88 mmol), palladium(II) acetate (2.65 g, 11.8 mmol), and BINAP (14.7 g, 22.36 mmol). The reaction was stirred at 120 °C for 16 h under nitrogen atmosphere. Then the reaction mixture was cooled down to room temperature and diluted with EtOAc (600 mL) and filtered. The precipitate was removed by filtration and the filtrate was concentrated *in vacuo* and the residue was purified by flash chromatography (silica gel, 0 to 5% EtOAc in petroleum ether) to afford the title compound (70 g, 74.1% yield) as a solid. MS obsd (ESI+) [$(\{^{35}Cl\}M+H)^+$] 400.0, [$(\{^{37}Cl\}M+H)^+$] 402.0.

***tert*-Butyl N-(3-chloro-6-fluoro-9H-pyrido[2,3-b]indol-8-yl)-N-ethyl-carbamate (6).** To a solution of *tert*-butyl N-[2-[(3,5-dichloro-2-pyridyl)amino]-5-fluoro-phenyl]-N-ethyl-carbamate (8 g, 20 mmol) and DBU (6.09 g, 40 mmol) in the mixture of o-xylene (13 mL) and N,N-dimethylacetamide (13 mL) was added $Pd_2(dba)_3$ (3.66 g, 4 mmol), and Xantphos (2.86 g, 6 mmol). The mixture was degassed with nitrogen for 5 min and then stirred at 130 °C for 3.5 h. The reaction mixture was cooled back to room temperature, poured into water (100 mL) and then extracted with EtOAc (300 mL) three times. The organic layer was washed with aqueous $CaCl_2$ solution (1N, 120 mL) three times, and brine (160 mL) twice. The organic layer was dried over anhy. Na_2SO_4, filtered, and concentrated *in vacuo*. The crude product was purified by flash chromatography (silica gel, EtOAc/pertrolieum ether = 30:1 to 3:1) and recrystallization in MeOH (40 mL) to afford the title compound (3.7 g, 50.9% yield) as a pale yellow solid. MS obsd (ESI+) [({^{35}Cl}M+H)$^+$] 364.1, [({^{37}Cl}M+H)$^+$] 366.1.

***tert*-Butyl N-(3,4-dichloro-6-fluoro-9H-pyrido[2,3-b]indol-8-yl)-N-ethyl-carbamate (7).** To a solution of *tert*-butyl N-(3-chloro-6-fluoro-9H-pyrido[2,3-b]indol-8-yl)-N-ethyl-carbamate (6 g, 16.5 mmol) in DCM (200 mL) was added 3-chloroperbenzoic acid (11.4 g, 66 mmol) at 0 °C. After the addition, the reaction was continued at 30 °C for 12 h. The reaction mixture was then poured into aqueous sodium sulfite solution (10%, 150 mL) and stirred for 1 h followed by the extraction with EtOAc (750 mL) three times. Combined organics were washed with aqueous sodium bicarbonate solution (5N, 200 mL) and brine (250 mL), dried over anhy. Na_2SO_4, filtered, and concentrated *in vacuo* to give *tert*-butyl N-(3-chloro-6-fluoro-1-oxido-9H-pyrido[2,3-b]indol-1-ium-8-yl)-N-ethyl-carbamate (6 g, 96% yield) as a brown solid. MS obsd (ESI+) [({^{35}Cl}M+H)$^+$] 380.1, [({^{37}Cl}M+H)$^+$] 382.0.

To a solution of *tert*-butyl N-(3-chloro-6-fluoro-1-oxido-9H-pyrido[2,3-b]indol-1-ium-8-yl)-N-ethyl-carbamate (6 g, 15.8 mmol) in DMF (100 mL) was added phosphorus(V) oxychloride (27.1 g, 176.2 mmol) dropwise at -5 °C. The mixture was stirred at -5 °C to 0 °C for 1 h before poured into saturated aqueous sodium bicarbonate solution (300 mL) at 0 °C. The mixture was extracted by EtOAc (750 mL) twice and combined organics were washed with saturated aqueous $NaHCO_3$ solution (150 mL x 2), aqueous $CaCl_2$ solution (1N, 150 mL x 2), and brine (150 mL x 2). The organic layer was dried over anhy. Na_2SO_4, filtered, and concentrated *in vacuo*. The crude product was washed with MeOH (120

mL) to afford the title compound (2.76 g, 43.8% yield) as a pale yellow solid. MS obsd (ESI+) 398 [({^{35}Cl}M+H)$^+$] 398.0, [({^{37}Cl}M+H)$^+$] 400.0. ^{1}H NMR (400 MHz, DMSO-*d6*) δ ppm 12.57 (br. s., 1 H) 8.65 (s, 1 H) 8.08 (d, 1 H) 7.42 (dd, 2.13 Hz, 1 H) 3.67 (br. s., 2 H) 0.98-1.60 (m, 12 H).

Synthetic procedure for the synthesis of 5-(8-(ethylamino)-6-fluoro-4-(3-(trifluoromethyl)-1H-pyrazol-1-yl)-9H-pyrido[2,3-b]indol-3-yl)nicotinic acid (10a).

Step (a). Preparation of methyl 5-[8-(ethylamino)-6-fluoro-4-[3-(trifluoromethyl)pyrazol-1-yl]-9H-pyrido[2,3-b]indol-3-yl]pyridine-3-carboxylate. To a stirred solution of *tert*-butyl N-[3-chloro-6-fluoro-4-[3-(trifluoromethyl)pyrazol-1-yl]-9H-pyrido[2,3-b]indol-8-yl]-N-ethyl-carbamate (**Intermediate 8**, 70 mg, 141 μmol) and methyl 5-(4,4,5,5-tetramethyl-1,3,2-dioxaborolan-2-yl)nicotinate (74 mg, 281 μmol) in 1,4-dioxane (4 mL) and H_2O (1.33 mL) was added dicyclohexyl(2',4',6'-triisopropyl-[1,1'-biphenyl]-2-yl)phosphine (13.4 mg, 28.1 μmol), potassium phosphate (89.5 mg, 422 μmol) and Pd_2dba_3 (12.9 mg, 14.1 μmol). The resulting mixture solution was heated at 110 ^{o}C for 4 h under N_2. The mixture was then cooled down to room temperature and evaporated to dryness under the reduced pressure. The residue was partitioned between EtOAc and water, and the separated organic layer was dried over anhy. Na_2SO_4, filtered, and concentrated *in vacuo*. The residue was re-dissolved in DCM (5 mL) and added TFA (0.5 mL) and stirred at room temperature for 2 h. After the mixture was concentrated under the reduced pressure, the residue was subject to prep-HPLC purification to afford the title compound (40 mg, 57% yield) as a while solid. MS obsd (ESI+) [(M+H)$^+$] 499.4.

Step (b). Preparation of 5-(8-(ethylamino)-6-fluoro-4-(3-(trifluoromethyl)-1H-pyrazol-1-yl)-9H-pyrido[2,3-b]indol-3-yl)nicotinic acid. To a solution of methyl 5-(8-(ethylamino)-6-fluoro-4-(3-(trifluoromethyl)-1H-pyrazol-1-yl)-9H-pyrido[2,3-b]indol-3-yl)nicotinate (40 mg, 80.3 μmol) in CH_3CN (4 mL) was added aqueous NaOH solution (1N, 1 mL). The reaction mixture was stirred at room temperature for 3 h before it was concentrated *in vacuo* to give a crude product, which was purified by prep-HPLC to afford the title compound (7 mg, 18% yield) as a white solid. MS obsd (ESI+) 485.4. HRMS calcd [(M+H)$^+$] 485.1349, measured [(M+H)$^+$] 485.1349. ^{1}H NMR (400 MHz, MeOH-*d*4) δ

ppm 8.94 (brs, 1H), 8.55 (s, 1H), 8.48 (brd, 1H), 8.04 (s, 1H), 7.85 (d, 1H), 6.78 (d, 1H), 6.37 (dd, 1H), 5.82 (dd, 1H), 2.66-2.99 (m, 2H), 0.91-1.37 (m, 3H).

Synthetic procedure for the synthesis of 5-[8-(ethylamino)-6-fluoro-4-[3-(trifluoromethyl)pyrazol-1-yl]-9H-pyrido[2,3-b]indol-3-yl]pyridine-3-carbonitrile (10d).

***tert*-Butyl N-[3-chloro-6-fluoro-4-[3-(trifluoromethyl)pyrazol-1-yl]-9H-pyrido[2,3-b]indol-8-yl]-N-ethyl-carbamate (8).** To a solution of *tert*-butyl N-(3,4-dichloro-6-fluoro-9H-pyrido[2,3-b]indol-8-yl)-N-ethyl-carbamate (Intermediate **7**, 80 mg, 0.2 mmol) in DMSO (1 mL) was added 3-(trifluoromethyl)pyrazole (54.4 mg, 0.4 mmol) and K_2CO_3 (82.9 mg, 0.6 mmol). The resulting mixture was stirred at 120 ^oC for 12 h. The reaction mixture was then cooled back to room temperature, filtered through a thin Celite pad, and concentrated *in vacuo*. The residue was purified by prep-HPLC to afford the title compound (85 mg, 86% yield) as a white solid. MS obsd (ESI+) [$(M+H)^+$] 498.2.

***tert*-Butyl N-[3-(5-cyano-3-pyridyl)-6-fluoro-4-[3-(trifluoromethyl)pyrazol-1-yl]-9H-pyrido[2,3-b]indol-8-yl]-N-ethyl-carbamate (9d).** A solution of *tert*-butyl N-[3-chloro-6-fluoro-4-[3-(trifluoromethyl)pyrazol-1-yl]-9H-pyrido[2,3-b]indol-8-yl]-N-ethyl-carbamate (Intermediate **8**, 60 mg, 0.12 mmol), 3-cyanopyridine-5-boronic acid pinacol ester (55.7 mg, 0.24 mmol), Pd_2dba_3 (21.9 mg, 0.024 mmol), Xantphos (11.4 mg, 0.024 mmol), and potassium phosphate tribasic (144.7 mg, 0.69 mmol) in 1,4-dioxane (4 mL) and water (0.4 mL) was stirred at 100 ^oC for 12 h under N_2 atmosphere. The mixture was cooled down to room temperature and poured into water (50 mL) and extracted with EtOAc (50 mL) three times. Combined organics were dried over anhy. Na_2SO_4, filtered, and concentrated *in vacuo*. The residue was purified by prep-TLC to afford the title compound (45.3 mg, 66% yield) as yellow oil. MS obsd (ESI+) [$(M+H)^+$] 566.3.

5-[8-(Ethylamino)-6-fluoro-4-[3-(trifluoromethyl)pyrazol-1-yl]-9H-pyrido[2,3-b]indol-3-yl]pyridine-3-carbonitrile (10d). To a solution of *tert*-butyl N-[3-(5-cyano-3-pyridyl)-6-fluoro-4-[3-(trifluoromethyl)pyrazol-1-yl]-9H-pyrido[2,3-b]indol-8-yl]-N-ethyl-carbamate (45 mg, 0.08 mmol) in DCM (3 mL) was added TFA (2 mL) at 10 ^oC. Then the solution was stirred at room temperature for 2

h before it was concentrated *in vacuo*. The residue was purified by prep-HPLC to afford the title compound (30 mg, 81% yield) as a yellow solid. MS obsd (ESI+) [(M+H)$^+$] 466.1. HRMS calcd [(M+H)$^+$] 466.1403, measured [(M+H)$^+$] 466.1407. ^{1}H NMR (400MHz, DMSO-*d6*) δ ppm 12.192 (s, 1H), 8.977-8.982 (d, 1H), 8.799 (s, 2H), 8.763 (s, 1H), 8.572-8.577 (d, 1H), 8.329 (s, 1H), 8.115 (s, 1H), 7.129-7.135 (d, 1H), 6.480-6.510 (m, 1H), 5.915 (m, 1H), 5.794-5.817 (m, 1H), 3.237-3.283 (m, 2H), 1.297-1.332 (s, 3H). ^{13}C NMR (126 MHz, DMSO-*d6*) δ ppm 160.1, 158.2, 153.1, 153.0, 151.5, 148.3, 143.6, 143.3, 140.2, 138.3, 136.9, 136.8, 136.2, 131.8, 125.1, 122.7, 120.8, 120.5, 117.0, 116.9, 116.8, 111.8, 109.3, 106.7, 95.6, 93.5, 38.1, 14.5.

The following compounds were prepared by a similar procedure to that described for compound **10d**.

5-(8-(Ethylamino)-6-fluoro-4-(3-(trifluoromethyl)-1H-pyrazol-1-yl)-9H-pyrido[2,3-b]indol-3-yl)nicotinamide (10b). MS obsd (ESI+) [(M+H)$^+$] 484.2. HRMS calcd [(M+H)$^+$] 484.1509, measured [(M+H)$^+$] 484.1510. ^{1}H NMR (400 MHz, DMSO-*d6*) δ ppm 12.13 (s, 1H), 8.95 (d, 1H), 8.70-8.79 (m, 1H), 8.42 (d, 1H), 8.27 (d, 1H), 8.15 (s, 1H), 8.08 (m, 1H), 7.63 (br. s., 1H), 7.08 (d, 1H), 6.50 (m, 1H), 5.89 (br. s., 1H), 5.76 (m, 1H), 3.27 (m, 2H), 1.31-1.36 (m, 3H). ^{13}C NMR (101 MHz, DMSO-*d6*) δ ppm δ ppm 166.40, 157.94, 153.96, 152.92, 151.50, 148.39, 147.95, 143.28, 138.25, 136.82, 136.70, 135.92, 131.05, 129.89, 125.10, 122.07, 116.93, 112.06, 106.62, 95.54, 93.39, 38.09, 14.53.

5-(8-(Ethylamino)-6-fluoro-4-(3-(trifluoromethyl)-1H-pyrazol-1-yl)-9H-pyrido[2,3-b]indol-3-yl)-N-methylnicotinamide (10c). MS obsd (ESI+) [(M+H)$^+$] 498.1. ^{1}H NMR (400 MHz, MeOH-*d4*) δ ppm 8.78 (d, 1H), 8.56 (s, 1H), 8.31 (d, 1H), 8.04 (m, 1H), 7.87 (d, 1H), 6.79 (d, 1H), 6.39 (m, 1H), 5.79-5.86 (m, 1H), 3.15-3.20 (m, 2H), 2.84 (s, 3H), 1.26-1.35 (t, 3H). ^{13}C NMR (101 MHz, DMSO-*d6*) δ ppm 165.16, 157.95, 152.92, 151.30, 148.37, 147.52, 143.46, 138.23, 136.77, 135.93, 135.59, 131.07, 130.13, 125.10, 122.06, 116.93, 112.07, 106.64, 95.56, 93.92, 93.18, 38.09, 26.66, 14.52.

5-[8-(Ethylamino)-6-fluoro-4-[3-(trifluoromethyl)pyrazol-1-yl]-9H-pyrido[2,3-b]indol-3-yl]-N-methyl-pyridine-3-carboxamidine (10g). MS obsd (ESI+) [(M+H)$^+$] 497.1. HRMS calcd [(M+H)$^+$] 497.1825, measured [(M+H)$^+$] 497.1826. ^{1}H NMR (400 MHz, MeOH-*d*4) δ ppm 8.74 (br s, 1H), 8.65

(s, 1H), 8.48 (s, 1H), 8.20 (m, 2H), 6.95 (d, 1H), 6.52 (m, 1H), 5.78 (dd, 1H), 3.21 (m, 2H), 3.05 (s, 3H), 1.42 (m, 3H).

N-Ethyl-6-fluoro-3-(pyrimidin-5-yl)-4-(3-(trifluoromethyl)-1H-pyrazol-1-yl)-9H-pyrido[2,3-b]indol-8-amine (10h). MS obsd (ESI+) [(M+H)$^+$] 442.2. HRMS calcd [(M+H)$^+$] 442.1403, measured [(M+H)$^+$] 442.1404. ^{1}H NMR (400 MHz, DMSO-*d6*) δ ppm 12.18 (br. s., 1H), 9.14 (s, 1H), 8.78 (s, 1H), 8.60 (s, 2H), 8.37 (d, 1H), 7.14 (d, 1H), 6.51 (m, 1H), 5.90 (br. s., 1H), 5.78 (m, 1H), 3.22-3.29 (m, 2H), 1.33 (m, 3H).

3-(5-Aminopyridin-3-yl)-N-ethyl-6-fluoro-4-(3-(trifluoromethyl)-1H-pyrazol-1-yl)-9H-pyrido[2,3-b]indol-8-amine (10i). MS obsd (ESI+) [(M+H)$^+$] 456.1. HRMS calcd [(M+H)$^+$] 456.1560, measured [(M+H)$^+$] 456.1661. ^{1}H NMR (400 MHz, MeOH-*d4*) δ ppm 8.62 (s, 1H), 8.08 (d, 1H), 7.95 (br s, 1H), 7.63 (s, 1H), 7.32-7.45 (m, 1H), 6.99 (d, 1H), 6.50 (dd, 1H), 5.98 (dd, 1H), 3.34-3.47 (m, 2H), 1.42 (t, 3H). ^{13}C NMR (101 MHz, DMSO-*d6*) δ ppm 159.1, 153.0, 148.0, 146.7, 143.3, 138.2, 136.8, 136.0, 133.5, 131.8, 130.0, 125.1, 124.6, 121.6, 121.5, 116.9, 111.9, 106.6, 95.6, 93.5, 38.1, 14.5.

N-Ethyl-6-fluoro-3-(5-morpholinopyridin-3-yl)-4-(3-(trifluoromethyl)-1H-pyrazol-1-yl)-9H-pyrido[2,3-b]indol-8-amine (10j). MS obsd (ESI+) [(M+H)$^+$] 526.3. HRMS calcd [(M+H)$^+$] 526.1978, measured [(M+H)$^+$] 526.1980. ^{1}H NMR (400 MHz, MeOH-*d4*) δ ppm 8.59-8.70 (m, 1H), 8.21-8.36 (m, 1H), 7.89-8.06 (m, 2H), 7.20-7.37 (m, 1H), 6.96 (d, 1H), 6.50 (dd, 1H), 5.90 (dd, 1H), 3.75-3.87 (m, 4H), 3.03-3.24 (m, 4H), 2.84-3.02 (m, 2H), 1.27-1.49 (m, 3H). ^{13}C NMR (101 MHz, DMSO-*d6*) δ ppm 159.1, 152.7, 148.2, 146.8, 143.1, 138.9, 138.2, 136.7, 136.2, 135.9, 131.4, 125.0, 122.7, 122.1, 121.2, 116.9, 112.3, 106.6, 95.5, 93.4, 66.2, 47.8, 38.1, 14.5.

N-Ethyl-6-fluoro-3-(2-(piperazin-1-yl)pyridin-4-yl)-4-(3-(trifluoromethyl)-1H-pyrazol-1-yl)-9H-pyrido[2,3-b]indol-8-amine (10k). MS obsd (ESI+) [(M+H)$^+$] 525.5. HRMS calcd [(M+H)$^+$] 525.2138, measured [(M+H)$^+$] 525.2138. ^{1}H NMR (400 MHz, MeOH-*d*4) δ ppm 8.55 (s, 1H), 7.98-8.10 (m, 1H), 7.85 (dd, 1H), 6.86 (d, 1H), 6.58-6.69 (m, 2H), 6.40 (dd, 1H), 5.79 (dd, 1H), 3.56-3.74 (m, 4H), 3.12-3.23 (m, 6H), 1.32 (t, 3H).

3-(5-(Aminomethyl)pyridin-3-yl)-N-ethyl-6-fluoro-4-(3-(trifluoromethyl)-1H-pyrazol-1-yl)-9H-pyrido[2,3-b]indol-8-amine (10l). MS obsd (ESI+) [(M+H)$^+$] 470.4. HRMS calcd [(M+H)$^+$] 470.1716, measured [(M+H)$^+$] 470.1715. ^{1}H NMR (400 MHz, MeOH-*d4*) δ ppm 8.57-8.68 (m, 2H), 8.34 (d, 1H), 7.93-8.09 (m, 2H), 6.95 (d, 1H), 6.43-6.57 (m, 1H), 5.93 (dd, 1H), 4.23 (s, 2H), 3.21-3.24 (m, 2H), 1.33-1.50 (m, 3H).

(5-(8-(Ethylamino)-6-fluoro-4-(3-(trifluoromethyl)-1H-pyrazol-1-yl)-9H-pyrido[2,3-b]indol-3-yl)pyridin-3-yl)methanol (10m). MS obsd (ESI+) [(M+H)$^+$] 471.1. HRMS calcd [(M+H)$^+$] 471.1556, measured [(M+H)$^+$] 471.1556. ^{1}H NMR (400 MHz, MeOH-*d4*) δ ppm 8.64 (s, 1H), 8.55 (s, 1H), 8.31 (s, 1H), 7.98 (d, 1H), 7.82 (s, 1H), 6.92 (d, 1H), 6.49 (dd, 1H), 5.93 (dd, 1H), 4.68 (s, 2H), 3.34-3.45 (m, 2H), 1.42 (t, 3H). ^{13}C NMR (101 MHz, DMSO-*d6*) δ ppm 159.1, 152.8, 148.2, 147.5, 147.0, 143.2, 138.2, 138.0, 136.7, 135.9, 135.3, 131.0, 125.1, 122.6, 121.7, 116.9, 112.2, 106.5, 95.5, 93.5, 60.8, 38.1, 14.5.

N-Ethyl-6-fluoro-3-[5-(oxazol-2-ylmethyl)-3-pyridyl]-4-[3-(trifluoromethyl)pyrazol-1-yl]-9H-pyrido[2,3-b]indol-8-amine (10q). MS obsd (ESI+) [(M+H)$^+$] 522.0. HRMS calcd [(M+H)$^+$] 522.1665, measured [(M+H)$^+$] 522.1666. ^{1}H NMR (400MHz, DMSO-*d6*) δ ppm 12.2 (s, 1H), 8.68 (s, 1H), 8.46 (s, 1H), 8.35 (s, 1H), 8.20 (s, 1H), 7.99 (s, 1H), 7.42 (s, 1H),7.12 (s, 1H), 7.01 (s, 1H), 6.46 (d, 1H), 5.95 (s, 1H), 5.68 (d, 1H), 4.12 (s, 2H), 3.20 (m, 2H), 1.31 (t, 3H).

N-Ethyl-6-fluoro-3-(pyrazolo[1,5-a]pyrimidin-6-yl)-4-(3-(trifluoromethyl)-1H-pyrazol-1-yl)-9H-pyrido[2,3-b]indol-8-amine (10t). MS obsd (ESI+) [(M+H)$^+$] 481.3. HRMS calcd [(M+H)$^+$] 481.1512, measured [(M+H)$^+$] 481.1512. ^{1}H NMR (400 MHz, DMSO-*d6*) δ ppm 12.16 (s, 1H), 9.15 (d, 1H), 8.84 (s, 1H), 8.40 (d, 1H), 8.28 (d, 1H), 8.10 (d, 1H), 7.13 (d, 1H), 6.76 (d, 1H), 6.51 (m, 1H), 5.90 (br. s., 1H), 5.81 (m, 1H), 3.22-3.31 (m, 2H), 1.30-1.37 (t, 3H). ^{13}C NMR (126 MHz, DMSO-*d6*) δ ppm 160.0, 158.2, 153.0, 150.0, 148.8, 147.1, 146.0, 138.5, 136.8, 136.7, 136.2, 135.1, 125.1, 119.0, 116.9, 116.8, 112.0, 106.8, 96.8, 95.5, 93.5, 38.1, 14.5.

N-Ethyl-6-fluoro-3-(2-methylpyrimidin-5-yl)-4-(3-(trifluoromethyl)-1H-pyrazol-1-yl)-9H-pyrido[2,3-b]indol-8-amine (12a). MS obsd (ESI+) [(M+H)$^+$] 456.2. HRMS calcd [(M+H)$^+$]

456.1560, measured [(M+H)$^+$] 456.1661. ^{1}H NMR (400 MHz, DMSO-*d6*) δ ppm 12.15 (s, 1H), 8.75 (s, 1H), 8.48 (s, 2H), 8.33 (s, 1H), 7.14 (d, 1H), 6.44-6.54 (m, 1H), 5.88 (br s, 1H), 5.73 (dd, 1H), 3.22-3.30 (m, 2H), 2.62 (s, 3H), 1.32 (t, 3H). ^{13}C NMR (126 MHz, DMSO-*d6*) δ ppm 166.7, 160.0, 158.2, 156.6, 153.0, 148.2, 143.5, 143.2, 138.2, 136.8, 136.7, 136.0, 126.5, 125.1, 122.7, 120.6, 119.6, 116.9, 116.8, 112.1, 106.8, 95.6, 93.4, 38.1, 25.8, 14.5.

(*S*)-1-(5-(8-(Ethylamino)-6-fluoro-4-(3-(trifluoromethyl)-1H-pyrazol-1-yl)-9H-pyrido[2,3-b]indol-3-yl)pyrimidin-2-yl)ethanol (12b). MS obsd (ESI+) [(M+H)$^+$] 486.2. HRMS calcd [(M+H)$^+$] 486.1665, measured [(M+H)$^+$] 486.1665. ^{1}H NMR (400 MHz, MeOH-*d*4,) δ ppm 8.6-8.7 (m, 1H), 8.6-8.6 (m, 2H), 8.0-8.1 (m, 1H), 6.9-7.0 (m, 1H), 6.4-6.5 (m, 1H), 5.9-5.9 (m, 1H), 4.94 (q, 1H), 3.2-3.3 (m, 2H), 1.5-1.5 (m, 3H), 1.4-1.4 (m, 3H). ^{13}C NMR (101 MHz, DMSO-*d6*) δ ppm 171.4, 159.1, 156.6, 153.1, 148.3, 143.4, 138.3, 136.8, 136.1, 127.6, 125.1, 123.0, 120.3, 119.5, 116.8, 112.2, 106.8, 95.6, 93.4, 70.1, 38.1, 23.2, 14.5.

(*R*)-1-(5-(8-(Ethylamino)-6-fluoro-4-(3-(trifluoromethyl)-1H-pyrazol-1-yl)-9H-pyrido[2,3-b]indol-3-yl)pyrimidin-2-yl)ethanol (12c). MS obsd (ESI+) [(M+H)$^+$] 486.2. HRMS calcd [(M+H)$^+$] 486.1665, measured [(M+H)$^+$] 486.1665. ^{1}H NMR (400 MHz, MeOH-*d*4) δ ppm 8.6-8.7 (m, 1H), 8.61 (s, 2H), 8.1-8.1 (m, 1H), 6.9-7.0 (m, 1H), 6.5-6.5 (m, 1H), 5.9-6.0 (m, 1H), 4.95 (q, 1H), 3.3-3.3 (m, 2H), 1.5-1.5 (m, 3H), 1.4-1.5 (m, 3H). ^{13}C NMR (101 MHz, DMSO-*d6*) δ ppm 171.4, 160.3, 158.0, 156.6, 153.1, 148.3, 143.4, 138.3, 136.8, 136.1, 127.6, 125.1, 119.5, 121.9, 116.8, 112.2, 106.8, 95.6, 93.4, 70.1, 38.1, 23.2, 14.5.

2-(5-(8-(Ethylamino)-6-fluoro-4-(3-(trifluoromethyl)-1H-pyrazol-1-yl)-9H-pyrido[2,3-b]indol-3-yl)pyrimidin-2-yl)propan-2-ol (12d). MS obsd (ESI+) [(M+H)$^+$] 500.3. HRMS calcd [(M+H)$^+$] 500.1822, measured [(M+H)$^+$] 500.1824. ^{1}H NMR (400 MHz, MeOH-*d4*) δ ppm 8.66 (s, 1H), 8.60 (s, 2H), 8.10 (d, 1H), 6.97 (d, 1H), 6.51 (m, 1H), 5.96 (m, 1H), 1.60 (s, 6H), 1.43 (t, 3H). ^{13}C NMR (101 MHz, DMSO-*d6*) δ ppm 173.5, 160.3, 158.0, 156.3, 153.1, 148.3, 143.6, 138.3, 136.7, 136.1, 127.2, 125.1, 123.0, 120.3, 119.4, 116.9, 116.8, 112.0, 106.8, 95.6, 93.4, 73.1, 38.1, 30.1, 14.5.

5-(8-(Ethylamino)-6-fluoro-4-(3-(trifluoromethyl)-1H-pyrazol-1-yl)-9H-pyrido[2,3-b]indol-3-yl)pyrimidine-2-carboxamide (12h). MS obsd (ESI+) [(M+H)$^+$] 485.2. HRMS calcd [(M+H)$^+$] 485.1461, measured [(M+H)$^+$] 485.1463. ^{1}H NMR (400 MHz, MeOH-*d4*) δ ppm 8.7-8.8 (m, 3H), 8.0-8.1 (m, 1H), 6.9-7.0 (m, 1H), 6.5-6.6 (m, 1H), 5.9-6.0 (m, 1H), 3.3-3.3 (m, 2H), 1.3-1.5 (m, 3H). ^{13}C NMR (101 MHz, MeOH-*d4*) δ ppm -1.46, 13.12, 29.52, 37.84, 93.91, 94.11, 95.86, 96.11, 105.99, 112.66, 112.69, 117.06, 118.43, 125.05, 131.34, 134.78, 136.22, 136.31, 138.37, 146.90, 153.32, 156.63, 156.76, 158.59, 160.45, 165.29.

N-Ethyl-6-fluoro-3-(2-methoxypyrimidin-5-yl)-4-[3-(trifluoromethyl)pyrazol-1-yl]-9H-pyrido[2,3-b]indol-8-amine (12j). MS obsd (ESI+) [(M+H)$^+$] 472.2. HRMS calcd [(M+H)$^+$] 472.1509, measured [(M+H)$^+$] 472.1509. ^{1}H NMR (400 MHz, DMSO-*d6*) δ ppm 8.70 (s, 1H), 8.38 (s, 2H), 8.29 (s, 1H), 7.10 (s, 1H), 6.46 (m, 1H), 5.72 (m, 1H), 3.92 (s, 3H), 3.24 (m, 2H), 1.32 (m, 3H). ^{13}C NMR (101 MHz, DMSO-*d6*) δ ppm 164.7, 159.1, 159.1, 152.9, 148.1, 143.3, 138.2, 136.7, 136.0, 125.1, 123.3, 119.4, 121.8, 116.8, 112.1, 106.7, 106.7, 95.5, 93.4, 55.2, 38.1, 14.5.

3-(2-Ethoxypyrimidin-5-yl)-N-ethyl-6-fluoro-4-(3-(trifluoromethyl)-1H-pyrazol-1-yl)-9H-pyrido[2,3-b]indol-8-amine (12k). MS obsd (ESI+) [(M+H)$^+$] 486.5. ^{1}H NMR (400 MHz, MeOH-*d4*) δ ppm 8.50 (s, 1H), 8.26 (s, 2H), 7.94 (d, 1H), 6.85 (d, 1H), 6.38 (m, 1H), 5.79 (m, 1H), 4.34 (m, 2H), 3.21 (d, 2H), 1.26-1.35 (m, 6H).

3-(2-(Azetidin-3-yloxy)pyrimidin-5-yl)-N-ethyl-6-fluoro-4-(3-(trifluoromethyl)-1H-pyrazol-1-yl)-9H-pyrido[2,3-b]indol-8-amine (12l). MS obsd (ESI+) [(M+H)$^+$] 513.2. HRMS calcd [(M+H)$^+$] 513.1774, measured [(M+H)$^+$] 513.1774. ^{1}H NMR (400 MHz, MeOH-*d4*) δ ppm 8.61 (s, 1H), 8.38 (s, 2H), 8.07 (s, 1H), 6.97 (s, 1H), 6.51 (m, 1H), 5.90 (m, 1H), 5.50 (m, 1H), 4.00 (m, 2H), 3.75 (m, 2H), 3.51 (m, 1H), 3.31 (m, 2H), 1.42 (m, 3H). ^{13}C NMR (126 MHz, DMSO-*d6*) δ ppm 163.4, 160.0, 159.2, 158.2, 152.9, 148.1, 143.5, 143.2, 138.2, 136.8, 136.7, 136.1, 125.1, 123.7, 122.7, 120.6, 119.4, 116.8, 116.7, 112.0, 112.0, 106.7, 95.5, 93.4, 70.7, 53.8, 38.1, 14.5.

N-Ethyl-6-fluoro-3-(2-(pyrrolidin-3-yloxy)pyrimidin-5-yl)-4-(3-(trifluoromethyl)-1H-pyrazol-1-yl)-9H-pyrido[2,3-b]indol-8-amine (12m). MS obsd (ESI+) [(M+H)$^+$] 527.3. HRMS calcd [(M+H)$^+$]

527.1931, measured [(M+H)$^+$] 527.1931. ^{1}H NMR (400 MHz, MeOH-*d4*) δ ppm 8.51 (s, 1H), 8.33 (s, 2H), 7.98 (s, 1H), 6.86 (s, 1H), 6.40 (m, 1H), 5.80 (m, 1H), 5.60 (s, 1H), 3.40 (m, 2H), 3.31 (m, 2H), 3.20 (m, 2H), 2.20 (m, 3H), 1.32 (m, 3H). ^{13}C NMR (126 MHz, DMSO-*d6*) δ ppm 163.3, 160.0, 159.3, 158.2, 152.9, 148.1, 143.5, 143.2, 138.2, 136.8, 136.7, 136.1, 125.1, 124.0, 122.7, 119.2, 116.8, 116.7, 112.1, 106.7, 95.5, 93.3, 76.2, 50.8, 44.3, 38.1, 31.1, 14.5.

N-Ethyl-6-fluoro-3-(2-(piperidin-4-yloxy)pyrimidin-5-yl)-4-(3-(trifluoromethyl)-1H-pyrazol-1-yl)-9H-pyrido[2,3-b]indol-8-amine (12n). MS obsd (ESI+) [(M+H)$^+$] 541.3. HRMS calcd [(M+H)$^+$] 541.2087, measured [(M+H)$^+$] 541.2090. ^{1}H NMR (400 MHz, MeOH-*d4*) δ ppmppm 8.5-8.5 (m, 1H), 8.3-8.3 (m, 2H), 8.0-8.0 (m, 1H), 7.2-7.3 (m, 1H), 6.8-6.9 (m, 1H), 6.4-6.4 (m, 1H), 5.8-5.8 (m, 1H), 5.2-5.3 (m, 1H), 3.3-3.3 (m, 1H), 3.1-3.1 (m, 1H), 3.0-3.0 (m, 1H), 2.1-2.2 (m, 2H), 1.9-2.0 (m, 3H), 1.7-1.9 (m, 1H), 1.3-1.3 (m, 3H).

3-(2-Aminopyrimidin-5-yl)-N-ethyl-6-fluoro-4-(3-(trifluoromethyl)-1H-pyrazol-1-yl)-9H-pyrido[2,3-b]indol-8-amine (12p). MS obsd (ESI+) [(M+H)$^+$] 457.2. HRMS calcd [(M+H)$^+$] 457.1512, measured [(M+H)$^+$] 457.1513. ^{1}H NMR (400 MHz, DMSO-*d6*) δ ppm 12.01 (s, 1H), 8.66 (s, 1H), 8.30 (d, 1H), 8.01 (s, 2H), 7.13 (d, 1H), 6.80 (s, 2H), 6.47 (m, 1H), 5.86 (m, 1H), 5.67 (m, 1H), 3.22-3.28 (m, 2H), 1.32 (m, 3H). ^{13}C NMR (126 MHz, DMSO-*d6*) δ ppm 163.1, 159.9, 158.1, 157.6, 152.4, 147.9, 142.9, 137.8, 136.7, 136.6, 135.8, 125.0, 122.8, 121.0, 120.7, 117.5, 116.9, 116.8, 112.3, 106.6, 95.3, 93.3, 38.1, 14.5,

N-Ethyl-6-fluoro-3-(2-(methylamino)pyrimidin-5-yl)-4-(3-(trifluoromethyl)-1H-pyrazol-1-yl)-9H-pyrido[2,3-b]indol-8-amine (12q). MS obsd (ESI+) [(M+H)$^+$] 471.3. HRMS calcd [(M+H)$^+$] 471.1669, measured [(M+H)$^+$] 471.1669. ^{1}H NMR (400 MHz, DMSO-*d6*) δ ppm 12.03 (s, 1H), 8.66 (s, 1H), 8.31 (s, 1H), 7.22 (br. s., 1H), 7.14 (d, 1H), 6.68 (br. s., 1H), 6.47 (m, 1H), 5.86 (br. s., 1H), 5.66 (m, 1H), 5.33 (m, 1H), 3.19-3.29 (m, 2H), 2.74 (d., 3H), 1.29-1.35 (t, 3H).

3-(2-(Azetidin-3-ylamino)pyrimidin-5-yl)-N-ethyl-6-fluoro-4-(3-(trifluoromethyl)-1H-pyrazol-1-yl)-9H-pyrido[2,3-b]indol-8-amine (12r). MS obsd (ESI+) [(M+H)$^+$] 512.1. HRMS calcd [(M+H)$^+$] 512.1934, measured [(M+H)$^+$] 512.1937. ^{1}H NMR (400 MHz, MeOH-*d*4) δ ppm 8.548 (s, 1 H), 8.119

(s, 2 H), 8.017(s, 1 H), 6.961-6.966 (d, 1 H), 6.462-6.489 (d, 1 H), 5.847-5.874 (d, 1 H), 3.879-3.974 (m, 2 H), 3.699-3.770 (m, 2 H), 3.369 (m, 1 H), 3.281-3.368 (m, 2 H), 1.399-1.435 (m, 3 H).

N-Ethyl-6-fluoro-3-[2-(pyrrolidin-3-ylamino)pyrimidin-5-yl]-4-[3-(trifluoromethyl)pyrazol-1-yl]-9H-pyrido[2,3-b]indol-8-amine (12s). MS obsd (ESI+) [(M+H)$^+$] 526.2. HRMS calcd [(M+H)$^+$] 526.2091, measured [(M+H)$^+$] 526.2093. ^{1}H NMR (400 MHz, MeOH-*d4*) δ ppm 8.54 (s, 1H), 8.17 (s, 2H), 8.02 (s, 1H), 6.96 (s, 1H),6.47 (d, 1H), 5.86 (d, 1H), 4.59 (m, 1H), 3.57 (m, 2H), 3.01 (m, 1H), 2.88 (m, 1H), 2.41 (m, 1H), 2.25 (m, 1H), 1.40-1.43 (m, 5H).

N-Ethyl-6-fluoro-3-(2-(piperidin-4-ylamino)pyrimidin-5-yl)-4-(3-(trifluoromethyl)-1H-pyrazol-1-yl)-9H-pyrido[2,3-b]indol-8-amine (12t). MS obsd (ESI+) [(M+H)$^+$] 540.3. HRMS calcd [(M+H)$^+$] 540.2247, measured [(M+H)$^+$] 540.2247. ^{1}H NMR (400 MHz, DMSO-*d6*) δ ppm 12.05 (br. s., 1H), 8.66 (s, 1H), 8.34 (d, 1H), 8.06 (br. s., 1H), 7.42 (d, 1H), 7.15 (d, 1H), 6.47 (m, 1H), 5.87 (br. s., 1H), 5.66 (m, 1H), 5.27-5.36 (m, 1H), 3.25 (br. s., 2H), 3.10 (br. s., 1H), 2.65-2.76 (m, 2H), 1.97-2.06 (m, 2H), 1.87 (d, 2H), 1.46 (d, 2H), 1.27-1.34 (m, 3H). ^{13}C NMR (101 MHz, DMSO-*d6*) δ ppm 161.0, 160.2, 157.8, 157.5, 152.4, 147.9, 143.3, 142.9, 137.8, 136.7, 135.8, 125.0, 123.1, 120.9, 120.5, 117.1, 116.8, 112.3, 106.6, 95.3, 93.3, 48.8, 45.6, 38.1, 33.4, 14.5.

N-Ethyl-6-fluoro-3-(2-(piperazin-1-yl)pyrimidin-5-yl)-4-(3-(trifluoromethyl)-1H-pyrazol-1-yl)-9H-pyrido[2,3-b]indol-8-amine (12u). MS obsd (ESI+) [(M+H)$^+$] 526.4. HRMS calcd [(M+H)$^+$] 526.2091, measured [(M+H)$^+$] 526.2092. ^{1}H NMR (400 MHz, DMSO-*d6*) δ ppm 8.6-8.7 (m, 1H), 8.3-8.4 (m, 1H), 8.13 (s, 1H), 7.6-7.7 (m, 1H), 7.16 (d, 1H), 6.4-6.5 (m, 1H), 5.8-5.9 (m, 1H), 5.6-5.7 (m, 1H), 5.3-5.4 (m, 1H), 3.6-3.7 (m, 2H), 3.2-3.3 (m, 2H), 2.7-2.8 (m, 2H), 1.9-2.1 (m, 2H), 1.6-1.7 (m, 1H), 1.4-1.5 (m, 1H), 1.3-1.3 (m, 3H).

N-Ethyl-6-fluoro-3-(2-morpholinopyrimidin-5-yl)-4-(3-(trifluoromethyl)-1H-pyrazol-1-yl)-9H-pyrido[2,3-b]indol-8-amine (12v). MS obsd (ESI+) [(M+H)$^+$] 527.4. HRMS calcd [(M+H)$^+$] 527.1931, measured [(M+H)$^+$] 527.1932. ^{1}H NMR (400 MHz, DMSO-*d6*) δ ppm 12.06 (br. s., 1H), 8.67 (s, 1H), 8.33 (d, 1H), 8.18 (s, 2H), 7.17 (d, 1H), 6.47 (m, 1H), 5.86 (br. s., 1H), 5.65 (m, 1H), 3.53-3.74 (m, 6H), 3.14-3.30 (m, 2H), 1.96-2.05 (m, 2H), 1.32 (m, 3H).

5-[4-(3-Cyanopyrazol-1-yl)-8-(ethylamino)-6-fluoro-9H-pyrido[2,3-b]indol-3-yl]pyridine-3-carbonitrile (15a). MS obsd (ESI+) [(M+H)$^+$] 423.2. HRMS calcd [(M+H)$^+$] 423.1482, measured [(M+H)$^+$] 423.1482. ^{1}H NMR (400 MHz, DMSO-*d6*) δ ppm 12.22 (s, 1H), 9.01 (d, 1H), 8.77 (s, 1H), 8.56 (d, 1H), 8.43 (d, 1H), 8.21 (s, 1H), 7.37 (d, 1H), 6.52 (m, 1H), 5.76 (m, 1H), 3.27 (q, 2H), 1.33 (t, 3H).

5-[4-(3-Aminopyrazol-1-yl)-8-(ethylamino)-6-fluoro-9H-pyrido[2,3-b]indol-3-yl]pyridine-3-carbonitrile (15c). MS obsd (ESI+) [(M+H)$^+$] 413.2. HRMS calcd [(M+H)$^+$] 413.1638, measured [(M+H)$^+$] 413.1636. ^{1}H NMR (400 MHz, DMSO-*d*6) δ ppm 11.97 (s, 1 H), 8.96 (d, 1 H), 8.66 (s, 1 H), 8.53 (d, 1 H), 8.10 (t, 1 H), 7.58 (d, 1 H), 6.35-6.55 (m, 2 H), 5.91 (d, 1 H), 3.25 (q, 2 H), 1.32 (t, 3 H). ^{13}C NMR (101 MHz, DMSO-*d6*) δ ppm 158.6, 158.3, 153.4, 153.0, 151.0, 148.5, 140.1, 139.7, 136.3, 134.1, 133.0, 124.6, 120.3, 117.9, 117.4, 109.3, 96.9, 95.3, 38.1, 14.6.

5-[8-(Ethylamino)-6-fluoro-4-(3-methylpyrazol-1-yl)-9H-pyrido[2,3-b]indol-3-yl]pyridine-3-carbonitrile (15e). MS obsd (ESI+) [(M+H)$^+$] 412.1. ^{1}H NMR (400 MHz, MeOH-*d*4) δ ppm 8.936 (s, 1 H), 8.691 (s, 1 H), 8.505 (s, 1 H), 8.066 (s, 1 H), 7.823 (s, 1 H), 6.454-6.482 (d, 1 H), 6.397 (s, 1 H), 6.040-6.063 (d, 1 H), 5.860 (s, 3 H), 3.230-3.276 (m, 2 H), 2.281 (s, 1 H), 1.295-1.331 (t, 3 H).

5-[8-(Ethylamino)-4-(3-ethylpyrazol-1-yl)-6-fluoro-9H-pyrido[2,3-b]indol-3-yl]pyridine-3-carbonitrile (15f). MS obsd (ESI+) [(M+H)$^+$] 426.1. HRMS calcd [(M+H)$^+$] 426.1842, measured [(M+H)$^+$] 426.1843. ^{1}H NMR (400 MHz, DMSO-*d6*) δ ppm 12.01 (s, 1H), 8.94 (d, 1H), 8.71 (s, 1H), 8.56 (d, 1H), 7.97 (t, 1H), 7.83 (d, 1H), 6.43-6.49 (m, 2H), 6.10 (m, 1H), 5.84 (br. s, 1H), 3.26 (q, 2H), 2.64 (m, 2H), 1.32 (t, 3H), 1.19 (t, 3H). ^{13}C NMR (126 MHz, DMSO-*d6*) δ ppm 159.9, 158.2, 156.5, 153.3, 153.0, 151.0, 148.3, 139.8, 139.8, 136.5, 133.9, 132.6, 124.8, 120.6, 117.6, 117.2, 112.1, 109.2, 106.6, 95.4, 94.4, 38.1, 21.4, 14.6, 14.6.

5-[8-(Ethylamino)-6-fluoro-4-(3-isopropylpyrazol-1-yl)-9H-pyrido[2,3-b]indol-3-yl]pyridine-3-carbonitrile (15g). MS obsd (ESI+) [(M+H)$^+$] 538.2. HRMS calcd [(M+H)$^+$] 440.1999, measured [(M+H)$^+$] 440.2001. ^{1}H NMR (400 MHz, DMSO-*d*6) δ ppm 12.01 (s, 1 H) 8.94 (d, 1 H) 8.71 (s, 1 H) 8.59 (d, 1 H) 7.77-7.92 (m, 2 H) 6.40-6.50 (m, 2 H) 6.11 (dd, 1 H) 5.84 (br. s., 1 H) 3.20-3.28 (m, 2 H) 2.94-3.05 (m, 1 H) 1.32 (t, 3 H) 1.23 (d, 6 H). ^{13}C NMR (126 MHz, DMSO-*d6*) δ ppm 160.9, 159.9,

158.1, 153.3, 153.0, 151.0, 148.2, 139.8, 139.7, 136.6, 136.5, 133.7, 132.6, 124.8, 120.6, 117.6, 117.5, 117.2, 112.1, 112.1, 109.2, 105.3, 95.3, 94.4, 38.1, 27.8, 23.1, 14.5.

5-[4-(3-*tert*-Butylpyrazol-1-yl)-8-(ethylamino)-6-fluoro-9H-pyrido[2,3-b]indol-3-yl]pyridine-3-carbonitrile (15h). MS obsd (ESI+) [(M+H)$^+$] 454.3. HRMS calcd [(M+H)$^+$] 454.2155, measured [(M+H)$^+$] 454.2155. ^{1}H NMR (400 MHz, DMSO-*d6*) δ ppm 12.01 (s, 1 H), 8.93 (s, 1 H), 8.70 (s, 1 H), 8.60 (d, 1 H), 7.77-7.82 (m, 2 H), 6.42-6.50 (m, 2 H), 6.14 (d, 1 H), 5.84 (br. s., 1 H), 3.20-3.28 (m, 2 H), 1.25-1.34 (m, 12 H).

5-[8-(Ethylamino)-6-fluoro-4-(3-fluoropyrazol-1-yl)-9H-pyrido[2,3-b]indol-3-yl]pyridine-3-carbonitrile (15i). MS obsd (ESI+) [(M+H)$^+$] 448.3. HRMS calcd [(M+H)$^+$] 448.1498, measured [(M+H)$^+$] 448.1498. ^{1}H NMR (400 MHz, MeOH-*d4*) δ ppm 8.84 (d, 1H), 8.64 (s, 1H), 8.58 (d, 1H), 8.02 (m, 1H), 7.96 (d, 1H), 6.83 (d, 1H), 6.49 (m, 1H), 5.99 (m, 1H), 5.17 (s, 1H), 4.58 (m, 2H), 1.41 (t, 3H). ^{13}C NMR (101 MHz, DMSO-*d6*) δ ppm 159.9, 157.6, 154.5, 151.8, 150.9, 147.2, 143.2, 141.3, 136.6, 136.4, 134.5, 133.4, 129.8, 124.7, 124.4, 119.4, 119.3, 118.3, 117.3, 114.8, 114.7, 113.2, 110.8, 109.0, 94.8, 93.8, 38.1, 14.6.

5-(8-(Ethylamino)-6-fluoro-4-(3-(trifluoromethyl)phenyl)-9H-pyrido[2,3-b]indol-3-yl)nicotinonitrile (15j). MS obsd (ESI+) [(M+H)$^+$] 476.0. HRMS calcd [(M+H)$^+$] 476.1498, measured [(M+H)$^+$] 476.1501. ^{1}H NMR (400 MHz, DMSO-*d6*) δ ppm 8.84 (d, 1H), 8.63-8.57 (m, 2H), 8.20-8.17 (m, 1H), 7.85 (br d, 1H), 7.78-7.67 (m, 3H), 6.42 (br d, 1H), 5.75 (dd, 1H), 3.25 (q, 2H), 1.38-1.29 (t, 3H). ^{13}C NMR (126 MHz, DMSO-*d6*) δ ppm 159.6, 157.8, 154.6, 151.8, 150.8, 147.4, 141.6, 141.4, 137.3, 134.3, 134.3, 129.9, 127.0, 125.7, 124.8, 123.3, 119.0, 119.1, 117.2, 113.8, 108.8, 94.8, 93.6, 38.1, 14.6.

5-[8-(Ethylamino)-6-fluoro-4-[4-(trifluoromethyl)imidazol-1-yl]-9H-pyrido[2,3-b]indol-3-yl]pyridine-3-carbonitrile (15k). MS obsd (ESI+) [(M+H)$^+$] 466.2. HRMS calcd [(M+H)$^+$] 466.1403, measured [(M+H)$^+$] 466.1403. ^{1}H NMR (400 MHz, DMSO-*d6*) δ ppm 12.19 (s, 1 H) 9.02 (d, 1 H) 8.68-8.78 (m, 2 H) 8.32 (s, 1 H) 8.18-8.27 (m, 2 H) 6.52 (dd, 1 H) 5.69 (dd, 1 H) 3.26 (q, 2 H) 1.32 (t, 3 H). ^{13}C NMR (101 MHz, DMSO-*d6*) δ ppm 160.4, 158.1, 151.8, 148.2, 140.5, 140.3, 137.0, 136.9,

135.5, 131.4, 125.0, 123.5, 122.7, 121.3, 120.8, 117.0, 116.9, 116.8, 112.1, 109.2, 109.3, 95.6, 92.7, 38.1, 14.5.

5-[8-(Ethylamino)-6-fluoro-4-[4-(trifluoromethyl)pyrazol-1-yl]-9H-pyrido[2,3-b]indol-3-yl]pyridine-3-carbonitrile (15l). MS obsd (ESI+) [(M+H)$^+$] 466.1. HRMS calcd [(M+H)$^+$] 466.1403, measured [(M+H)$^+$] 466.1404. ^{1}H NMR (400 MHz, DMSO-*d6*) δ ppm 12.19 (s, 1H), 9.00 (d, 1H), 8.82 (s, 1H), 8.77 (s, 1H), 8.58 (s, 1H), 8.44 (s, 1H), 8.12 (d, 1H), 6.51 (m, 1H), 5.84 (m, 1H), 3.26 (q, 2H), 1.32 (t, 3H). ^{13}C NMR (101 MHz, DMSO-*d6*) δ ppm 160.3, 158.0, 153.1, 151.5, 148.3, 140.1, 139.3, 136.9, 136.7, 134.0, 131.8, 125.1, 124.2, 120.8, 117.0, 116.8, 114.4, 112.0, 109.3, 95.6, 93.6, 38.1, 14.5.

5-(8-(Ethylamino)-6-fluoro-4-(4-(trifluoromethyl)thiazol-2-yl)-9H-pyrido[2,3-b]indol-3-yl)nicotinonitrile (15m). MS obsd (ESI+) [(M+H)$^+$] 483.2. HRMS calcd [(M+H)$^+$] 483.1015, measured [(M+H)$^+$] 483.1017. ^{1}H NMR (400 MHz, MeOH-*d*4) δ ppm 8.86 (d, 1H), 8.73 (d, 1H), 8.60 (s, 1H), 8.50 (s, 1H), 8.23 (t, 1H), 6.50 (dd, 1H), 6.08 (dd, 1H), 3.36-3.34 (m, 2H), 1.43 (t, 3H). ^{13}C NMR (126 MHz, DMSO-*d6*) δ ppm 164.8, 159.8, 157.9, 154.1, 151.8, 151.5, 147.6, 143.5, 143.2, 141.2, 136.7, 136.6, 133.7, 133.0, 127.9, 125.3, 124.1, 123.5, 122.0, 119.9, 118.3, 118.2, 117.1, 113.8, 113.8, 109.2, 95.5, 95.3, 94.0, 93.8, 38.1, 14.5.

1-(3-(5-Cyanopyridin-3-yl)-8-(ethylamino)-6-fluoro-9H-pyrido[2,3-b]indol-4-yl)-3-(trifluoromethyl)-1H-pyrazole-4-carboxylic acid (15n). MS obsd (ESI+) [(M+H)$^+$] 510.2. HRMS calcd [(M+H)$^+$] 510.1302, measured [(M+H)$^+$] 510.1302. ^{1}H NMR (400 MHz, DMSO-*d*6) δ ppm 13.39 (br. s., 1 H), 12.25 (s, 1 H), 9.02 (d, 1 H), 8.93 (s, 1 H), 8.78 (s, 1 H), 8.62 (d, 1 H), 8.22 (s, 1 H), 6.53 (dd, 1 H), 5.93 (br. s., 1 H), 5.78 (dd, 1 H), 3.27 (dd, 2 H), 1.33 (t, 3 H). ^{13}C NMR (101 MHz, DMSO-*d6*) δ ppm 161.6, 160.4, 158.1, 153.1, 151.8, 148.3, 142.5, 142.1, 140.5, 137.4, 137.0, 136.9, 131.5, 125.3, 122.1, 120.8, 119.4, 117.0, 116.7, 116.5, 115.4, 111.7, 111.7, 109.3, 95.8, 93.8, 38.1, 14.5.

Ethyl 1-[3-(5-cyano-3-pyridyl)-8-(ethylamino)-6-fluoro-9H-pyrido[2,3-b]indol-4-yl]-3-(trifluoromethyl)pyrazole-4-carboxylate (15o). MS obsd (ESI+) [(M+H)$^+$] 538.2. ^{1}H NMR (400 MHz, DMSO-*d*6) δ ppm 12.25 (s, 1 H), 8.98-9.08 (m, 2 H), 8.78 (s, 1 H), 8.62 (d, 1 H), 8.16-8.26 (m, 1 H), 6.53 (dd, 1 H), 5.77 (dd, 1 H), 4.29 (q, 2 H), 3.27 (q, 2 H), 1.20-1.39 (m, 6 H).

5-[8-(Ethylamino)-6-fluoro-4-[5-methyl-3-(trifluoromethyl)pyrazol-1-yl]-9H-pyrido[2,3-b]indol-3-yl]pyridine-3-carbonitrile (15s). MS obsd (ESI+) [(M+H)$^+$] 480.2. HRMS calcd [(M+H)$^+$] 480.1560, measured [(M+H)$^+$] 480.1561. ^{1}H NMR (400 MHz, DMSO-*d*6) δ ppm 12.219 (s, 1H), 8.992-8.996 (d, 1H), 8.832 (s, 1H), 8.625 (s, 1H), 8.147-8.152 (d, 1H), 6.911 (s, 1H), 6.490-6.526 (m, 1H), 5.549-5.577 (m, 1H), 3.236-3.254 (m, 2H), 1.882 (s, 3H), 1.301-1.336 (m, 3H). ^{13}C NMR (101 MHz, DMSO-*d6*) δ ppm 160.5, 158.2, 153.1, 153.0, 151.7, 148.5, 143.7, 143.2, 140.2, 137.0, 136.9, 136.5, 131.5, 125.2, 117.0, 117.0, 116.9, 112.7, 112.7, 109.5, 105.6, 95.7, 92.6, 38.1, 14.5, 10.9.

5-[8-(Ethylamino)-6-fluoro-4-[5-(hydroxymethyl)-3-(trifluoromethyl)pyrazol-1-yl]-9H-pyrido[2,3-b]indol-3-yl]pyridine-3-carbonitrile (15t). MS obsd (ESI+) [(M+H)$^+$] 496.1. HRMS calcd [(M+H)$^+$] 496.1509, measured [(M+H)$^+$] 496.1509. ^{1}H NMR (400 MHz, MeOH-*d*4) δ ppm 13.534 (s, 1 H), 11.818 (s, 1 H), 8.890-8.925 (d, 1 H), 8.454 (s, 1 H), 8.239 (s, 1 H), 7.075-7.093 (d, 1 H), 6.488-6.519 (d, 1 H), 6.208 (s, 1 H), 5.826 (s, 1 H), 5.142 (s, 2 H), 3.264-3.403 (m, 2 H), 1.305-1.341(t, 3 H).

5-[8-(Ethylamino)-6-fluoro-4-[3-(trifluoromethyl)-5,6-dihydro-4H-pyrrolo[3,4-c]pyrazol-1-yl]-9H-pyrido[2,3-b]indol-3-yl]pyridine-3-carbonitrile (15u). MS obsd (ESI+) [(M+H)$^+$] 507.1. HRMS calcd [(M+H)$^+$] 507.1669, measured [(M+H)$^+$] 507.1668. ^{1}H NMR (400 MHz, DMSO-*d*6) δ ppm 12.30 (s, 1 H), 10.22 (br. s., 2 H), 9.05 (d, 1 H), 8.78 (s, 1 H), 8.56 (d, 1 H), 8.19 (s, 1 H), 6.54 (dd, 1 H), 6.11 (dd, 1 H), 4.55-4.64 (m, 1 H), 4.43-4.51 (m, 1 H), 4.22 (d, 1 H), 3.84 (d, 1 H), 3.27 (q, 2 H), 1.33 (t, 3 H). ^{13}C NMR (101 MHz, DMSO-*d6*) δ ppm 160.5, 158.9, 158.2, 153.1, 151.9, 148.6, 147.9, 140.2, 136.9, 136.0, 131.3, 125.3, 122.1, 121.8, 120.3, 117.1, 116.7, 116.6, 111.2, 109.7, 95.8, 93.8, 44.2, 38.1, 14.5.

5-[4-[3-(Difluoromethyl)-5,6-dihydro-4H-pyrrolo[3,4-c]pyrazol-1-yl]-8-(ethylamino)-6-fluoro-9H-pyrido[2,3-b]indol-3-yl]pyridine-3-carbonitrile (15v). MS obsd (ESI+) [(M+H)$^+$] 507.1. ^{1}H NMR (400 MHz, DMSO-*d6*) δ ppm 12.30 (s, 1H), 10.22 (br. s, 2H), 9.05 (d, 1H), 8.78 (s, 1H), 8.56 (d, 1H), 8.19 (s, 1H), 6.56 (m, 1H), 6.10 (m, 1H), 4.45-4.61 (m, 2H), 4.22 (d, 1H), 3.84 (d, 1H), 3.28 (q, 2H), 1.33 (t, 3H).

5-[4-(5,6-Dihydro-4H-pyrrolo[3,4-c]pyrazol-2-yl)-8-(ethylamino)-6-fluoro-9H-pyrido[2,3-b]indol-3-yl]pyridine-3-carbonitrile (15w). MS obsd (ESI+) [(M+H)$^+$] 439.3. HRMS calcd [(M+H)$^+$] 439.1795, measured [(M+H)$^+$] 439.1795. ^{1}H NMR (400 MHz, DMSO-*d*6) δ ppm 12.19 (s, 1 H), 10.16 (br. s., 2 H), 8.96 (d, 1 H), 8.65-8.71 (m, 1 H), 8.45-8.54 (m, 1 H), 8.16-8.29 (m, 1 H), 7.93 (s, 1 H), 6.46 (dd, 1 H), 6.07 (dd, 1 H), 4.45 (d, 4 H), 3.24 (q, 2 H), 1.31 (t, 3 H). ^{13}C NMR (101 MHz, DMSO-*d6*) δ ppm 158.6, 157.9, 155.7, 153.3, 153.0, 151.4, 148.6, 140.2, 139.1, 132.5, 128.0, 125.0, 120.9, 120.4, 117.2, 109.5, 95.7, 95.4, 44.4, 43.8, 38.1, 14.5.

5-[4-(5,6-Dihydro-4H-pyrrolo[3,4-c]pyrazol-1-yl)-8-(ethylamino)-6-fluoro -9H-pyrido[2,3-b]indol-3-yl]pyridine-3-carbonitrile (15x). MS obsd (ESI+) [(M+H)$^+$] 439.3. HRMS calcd [(M+H)$^+$] 439.1795, measured [(M+H)$^+$] 439.1792. ^{1}H NMR (400 MHz, DMSO-*d*6) δ ppm 12.26 (s, 1 H), 10.18 (br. s., 2 H), 9.03 (d, 1 H), 8.78 (s, 1 H), 8.55 (d, 1 H), 8.18 (s, 1 H), 7.89 (s, 1 H), 6.54 (dd, 1 H), 6.14 (dd, 1 H), 4.28-4.55 (m, 2 H), 4.15 (d, 1 H), 3.69 (d, 1 H), 3.30 (q, 2 H), 1.36 (t, 3 H).

N-Ethyl-6-fluoro-3-(2-methoxypyrimidin-5-yl)-4-[3-(trifluoromethyl)-5,6-dihydro-4H-pyrrolo[3,4-c]pyrazol-1-yl]-9H-pyrido[2,3-b]indol-8-amine (17u). MS obsd (ESI+) [(M+H)$^+$] 513.1. HRMS calcd [(M+H)$^+$] 513.1774, measured [(M+H)$^+$] 513.1776. ^{1}H NMR (400 MHz, DMSO-*d6*) δ ppm 12.25 (s, 1H), 10.26 (br. s, 2H), 8.73 (s, 1H), 8.43 (s, 2H), 6.53 (m, 1H), 6.04 (m, 1H), 4.62 (d, 1H), 4.52 (d, 1H), 4.24 (d, 1H), 3.94 (d, 1H), 3.27 (q, 2H), 1.32 (t, 3H). ^{13}C NMR (101 MHz, DMSO-*d6*) δ ppm 164.8, 159.2, 158.0, 154.9, 153.1, 152.9, 148.3, 136.9, 136.7, 135.8, 133.4, 125.4, 125.1, 123.2, 120.8, 119.0, 117.6, 108.5, 95.7, 93.4, 55.3, 44.7, 44.4, 38.1, 14.5.

4-(5,6-Dihydro-4H-pyrrolo[3,4-c]pyrazol-1-yl)-N-ethyl-6-fluoro-3-(2-methoxypyrimidin-5-yl)-9H-pyrido[2,3-b]indol-8-amine (17x). MS obsd (ESI+) [(M+H)$^+$] 445.3. HRMS calcd [(M+H)$^+$] 445.1901, measured [(M+H)$^+$] 445.1902. ^{1}H NMR (400 MHz, DMSO-*d6*) δ ppm 12.13 (s, 1H), 10.00 (br. s., 2H), 8.70 (s, 1H), 8.38 (s, 2H), 7.84 (s, 1H), 6.51 (m, 1H), 6.02 (m, 1H), 4.35-4.42 (m, 2H), 4.10 (s, 1H), 3.95 (s, 3H) 3.80 (m, 1H), 3.26 (m, 2H), 1.32 (t, 3H). ^{13}C NMR (101 MHz, DMSO-*d6*) δ ppm 164.6, 160.2, 159.0, 157.9, 153.0, 151.6, 148.0, 138.4, 136.6, 134.5, 129.1, 124.9, 123.8, 119.1, 117.5, 117.3, 112.4, 95.3, 94.2, 55.2, 44.6, 38.1, 14.6.

Synthetic procedure for the synthesis of 5-(8-(ethylamino)-6-fluoro-4-(3-(trifluoromethyl)-1H-pyrazol-1-yl)-9H-pyrido[2,3-b]indol-3-yl)-N-hydroxynicotinamide (10e).

Step (a). Preparation of methyl 5-(8-((*tert*-butoxycarbonyl)(ethyl)amino)-6-fluoro-4-(3-(trifluoromethyl)-1H-pyrazol-1-yl)-9H-pyrido[2,3-b]indol-3-yl)nicotinate. A mixture solution of *tert*-butyl N-[3-chloro-6-fluoro-4-[3-(trifluoromethyl)pyrazol-1-yl]-9H-pyrido[2,3-b]indol-8-yl]-N-ethyl-carbamate (**Intermediate 8**, 50 mg, 100 μmol), methyl 5-(4,4,5,5-tetramethyl-1,3,2-dioxaborolan-2-yl)nicotinate (52.8 mg, 201 μmol) and CsF (61 mg, 402 μmol) in 1,4-dioxane (6 mL) were degassed with N_2 several times. It was followed by the addition of dicyclohexyl(2',4',6'-triisopropyl-[1,1'-biphenyl]-2-yl)phosphine (23.9 mg, 50.2 μmol) and Pd_2dba_3 (23 mg, 25.1 μmol) at 0 °C, and the resulting mixture was heated at 110 °C for 4 h. The mixture was cooled down to room temperature and concentrated *in vacuo*. The residue was diluted with EtOAc (50 mL) and washed with water (20 mL). The organic layer was then dried over anhy. Na_2SO_4, filtered, and concentrated *in vacuo* to give a crude product of the title compound (60 mg) as a solid. It was used directly in the next step without further purification. MS obsd (ESI+) [$(M+H)^+$] 599.3.

Step (b). Preparation of *tert*-butyl ethyl(6-fluoro-3-(5-(hydroxycarbamoyl)pyridin-3-yl)-4-(3-(trifluoromethyl)-1H-pyrazol-1-yl)-9H-pyrido[2,3-b]indol-8-yl)carbamate. A solution of methyl 5-(8-((*tert*-butoxycarbonyl)(ethyl)amino)-6-fluoro-4-(3-(trifluoromethyl)-1H-pyrazol-1-yl)-9H-pyrido[2,3-b]indol-3-yl)nicotinate (60 mg, 100 μmol) and hydroxylamine (662 mg, 591 μl, 10 mmol) in MeOH (6 mL) was stirred at room temperature overnight. The reaction mixture was concentrated *in vacuo* to give a crude product of the title compound (60 mg) as a solid. It was used directly in the next step without further purification. MS obsd (ESI+) [$(M+H)^+$] 600.3.

Step (c). Preparation of 5-(8-(ethylamino)-6-fluoro-4-(3-(trifluoromethyl)-1H-pyrazol-1-yl)-9H-pyrido[2,3-b]indol-3-yl)-N-hydroxynicotinamide. To a solution of *tert*-butyl ethyl(6-fluoro-3-(5-(hydroxycarbamoyl)pyridin-3-yl)-4-(3-(trifluoromethyl)-1H-pyrazol-1-yl)-9H-pyrido[2,3-b]indol-8-yl)carbamate (60 mg, 100 μmol) in DCM (3 mL) was added TFA (2 mL, 26.3 mmol) and the resulting mixture was stirred at room temperature for 2 h. The mixture solution was concentrated under the reduced pressure and the residue was subject to prep-HPLC purification to afford the title compound

(15 mg, 29% yield) as a white solid. MS obsd (ESI+) [(M+H)$^+$] 500.1. HRMS calcd [(M+H)$^+$] 500.1458, measured, 500.1456. ^{1}H NMR (400 MHz, DMSO-*d*6) δ ppm 12.1-12.2 (m, 1H), 11.3-11.5 (m, 1H), 9.2-9.3 (m, 1H), 8.8-8.9 (m, 1H), 8.7-8.8 (m, 1H), 8.4-8.4 (m, 1H), 8.2-8.3 (m, 1H), 7.9-8.0 (m, 1H), 7.0-7.1 (m,1H), 6.5-6.5 (m, 1H), 5.9-5.9 (m, 1H), 5.7-5.8 (m, 1H), 3.2-3.3 (m, 2H), 1.3-1.3 (m, 3H). ^{13}C NMR (101 MHz, DMSO-*d*6) δ ppm 162.5, 160.2, 157.9, 152.9, 151.5, 148.4, 147.1, 138.2, 135.9, 135.4 , 131.2,128.7, 125.1,123.0, 121.9, 120.3,117.0 ,112.1, 106.3, 95.7, 93.6, 38.1, 14.5.

5-(8-(Ethylamino)-6-fluoro-4-(3-(trifluoromethyl)-1H-pyrazol-1-yl)-9H-pyrido[2,3-b]indol-3-yl)-N-methylpyrimidine-2-carboxamide (12i). The title compound was prepared by a similar procedure to that described for compound **10e**. MS obsd (ESI+) [(M+H)$^+$] 499.0. HRMS calcd [(M+H)$^+$] 500.1458, measured [(M+H)$^+$] 500.1457. ^{1}H NMR (400 MHz, MeOH-*d*4) δ ppm 8.97 (d, 1H), 8.6-8.6 (m, 1H), 8.0-8.1 (m, 1H), 7.9-8.0 (m, 1H), 6.8-6.9 (m, 1H), 6.4-6.4 (m, 1H), 5.85 (dd, 1H), 3.2-3.2 (m, 2H), 3.1-3.1 (m, 3H), 1.3-1.3 (m, 3H).

Synthetic procedure for the synthesis of 5-(8-(ethylamino)-6-fluoro-4-(3-(trifluoromethyl)-1H-pyrazol-1-yl)-9H-pyrido[2,3-b]indol-3-yl)-N-methoxynicotinamide (10f).

Step (a). Preparation of 5-(8-((*tert*-butoxycarbonyl)(ethyl)amino)-6-fluoro-4-(3-(trifluoromethyl)-1H-pyrazol-1-yl)-9H-pyrido[2,3-b]indol-3-yl)nicotinic acid. A solution of methyl 5-(8-((*tert*-butoxycarbonyl)(ethyl)amino)-6-fluoro-4-(3-(trifluoromethyl)-1H-pyrazol-1-yl)-9H-pyrido[2,3-b]indol-3-yl)nicotinate (61 mg, 102 μmol), sodium hydroxide (40.8 mg, 1.02 mmol) in THF (3 mL) and H_2O (3 mL) was stirred at room temperature for 30 min. Afterwards, the mixture solution was concentrated *in vacuo* and the residue was diluted with EtOAc (50 mL) and washed with water (20 mL). The organic layer was dried over anhy. Na_2SO_4, filtered, and evaporated to dryness to afford a crude product of the title compound (61 mg) as a solid. It was used directly in the next step without further purification. MS obsd (ESI+) [(M+H)$^+$] 585.4.

Step (b). Preparation of *tert*-butyl ethyl(6-fluoro-3-(5-(methoxycarbamoyl)pyridin-3-yl)-4-(3-(trifluoromethyl)-1H-pyrazol-1-yl)-9H-pyrido[2,3-b]indol-8-yl)carbamate. A mixture solution of 5-(8-((*tert*-butoxycarbonyl)(ethyl)amino)-6-fluoro-4-(3-(trifluoromethyl)-1H-pyrazol-1-yl)-9H-pyrido[2,3-

b]indol-3-yl)nicotinic acid (61 mg, 104 μmol), 2-(3H-[1,2,3]triazolo[4,5-b]pyridin-3-yl)-1,1,3,3-tetramethylisouronium hexafluorophosphate(V) (71.4 mg, 188 μmol), O-methylhydroxylamine hydrochloride (26.1 mg, 313 μmol), and N-ethyl-N-isopropylpropan-2-amine (80.9 mg, 626 μmol) in DCM (3 mL) was stirred at room temperature overnight. Afterwards, the mixture was diluted with DCM (50 mL) and washed with water (20 mL). The separated organic layer was dried over anhy. Na_2SO_4, filtered, and concentrated *in vacuo* to give a crude product of the title compound (61 mg) as a solid. It was used directly in the next step without further purification. MS obsd (ESI+) [$(M+H)^+$] 614.2.

Step (c). Preparation of 5-(8-(ethylamino)-6-fluoro-4-(3-(trifluoromethyl)-1H-pyrazol-1-yl)-9H-pyrido[2,3-b]indol-3-yl)-N-methoxynicotinamid. A solution of *tert*-butyl ethyl(6-fluoro-3-(5-(methoxycarbamoyl)pyridin-3-yl)-4-(3-(trifluoromethyl)-1H-pyrazol-1-yl)-9H-pyrido[2,3-b]indol-8-yl)carbamate (61 mg, 99.4 μmol) and TFA (11.3 mg, 99.4 μmol) in DCM (3 mL) was stirred at room temperature for 2 h. Afterward, the mixture solution was concentrated *in vacuo* to give a crude product, which was purified by prep-HPLC to afford the title compound (16 mg, 31% yield) as a while solid. MS obsd (ESI+) [$(M+H)^+$] 514.1. HRMS calcd [$(M+H)^+$] 514.1615, measured [$(M+H)^+$] 514.1617. ^{1}H NMR (400 MHz, MeOH-*d4*) δ ppm 8.7-8.8 (m, 1H), 8.5-8.6 (m, 1H), 8.4-8.4 (m, 1H), 7.9-8.0 (m, 1H), 7.8-7.9 (m, 1H), 6.7-6.8 (m, 1H), 6.3-6.4 (m, 1H), 5.8-5.9 (m, 1H), 3.7-3.8 (m, 3H), 1.3-1.3 (m, 3H).

Synthetic procedure for the synthesis of 2-(5-(8-(ethylamino)-6-fluoro-4-(3-(trifluoromethyl)-1H-pyrazol-1-yl)-9H-pyrido[2,3-b]indol-3-yl)pyridin-3-yl)acetic acid (10n).

Step (a). Preparation of methyl 2-(5-(8-((*tert*-butoxycarbonyl)(ethyl)amino)-6-fluoro-4-(3-(trifluoromethyl)-1H-pyrazol-1-yl)-9H-pyrido[2,3-b]indol-3-yl)pyridin-3-yl)acetate. To a 25 mL microwave vial was added methyl 2-(5-bromopyridin-3-yl)acetate (100 mg, 435 μmol), bis(pinacolato)diboron (121 mg, 478 μmol), 1,1'-bis(diphenylphosphino)ferrocene-palladium(II)dichloride dichloromethane complex (35.5 mg, 43.5 μmol) and potassium acetate (128 mg, 1.3 mmol) in 1,4-dioxane (10 mL). The vial was capped and heated in the microwave reactor at 100 ºC for 1 h under N_2. Afterwards, the reaction was cooled to room temperature and added *tert*-butyl N-[3-chloro-6-fluoro-4-[3-(trifluoromethyl)pyrazol-1-yl]-9H-pyrido[2,3-b]indol-8-yl]-N-ethyl-carbamate

(Intermediate **8**, 216 mg, 435 μmol), 1,1'-bis(di-*tert*-butylphosphino)ferrocene palladium dichloride (14.2 mg, 21.7 μmol), cesium fluoride (198 mg, 1.3 mmol) and H_2O (2 mL). The resulting reaction mixture was re-heated to 120 °C and stirred for 15 h under N_2. The reaction mixture was cooled down to room temperature and filtered through glass fiber paper. The crude material was then purified by flash chromatography (silica gel, 0% to 10% MeOH in DCM) to afford the title compound (150 mg, 56.3 % yield) as a solid.

Step (b). Preparation of 2-(5-(8-((*tert*-butoxycarbonyl)(ethyl)amino)-6-fluoro-4-(3-(trifluoromethyl)-1H-pyrazol-1-yl)-9H-pyrido[2,3-b]indol-3-yl)pyridin-3-yl)acetic acid. To a solution of methyl 2-(5-(8-((*tert*-butoxycarbonyl)(ethyl)amino)-6-fluoro-4-(3-(trifluoromethyl)-1H-pyrazol-1-yl)-9H-pyrido[2,3-b]indol-3-yl)pyridin-3-yl)acetate (150 mg, 245 μmol) in MeOH (8 mL) was added LiOH (47.9 mg, 2 mmol) in H_2O (2 mL) and the resulting mixture was stirred at room temperature for 2h. After the solution was adjusted to pH ~ 7, it was concentrated *in vacuo*. The residue was partitioned between H_2O (25 mL) and EtOAc (25 mL). The organic layer was then dried over anhy. Na_2SO_4, filtered, and concentrated *in vacuo* to afford a crude product of the title compound (140 mg, 95.5 % yield) as a solid. It was used directly in the next step without further purification.

Step (c). Preparation of 2-(5-(8-(ethylamino)-6-fluoro-4-(3-(trifluoromethyl)-1H-pyrazol-1-yl)-9H-pyrido[2,3-b]indol-3-yl)pyridin-3-yl)acetic acid. To a solution of 2-(5-(8-((*tert*-butoxycarbonyl)(ethyl)amino)-6-fluoro-4-(3-(trifluoromethyl)-1H-pyrazol-1-yl)-9H-pyrido[2,3-b]indol-3-yl)pyridin-3-yl)acetic acid (140 mg, 234 μmol) in DCM (8 mL) was added TFA (1.33 g, 11.7 mmol). The resulting mixture was stirred at room temperature for 2h before it was concentrated *in vacuo*. The crude product was then subjected to prep-HPLC purification to afford the title compound (17.2 mg, 14 % yield) as a solid. MS obsd (ESI+) [$(M+H)^+$] 499.3. HRMS calcd [$(M+H)^+$] 499.1506, measured [$(M+H)^+$] 499.1509. ^{1}H NMR (400 MHz, DMSO-*d6*) δ ppm 12.0-12.2 (m, 1H), 8.7-8.8 (m, 1H), 8.5-8.6 (m, 1H), 8.3-8.4 (m, 1H), 8.2-8.3 (m, 1H), 7.6-7.7 (m, 1H), 7.0-7.1 (m, 1H), 6.4-6.5 (m, 1H), 5.6-5.8 (m, 1H), 3.6-3.7 (m, 2H), 3.2-3.3 (m, 2H), 1.3-1.4 (m, 3H). ^{13}C NMR (101 MHz, DMSO-*d6*) δ ppm 172.0, 159.0, 152.9, 148.2, 146.0, 143.1, 139.6, 138.3, 136.8, 136.0, 131.8, 125.1, 123.0, 121.8, 120.4, 116.9, 112.2, 106.7, 95.6, 93.4, 38.1, 37.7, 26.8, 14.5.

The following compounds were prepared by a similar procedure to that described for compound **10n**.

2-(5-(8-(Ethylamino)-6-fluoro-4-(3-(trifluoromethyl)-1H-pyrazol-1-yl)-9H-pyrido[2,3-b]indol-3-yl)pyrimidin-2-yl)acetic acid (12e). MS obsd (ESI+) [(M+H)$^+$] 500.3. ^{1}H NMR (400 MHz, DMSO-*d*6) δ ppm 8.7-8.8 (m, 1H), 8.5-8.6 (m, 2H), 8.3-8.4 (m, 1H), 7.1-7.2 (m, 1H), 6.6-6.7 (m, 1H), 6.5-6.5 (m, 1H), 5.9-5.9 (m, 1H), 5.7-5.8 (m, 1H), 5.3-5.4 (m, 1H), 3.8-3.9 (m, 2H), 3.3-3.3 (m, 2H), 1.3-1.3 (m, 3H).

5-(8-(Ethylamino)-6-fluoro-4-(3-(trifluoromethyl)-1H-pyrazol-1-yl)-9H-pyrido[2,3-b]indol-3-yl)pyrimidine-2-carboxylic acid (12g). MS obsd (ESI+) [(M+H)$^+$] 486.1. HRMS calcd [(M+H)$^+$] 486.1302, measured [(M+H)$^+$] 486.1302. ^{1}H NMR (400 MHz, MeOH-*d*4) δ ppm 8.6-8.6 (m, 1H), 8.54 (s, 2H), 7.9-7.9 (m, 1H), 6.8-6.8 (m, 1H), 6.4-6.4 (m, 1H), 5.8-5.8 (m, 1H), 3.2-3.2 (m, 2H), 1.3-1.3 (m, 3H). ^{13}C NMR (126 MHz, DMSO-*d6*) δ ppm 216.9, 160.1, 158.2, 156.5, 153.1, 148.2, 143.6, 143.3, 138.2, 136.9, 136.8, 136.1, 125.2, 122.7, 120.6, 119.3, 116.9, 116.8, 112.2, 112.2, 106.8, 95.5, 93.4, 40.6, 40.4, 40.2, 38.1, 14.5.

1-(5-(8-(Ethylamino)-6-fluoro-4-(3-(trifluoromethyl)-1H-pyrazol-1-yl)-9H-pyrido[2,3-b]indol-3-yl)pyrimidin-2-yl)cyclopropanecarboxylic acid (12f). MS obsd (ESI+) [(M+H)$^+$] 526.1. HRMS calcd [(M+H)$^+$] 526.1615, measured [(M+H)$^+$] 526.1617. ^{1}H NMR (MeOH-*d4*, 400 MHz) δ ppm 8.68 (s, 1H), 8.58 (s, 2H), 8.1-8.1 (m, 1H), 6.99 (d, 1H), 6.52 (dd, 1H), 5.98 (dd, 1H), 3.3-3.4 (m, 2H), 1.8-1.9 (m, 2H), 1.7-1.8 (m, 2H), 1.43 (t, 3H). ^{13}C NMR (101 MHz, DMSO-*d6*) δ ppm 173.3, 166.5, 160.3, 158.0, 156.4, 153.1, 148.2, 143.7, 143.3, 138.3, 136.8, 136.7, 136.1, 127.1, 125.1, 123.0, 120.3, 119.2, 116.9, 116.8, 112.1, 112.0, 106.8, 95.6, 93.4, 38.1, 31.2, 18.1, 14.5.

3-((5-(8-(Ethylamino)-6-fluoro-4-(3-(trifluoromethyl)-1H-pyrazol-1-yl)-9H-pyrido[2,3-b]indol-3-yl)pyrimidin-2-yl)oxy)-2,2-dimethylpropanoic acid (12o). MS obsd (ESI+) [(M+H)$^+$] 558.1. HRMS calcd [(M+H)$^+$] 558.1877, measured [(M+H)$^+$] 558.1878. ^{1}H NMR (400 MHz, MeOH-*d4*) δ ppm 8.63

(s, 1H), 8.39 (s, 2H), 8.05 (d, 1H), 6.98 (d, 1H), 6.50 (dd, 1H), 5.91 (dd, 1H), 4.43 (s, 2H), 3.3-3.4 (m, 1H), 3.29 (m, 2H), 1.43 (t, 3H), 1.34 (s, 6H).

1-(((5-(8-(Ethylamino)-6-fluoro-4-(3-(trifluoromethyl)-1H-pyrazol-1-yl)-9H-pyrido[2,3-b]indol-3-yl)pyrimidin-2-yl)amino)methyl)cyclopropanecarboxylic acid (12w). MS obsd (ESI+) [(M+H)$^+$] 555.1. HRMS calcd [(M+H)$^+$] 557.2037, measured [(M+H)$^+$] 557.2037. ^{1}H NMR (400 MHz, MeOH-*d4*) δ ppm 8.57 (s, 1H), 8.09 (s, 2H), 8.02 (d, 1H), 6.98 (d, 1H), 6.49 (dd, 1H), 5.87 (dd, 1H), 3.66 (s, 2H), 3.3-3.3 (m, 2H), 1.42 (t, 3H), 1.2-1.2 (m, 2H), 1.0-1.0 (m, 2H). ^{13}C NMR (101 MHz, DMSO-*d6*) δ ppm 178.5, 162.2, 157.4, 152.4, 147.9, 143.3, 137.8, 136.7, 135.9, 125.0, 123.1, 120.8, 117.6, 116.9, 112.3, 106.6, 95.3, 93.4, 48.6, 43.4, 38.1, 23.4, 14.5.

1-[5-[6-Fluoro-8-(methylamino)-4-[3-(trifluoromethyl)pyrazol-1-yl]-9H-pyrido[2,3-b]indol-3-yl]pyrimidin-2-yl]cyclopropanecarboxylic acid (12x). HRMS calcd [(M+H)$^+$] 512.1458, measured [(M+H)$^+$] 512.1460. ^{1}H NMR (400 MHz, DMSO-*d*6) δ ppm 8.76 (s, 1H), 8.53 (s, 2H), 8.38 (br d, *J* = 1.0 Hz, 1H), 7.16 (d, *J* = 2.2 Hz, 1H), 6.47 (dd, *J* = 2.1, 12.1 Hz, 1H), 6.08 (br d, *J* = 3.7 Hz, 1H), 5.92 - 5.61 (m, 1H), 2.92 (br d, *J* = 3.9 Hz, 3H), 1.50 - 1.62 (m, 2H), 1.34 - 1.47 (m, 2H). ^{13}C NMR (101 MHz, DMSO-*d6*) δ ppm 173.4, 166.6, 160.4, 158.1, 156.4, 153.1, 148.2, 143.5, 138.2, 137.8, 136.1, 127.1, 125.2, 119.2, 121.6, 116.7, 112.0, 106.8, 95.3, 93.4, 31.3, 30.2, 25.4, 18.0.

Synthetic procedure for the synthesis of 2-[5-[8-(Ethylamino)-6-fluoro-4-[3-(trifluoromethyl)pyrazol-1-yl]-9H-pyrido[2,3-b]indol-3-yl]-3-pyridyl]acetamide (10o).

Step (a). Preparation of *tert*-butyl (3-(5-(2-amino-2-oxoethyl)pyridin-3-yl)-6-fluoro-4-(3-(trifluoromethyl)-1H-pyrazol-1-yl)-9H-pyrido[2,3-b]indol-8-yl)(ethyl)carbamate. To a 25 mL microwave vial was added 2-(5-(8-((*tert*-butoxycarbonyl)(ethyl)amino)-6-fluoro-4-(3-(trifluoromethyl)-1H-pyrazol-1-yl)-9H-pyrido[2,3-b]indol-3-yl)pyridin-3-yl)acetic acid (128 mg, 214 μmol), and CDI (46.8 mg, 289 μmol) in THF (8 mL). The vial was capped and heated in the microwave reactor at 60 ºC for 2 h. Afterwards, the reaction was cooled down to room temperature and added ammonia in isopropyl alcohol (10.7 mL, 10.7 mmol). The resulting mixture was then stirred at room temperature overnight before it was concentrated *in vacuo*. The residue was suspended in H_2O (25 mL)

and extracted with EtOAc (25 mL x 3). Combined organics were washed with brine (25 mL), dried over anhy. Na_2SO_4, filtered, and concentrated *in vacuo* to afford a crude product of the title compound (120 mg, 93.9 % yield) as a solid.

Step (b). Preparation of 2-[5-[8-(ethylamino)-6-fluoro-4-[3-(trifluoromethyl)pyrazol-1-yl]-9H-pyrido[2,3-b]indol-3-yl]-3-pyridyl]acetamide. To a solution of *tert*-butyl (3-(5-(2-amino-2-oxoethyl)pyridin-3-yl)-6-fluoro-4-(3-(trifluoromethyl)-1H-pyrazol-1-yl)-9H-pyrido[2,3-b]indol-8-yl)(ethyl)carbamate (120 mg, 201 μmol) in DCM (10 mL) was added TFA (1.14 g, 10 mmol) and the resulting reaction mixture was stirred at room temperature for 2 h. Afterwards, the solution was concentrated *in vacuo* to give a crude product, which was purified by pHPLC to afford the title compound (22 mg, 19.5 % yield) as a white solid. MS obsd (ESI+) $[(M+H)^+]$ 498.4. HRMS calcd $[(M+H)^+]$ 498.1665, measured $[(M+H)^+]$ 498.1665. ^{1}H NMR (400 MHz, DMSO-*d6*) δ ppm 12.0-12.2 (m, 1H), 8.6-8.7 (m, 1H), 8.4-8.5 (m, 1H), 8.2-8.3 (m, 2H), 7.4-7.6 (m, 2H), 7.05 (d, 1H), 6.9-7.0 (m, 1H), 6.48 (dd, 1H), 5.88 (brs, 1H), 5.70 (dd, 1H), 3.38 (s, 2H), 3.2-3.3 (m, 2H), 1.3-1.4 (m, 3H). ^{13}C NMR (101 MHz, DMSO-*d6*) δ ppm 171.6, 160.2, 157.9, 152.8, 149.6, 148.3, 147.4, 143.3, 138.2, 137.2, 136.7, 135.9, 125.1, 123.1, 122.6, 120.4, 116.9, 112.2, 106.5, 95.5, 93.5, 38.1, 27.3, 14.5.

Synthetic procedure for the synthesis of N-ethyl-6-fluoro-3-[5-(1H-tetrazol-5-ylmethyl)-3-pyridyl]-4-[3-(trifluoromethyl)pyrazol-1-yl]-9H-pyrido[2,3-b]indol-8-amine (10p).

Step (a). Preparation of *tert*-butyl N-[3-[5-(cyanomethyl)-3-pyridyl]-6-fluoro-4-[3-(trifluoromethyl)pyrazol-1-yl]-9H-pyrido[2,3-b]indol-8-yl]-N-ethyl-carbamate. To a solution of *tert*-butyl N-(3,4-dichloro-6-fluoro-9H-pyrido[2,3-b]indol-8-yl)-N-ethyl-carbamate (250 mg, 0.502 mmol), [5-(cyanomethyl)-3-pyridyl]boronic acid (110 mg, 0.679 mmol) in THF/H_2O (10 mL/1 mL) was added Pd-Ad_2nBuP Biphenyl Precat (40 mg, 0.06 mmol) and K_3PO_4 (280 mg, 2.63 mmol), then the solution was stirred at 80 °C under Ar for 18 h. Then the mixture was cooled down to room temperature and concentrated *in vacuo*. The crude product was purified by prep-TLC (petroleum ether:EtOAc = 1:2) to afford the title compound (260 mg, 89.3% yield) as a yellow solid. MS obsd (ESI+) $[(M+H)^+]$ 580.1.

Step (b). Preparation of *tert*-butyl N-ethyl-N-[6-fluoro-3-[5-(1H-tetrazol-5-ylmethyl)-3-pyridyl]-4-[3-(trifluoromethyl)pyrazol-1-yl]-9H-pyrido[2,3-b]indol-8-yl]carbamate. To a solution of *tert*-butyl N-[3-[5-(cyanomethyl)-3-pyridyl]-6-fluoro-4-[3-(trifluoromethyl)pyrazol-1-yl]-9H-pyrido[2,3-b]indol-8-yl]-N-ethyl-carbamate (50 mg, 0.086 mmol) in DMF (3 mL) was added NaN_3 (10 mg, 0.154 mmol) and NH_4Cl (20 mg, 0.374mmol), then the resulting mixture was stirred at 100 °C for 72 h under N_2. The reaction mixture was cooled down to room temperature, poured into water (50 mL) and extracted with EtOAc (40 mL x 3). Combined organics were washed with brine (40 mL x 3), dried over anhy. Na_2SO_4, filtered, and concentrated *in vacuo* to give a crude of the title compound (70 mg) as yellow gum. It was used directly in the next step without further purification. MS obsd (ESI+) [$(M+H)^+$] 623.2.

Step (c). Preparation of 3-(5-((1H-tetrazol-5-yl)methyl)pyridin-3-yl)-N-ethyl-6-fluoro-4-(3-(trifluoromethyl)-1H-pyrazol-1-yl)-9H-pyrido[2,3-b]indol-8-amine formate. To a solution of *tert*-butyl N-ethyl-N-[6-fluoro-3-[5-(1H-tetrazol-5-ylmethyl)-3-pyridyl]-4-[3-(trifluoromethyl)pyrazol-1-yl]-9H-pyrido[2,3-b]indol-8-yl]carbamate (70 mg, 0.086 mmol) in DCM (2 mL) was added TFA (0.5 mL), then the solution was stirred at 20 °C for 3 h. The reaction mixture was concentrated *in vacuo* to give a crude material, which was purified by prep-HPLC to afford the title compound (30.5 mg, 61.6% yield) as a light-yellow solid. MS obsd (ESI+) [$(M+H)^+$] 523.2. HRMS calcd [$(M+H)^+$] 523.1730, measured [$(M+H)^+$] 523.1730. ^{1}H NMR (400 MHz, DMSO-*d6*) δ ppm 12.10 (brs, 1H), 8.66 (s, 1H), 8.48 (s, 1H), 8.23-8.20 (m, 2H), 8.15 (s, 0.25H), 7.52 (s, 1H), 7.00 (s, 1H), 6.49-6.45 (dd, 1H), 5.87 (s, 1H), 5.70 (m, 1H), 4.21 (s, 2H), 3.26-3.23 (q, 2H), 1.32-1.29 (t, 2H).

Synthetic procedure for the synthesis of 5-[[5-[8-(ethylamino)-6-fluoro-4-[3-(trifluoromethyl)pyrazol-1-yl]-9H-pyrido[2,3-b]indol-3-yl]-3-pyridyl]methyl]-3H-1,3,4-oxadiazol-2-one (10r).

Step (a). Preparation of ethyl 2-[5-[8-[*tert*-butoxycarbonyl(ethyl)amino]-6-fluoro-4-[3-(trifluoromethyl)pyrazol-1-yl]-9H-pyrido[2,3-b]indol-3-yl]-3-pyridyl]acetate. To a mixture of *tert*-butyl N-(3,4-dichloro-6-fluoro-9H-pyrido[2,3-b]indol-8-yl)-N-ethyl-carbamate (100 mg, 0.2 mmol),

ethyl 2-[5-(4,4,5,5-tetramethyl-1,3,2-dioxaborolan-2-yl)-3-pyridyl]acetate (83.56 mg, 0.4 mmol), K_3PO_4 (127.91 mg, 0.6 mmol), Catacxium A-PD-G2 (13.43 mg, 0.02 mmol) was added THF (2 mL) and H_2O (0.2 mL), then the solution was stirred at 80 °C under Ar for 16 h. After the reaction was completed by LC-MS detection, the crude product was purified by prep-TLC (petroleum ether:EtOAc = 2:1) to afford the title compound (100 mg, 79.5% yield) as a brown solid. MS obsd (ESI+) $[(M+H)^+]$ 627.2.

Step (b). Preparation of 2-[5-[8-[*tert*-butoxycarbonyl(ethyl)amino]-6-fluoro-4-[3-(trifluoromethyl)pyrazol-1-yl]-9H-pyrido[2,3-b]indol-3-yl]-3-pyridyl]acetic acid. To a solution of ethyl 2-[5-[8-[*tert*-butoxycarbonyl(ethyl)amino]-6-fluoro-4-[3-(trifluoromethyl)pyrazol-1-yl]-9H-pyrido[2,3-b]indol-3-yl]-3-pyridyl]acetate (100 mg, 0.16 mmol) in EtOH (5 mL) was added aqueous NaOH solution (1N, 1 mL, 1 mmol), then the mixture was stirred at 20 °C for 1 h. After LC-MS indicated the reaction was completed, the mixture was adjusted to pH = 4-5 with aqueous HCl solution (1N) and extracted with EtOAc (20 mL x 3). Combined organics were then dried over anhy. Na_2SO_4, filtered, and concentrated *in vacuo* to give a crude product of the title compound (90 mg, 94.2% yield) as a yellow solid. It was used directly in the next step without further purification. MS obsd (ESI+) $[(M+H)^+]$ 599.0.

Step (c). Preparation of *tert*-butyl N-[3-[5-[2-(2-tert-butoxycarbonylhydrazino)-2-oxo-ethyl]-3-pyridyl]-6-fluoro-4-[3-(trifluoromethyl)pyrazol-1-yl]-9H-pyrido[2,3-b]indol-8-yl]-N-ethyl-carbamate. A solution of 2-[5-[8-[*tert*-butoxycarbonyl(ethyl)amino]-6-fluoro-4-[3-(trifluoromethyl)pyrazol-1-yl]-9H-pyrido[2,3-b]indol-3-yl]-3-pyridyl]acetic acid (90 mg, 0.15 mmol), HATU (68.61 mg, 0.18 mmol), DIPEA (0.08 mL, 0.45 mmol) in DMF (3 mL) was stirred at 20 °C for 0.5 h, then *tert*-butyl carbazate (23.85 mg, 0.18 mmol) was added and the resulting mixture was stirred at 20 °C for additional 16 h. EtOAc (30 mL) was added and the mixture solution washed with brine (20 mL), saturated aqueous $NaHCO_3$ solution (20 mL). The separated organic layer was dried over anhy. Na_2SO_4, filtered, and concentrated *in vacuo* to give a crude product of the title compound (100 mg, 93.3% yield) as a yellow solid. It was used directly in the next step without further purification. MS obsd (ESI+) $[(M+H)^+]$ 713.2.

Step (d). Preparation of 2-[5-[8-(ethylamino)-6-fluoro-4-[3-(trifluoromethyl)pyrazol-1-yl]-9H-pyrido[2,3-b]indol-3-yl]-3-pyridyl]acetohydrazide. To a solution of *tert*-butyl N-[3-[5-[2-(2-*tert*-butoxycarbonylhydrazino)-2-oxo-ethyl]-3-pyridyl]-6-fluoro-4-[3-(trifluoromethyl)pyrazol-1-yl]-9H-pyrido[2,3-b]indol-8-yl]-N-ethyl-carbamate (100 mg, 0.14 mmol) in EtOAc (5 mL) was added HCl/EtOAc (4N, 1 mL, 4 mmol), then the mixture was stirred at 20 °C for 1 h until LC-MS indicated the completion of the reaction. The reaction mixture was then concentrated *in vacuo* to give a crude product of the title compound (100 mg, 65.2% yield) as a yellow solid. It was used directly in the next step without further purification. MS obsd (ESI+) [$(M+H)^+$] 513.1.

Step (e). Preparation of 5-[[5-[8-(ethylamino)-6-fluoro-4-[3-(trifluoromethyl)pyrazol-1-yl]-9H-pyrido[2,3-b]indol-3-yl]-3-pyridyl]methyl]-3H-1,3,4-oxadiazol-2-one. To a solution of 2-[5-[8-(ethylamino)-6-fluoro-4-[3-(trifluoromethyl)pyrazol-1-yl]-9H-pyrido[2,3-b]indol-3-yl]-3-pyridyl]acetohydrazide (100 mg, 0.2 mmol) in THF (5 mL) was added DIPEA (0.1 mL, 0.590 mmol) and the mixture was stirred at 20 °C for 0.5 h. Then CDI (63 mg, 0.390 mmol) was added and the resulting mixture was stirred at 20 °C for additional 16 h. EtOAc (20 mL) was added and the mixture was washed with brine (20 mL), saturated aqueous NH_4Cl solution (20 mL x 2). The organic layer was dried over anhy. Na_2SO_4, filtered and concentrated *in vacuo* to give a crude product, which was purified by prep-HPLC to afford the title compound (19.2 mg, 18.3% yield) as a yellow solid. MS obsd (ESI+) [$(M+H)^+$] 539.1. HRMS calcd [$(M+H)^+$] 539.1567, measured [$(M+H)^+$] 539.1566. ^{1}H NMR (400 MHz, DMSO-*d6*) δ ppm 12.22 (brs, 1H) 8.71 (s, 1H) 8.49 (d, 1H) 8.44 (brs, 1H) 8.36 (d, 1H) 8.25 (d, 1H) 7.48 (s, 1H) 7.02 (d, 1H) 6.48 (dd, 1H) 5.96 (brs, 1H) 5.71 (dd, 1H) 3.93 (s, 2H) 3.18 - 3.28 (m, 2 H) 1.32 (t, 3 H).

Synthetic procedure for the synthesis of N-ethyl-6-fluoro-3-[5-(1H-imidazol-2-ylmethyl)-3-pyridyl]-4-[3-(trifluoromethyl)pyrazol-1-yl]-9H-pyrido[2,3-b]indol-8-amine (10s).

Step (a). Preparation of *tert*-butyl (3-(5-(cyanomethyl)pyridin-3-yl)-6-fluoro-4-(3-(trifluoromethyl)-1H-pyrazol-1-yl)-9H-pyrido[2,3-b]indol-8-yl)(ethyl)carbamate. To a solution of *tert*-butyl N-[3-

chloro-6-fluoro-4-[3-(trifluoromethyl)pyrazol-1-yl]-9H-pyrido[2,3-b]indol-8-yl]-N-ethyl-carbamate (250 mg, 0.5 mmol) and (5-(cyanomethyl)pyridin-3-yl)boronic acid (110 mg, 0.68 mmol) in THF/H_2O (10 mL/1 mL) was added cataCXium® A Pd G2 (40 mg, 0.06 mmol) and K_3PO_4 (280 mg, 2.63 mmol). The resulting mixture was stirred at 80 °C for 18 h under Ar. Afterwards, the reaction was cooled down to room temperature and the solution was concentrated *in vacuo*. The crude product was purified by prep-TLC (petroleum ether:EtOAc = 1:2) to afford the title compound (260 mg, 89.3% yield) as a yellow solid. MS obsd (ESI+) [$(M+H)^+$] 580.1.

Step (b). Preparation of *tert*-butyl (3-(5-(2-amino-2-iminoethyl)pyridin-3-yl)-6-fluoro-4-(3-(trifluoromethyl)-1H-pyrazol-1-yl)-9H-pyrido[2,3-b]indol-8-yl)(ethyl)carbamate. To a solution of *tert*-butyl (3-(5-(cyanomethyl)pyridin-3-yl)-6-fluoro-4-(3-(trifluoromethyl)-1H-pyrazol-1-yl)-9H-pyrido[2,3-b]indol-8-yl)(ethyl)carbamate (80 mg, 0.138 mmol) in MeOH (5 mL) was added NaOMe (10 mg, 0.185 mmol). After the reaction mixture was stirred at 20 °C for 120 h under N_2, NH_4Cl (30 mg, 0.56 mmol) was added and then the resulting solution was stirred at 20 °C for additional 20 h. The reaction mixture was concentrated *in vacuo* to give a crude product, which was re-dissolved in EtOAc (50 mL) and filtered. The filtrate was concentrated *in vacuo* to give a crude product of the title compound (76 mg) as a white solid. It was used directly in the next step without further purification. MS obsd (ESI+) [$(M+H)^+$] 597.2.

Step (c). Preparation of 3-(5-((1H-imidazol-2-yl)methyl)pyridin-3-yl)-N-ethyl-6-fluoro-4-(3-(trifluoromethyl)-1H-pyrazol-1-yl)-9H-pyrido[2,3-b]indol-8-amine. To a solution of *tert*-butyl (3-(5-(2-amino-2-iminoethyl)pyridin-3-yl)-6-fluoro-4-(3-(trifluoromethyl)-1H-pyrazol-1-yl)-9H-pyrido[2,3-b]indol-8-yl)(ethyl)carbamate (76 mg, 0.051 mmol) in MeOH (5 mL) was added 2,2-dimethoxyethanamine (15 mg, 0.143 mmol). After being stirred at 70 °C for 18 h, the reaction mixture was concentrated *in vacuo* to give a crude solid, which was dissolved in aqueous oxalic acid solution (1N, 5 mL) and the resulting mixture was stirred at 80 °C for another 3 h. The reaction mixture was cooled back to room temperature, diluted with H_2O (30 mL), and basified with saturated aqueous Na_2CO_3 solution to pH ~ 9. The aqueous solution was extracted with EtOAc (30 mL) three times and the combined organics were dried over anhy. Na_2SO_4, filtered, and concentrated *in vacuo*. The crude

product was then purified by prep-HPLC to afford the title compound (13.2 mg, 49.8% yield) as a light-yellow solid. MS obsd (ESI+) [(M+H)$^+$] 521.1. HRMS calcd [(M+H)$^+$] 521.1825, measured [(M+H)$^+$] 521.1828. ^{1}H NMR (400 MHz, DMSO-*d6*) δ ppm 12.20 (brs, 1H), 8.65 (s, 1H), 8.41 (s, 1H), 8.30 (s, 1H), 8.26 (s, 0.23H), 8.19 (m, 2H), 7.50 (s, 1H), 7.02 (s, 1H), 6.89 (s, 2H), 6.48-6.45 (d, 1H), 5.95 (s, 1H), 5.69-5.67 (m, 1H), 3.95 (s, 2H), 3.27-3.22 (q, 2H), 1.32-1.29 (t, 2H).

Synthetic procedure for the synthesis of 6-(8-(Ethylamino)-6-fluoro-4-(3-(trifluoromethyl)-1H-pyrazol-1-yl)-9H-pyrido[2,3-b]indol-3-yl)-1-methyl-4-oxo-1,4-dihydro-1,8-naphthyridine-3-carboxylic acid (10u).

Step (a). Preparation of ethyl 6-[8-[*tert*-butoxycarbonyl(ethyl)amino]-6-fluoro-4-[3-(trifluoromethyl)pyrazol-1-yl]-9H-pyrido[2,3-b]indol-3-yl]-1-methyl-4-oxo-1,8-naphthyridine-3-carboxylate. To a solution of *tert*-butyl N-(3,4-dichloro-6-fluoro-9H-pyrido[2,3-b]indol-8-yl)-N-ethyl-carbamate (80 mg, 0.16 mmol), ethyl 1-methyl-4-oxo-6-(4,4,5,5-tetramethyl-1,3,2-dioxaborolan-2-yl)-1,8-naphthyridine-3-carboxylate (132.5 mg, 0.48 mmol) and K_3PO_4 (135.8 mg, 0.64 mmol) in THF/H_2O (2.5 mL, v/v=10:1) was added Ad_2nBuP Biphenyl (21.4 mg, 0.032 mmol) under N_2 at 0 ^{o}C. The resulting reaction solution was degassed with N_2 several before it was stirred at 70 ^{o}C for 12 h. After LC-MS showed the reaction was completed, the mixture was poured into water (50 mL), and extracted with EtOAc (50 mL x 3). Combined organics were dried over anhy. Na_2SO_4, filtered, and concentrated *in vacuo* to give a crude product, which was purified by prep-TLC (DCM:EtOH = 30:1) to afford the title compound (72.5 mg, 67.8% yield) as a yellow solid. MS obsd (ESI+) [(M+H)$^+$] 694.3.

Step (b). Preparation of 6-[8-[*tert*-butoxycarbonyl(ethyl)amino]-6-fluoro-4-[3-(trifluoromethyl)pyrazol-1-yl]-9H-pyrido[2,3-b]indol-3-yl]-1-methyl-4-oxo-1,8-naphthyridine-3-carboxylic acid. To a solution of ethyl 6-[8-[*tert*-butoxycarbonyl(ethyl)amino]-6-fluoro-4-[3-(trifluoromethyl)pyrazol-1-yl]-9H-pyrido[2,3-b]indol-3-yl]-1-methyl-4-oxo-1,8-naphthyridine-3-carboxylate (62.5 mg, 0.091 mmol) in THF (3 mL) was added NaOH (36.2 mg, 0.91 mmol), and the resulting mixture was stirred at 30 ^{o}C for 1 h. Afterwards, the reaction mixture was poured into water (5 mL), adjust pH to 7 and extracted with EtOAc (10 mL). The organic layer was washed with aqueous

$CaCl_2$ solution (1N, 100 mL) twice, and brine (100 mL) twice. The organic layer was dried over anhy. Na_2SO_4, filtered, and concentrated *in vacuo* to give a crude product of the title compound (59.3 mg) as yellow oil. It was used directly in the next step without further purification. MS obsd (ESI+) [$(M+H)^+$] 666.2 ([$M+H]^+$).

Step (c). Preparation of 6-[8-(ethylamino)-6-fluoro-4-[3-(trifluoromethyl)pyrazol-1-yl]-9H-pyrido[2,3-b]indol-3-yl]-1-methyl-4-oxo-1,8-naphthyridine-3-carboxylic acid. To a solution of 6-[8-[*tert*-butoxycarbonyl(ethyl)amino]-6-fluoro-4-[3-(trifluoromethyl)pyrazol-1-yl]-9H-pyrido[2,3-b]indol-3-yl]-1-methyl-4-oxo-1,8-naphthyridine-3-carboxylic acid (49.3 mg, 0.074 mmol) in DCM (2 mL) was added TFA (0.4 mL), and the resulting mixture was stirred at 20 ^oC for 1 h. Afterwards, the mixture was concentrated to give a crude product, which was purified by prep-HPLC to afford the title compound (4.5 mg, 10.7% yield) as a yellow solid. MS obsd (ESI+) [$(M+H)^+$] 566.1. ^1H NMR (400 MHz, MeOH-*d4*) δ ppm 9.198 (s, 1 H), 8.900 (s, 1 H), 8.840 (s, 1 H), 8.367 (s, 1 H), 8.316 (s, 1 H), 7.086 (s, 1 H), 6.469-6.499 (d, 1 H), 5.731-5.752 (d, 1 H), 4.0859 (s, 3 H), 3.252 (m, 2 H), 1.297-1.331 (m, 3 H).

Synthetic procedure for the synthesis of N-ethyl-6-fluoro-3-[5-(1H-imidazol-2-ylmethyl)-3-pyridyl]-4-[3-(trifluoromethyl)pyrazol-1-yl]-9H-pyrido[2,3-b]indol-8-amine (15b).

Step (a). Preparation of 1-[8-[*tert*-butoxycarbonyl(ethyl)amino]-3-chloro-6-fluoro-9H-pyrido[2,3-b]indol-4-yl]pyrazole-3-carboxylic acid. A mixture solution of methyl 1-[8-[*tert*-butoxycarbonyl(ethyl)amino]-3-chloro-6-fluoro-9H-pyrido[2,3-b]indol-4-yl]pyrazole-3-carboxylate (70 mg, 0.114 mmol) and NaOH (29 mg, 0.719 mmol) in MeOH (5 mL) and H_2O (2 mL) was stirred at 10 ^oC for 12 h. Afterwards, the mixture was first adjusted to pH = 3 with 15% aqueous HCl solution, and then concentrated *in vauco* to give a crude product, which was purified by prep-HPLC to afford the title compound (66.5 mg, 97.1% yield) as a yellow solid. MS obsd (ESI+) [({^{35}Cl}M+H)$^+$] 474.0.

Step (b). Preparation of 1-[8-[*tert*-butoxycarbonyl(ethyl)amino]-3-(5-cyano-3-pyridyl)-6-fluoro-9H-pyrido[2,3-b]indol-4-yl]pyrazole-3-carboxylic acid. A solution of 1-[8-[*tert*-

butoxycarbonyl(ethyl)amino]-3-chloro-6-fluoro-9H-pyrido[2,3-b]indol-4-yl]pyrazole-3-carboxylic acid (30 mg, 0.063 mmol), 5-(4,4,5,5-tetramethyl-1,3,2-dioxaborolan-2-yl)pyridine-3-carbonitrile (29.2 mg, 0.127 mmol) and CsF (28.7 mg, 0.189 mmol) in 1,4-dioxane/H_2O (4 mL/0.4 mL) was first degassed with N_2 several times at 20 °C, and then $Pd_2(dba)_3$ (29.3 mg, 0.032 mmol) and Xantphos (15.2 mg, 0.032 mmol) were added to the mixture. After the addition, the resulting reaction solution was again degassed with N_2 for five times at 20 °C before it was stirred at 110 °C for 12 h. The reaction mixture was cooled down to room temperature and concentrated *in vacuo* to give a crude product, which was purified by prep-TLC (petroleum ether:EtOAc = 2:1) to afford the title compound (26.3 mg, 76.6% yield) as a yellow solid. MS obsd (ESI+) [$(M+H)^+$] 542.1.

Step (c). Preparation of 1-(3-(5-cyanopyridin-3-yl)-8-(ethylamino)-6-fluoro-9H-pyrido[2,3-b]indol-4-yl)-1H-pyrazole-3-carboxylic acid**.** To a solution of 1-[8-[*tert*-butoxycarbonyl(ethyl)amino]-3-(5-cyano-3-pyridyl)-6-fluoro-9H-pyrido[2,3-b]indol-4-yl]pyrazole-3-carboxylic acid (45 mg, 0.083 mmol) in DCM (2 mL) was added TFA (1 mL), and the resulting reaction mixture was stirred at 20 °C for 30 min. Afterwards, the mixture was concentrated *in vacuo* to give a crude product, which was purified by prep-HPLC to afford the title compound (14 mg, 38.1% yield) as a yellow solid. MS obsd (ESI+) [$(M+H)^+$] 442.1. HRMS calcd [$(M+H)^+$] 442.1428, measured [$(M+H)^+$] 442.1428. ^{1}H NMR (DMSO 400MHz) δ ppm 12.142 (br, 1H), 8.971 (s, 1H), 8.755 (s, 1H), 8.545-8.550 (d, 1H), 8.150-8.188 (m, 2H), 7.016-7.022 (m, 1H), 6.476-6.511 (m, 1H), 5.887 (m, 1H), 5.808-5.831 (m, 1H), 3.243-3.261 (m, 2H), 1.304-1.340 (m, 3H).

Synthetic procedure for the synthesis of 5-[4-[3-(aminomethyl)pyrazol-1-yl]-8-(ethylamino)-6-fluoro-9H-pyrido[2,3-b]indol-3-yl]pyridine-3-carbonitrile (15d).

Step (a). Preparation of *tert*-butyl N-[3-chloro-4-(3-cyanopyrazol-1-yl)-6-fluoro-9H-pyrido[2,3-b]indol-8-yl]-N-ethyl-carbamate. To a solution of *tert*-butyl N-(3,4-dichloro-6-fluoro-9H-pyrido[2,3-b]indol-8-yl)-N-ethyl-carbamate (140 mg, 0.352 mmol) and K_2CO_3 (145.0 mg, 1.05 mmol) in DMSO (2 mL) was added 1H-pyrazole-3-carbonitrile (98.2 mg, 1.05 mmol), and the resulting reaction mixture was stirred at 120 °C for 12 h. The mixture was cooled down to room temperature and extracted between

water (50 mL) and EtOAc (100 mL) twice. Combined organics were washed with brine (50 mL x 2), dried with anhy. Na_2SO_4, filtered, and concentrated *in vacuo* to give a crude product, which was purified by prep-TLC (petroleum ether: EtOAc = 2:1) to afford the title compound (140 mg, 87.6% yield) as a yellow solid. MS obsd (ESI+) [({^{35}Cl}M+H)$^+$] 455.1, [({^{37}Cl}M+H)$^+$] 457.1.

Step (b). Preparation of *tert*-butyl N-[4-[3-(aminomethyl)pyrazol-1-yl]-3-chloro-6-fluoro-9H-pyrido[2,3-b]indol-8-yl]-N-ethyl-carbamate. To a solution *tert*-butyl N-[3-chloro-4-(3-cyanopyrazol-1-yl)-6-fluoro-9H-pyrido[2,3-b]indol-8-yl]-N-ethyl-carbamate (140 mg, 0.308 mmol) in EtOH (6 mL), was added $NaBH_4$ (58.3 mg, 1.54 mmol) and $CoCl_2$ (80 mg, 0.616 mmol) at 0 °C, then the reaction mixture was first stirred at 0 °C for 1 h and then warmed up to room temperature and stirred for additional 1 h. After LC-MS indicated the completion of the reaction, the mixture was poured into water (50 mL) and extracted with EtOA (60 mL) three times. Combined organics were washed with brine (50 mL), dried over anhy. Na_2SO_4, filtered, and concentrated *in vacuo* to give a crude product, which was purified by prep-TLC (DCM:MeOH = 10:1) to afford the title compound (80 mg, 56.4% yield) as a yellow solid. MS obsd (ESI+) [({^{35}Cl}M+H)$^+$] 459.2, [({^{37}Cl}M+H)$^+$] 461.3.

Step (c). Preparation of *tert*-butyl N-[4-[3-(aminomethyl)pyrazol-1-yl]-3-(5-cyano-3-pyridyl)-6-fluoro-9H-pyrido[2,3-b]indol-8-yl]-N-ethyl-carbamate. A solution of *tert*-butyl N-[4-[3-(aminomethyl)pyrazol-1-yl]-3-chloro-6-fluoro-9H-pyrido[2,3-b]indol-8-yl]-N-ethyl-carbamate (80 mg, 0.174 mmol), 5-(4,4,5,5-tetramethyl-1,3,2-dioxaborolan-2-yl)pyridine-3-carbonitrile (80.2 mg, 0.349 mmol) and CsF (106 mg, 0.698 mmol) in 1,4-dioxane/H_2O (3 mL, v/v=10:1) was first degassed with N_2 several times, and then $Pd_2(dba)_3$ (16 mg, 0.0174 mmol) and Xantphos (16.6 mg, 0.0349 mmol) were added to the mixture. After the addition, the resulting reaction solution was again degassed with N_2 for five times at 20 °C before it was stirred at 110 °C for 12 h. The reaction mixture was cooled down to room temperature and extracted between water (40 mL) and EtOAc (80 mL) four times. Combined organics were washed with brine (50 mL), dried over anhy. Na_2SO_4, filtered, and concentrated *in vacuo* to give a crude product, which was further purified by prep-TLC (DCM:MeOH = 10:1) to afford *the* title compound (68 mg, 74.1% yield) as a yellow solid. MS obsd (ESI+) [(M+H)$^+$] 527.3.

Step (d). Preparation of 5-[4-[3-(aminomethyl)pyrazol-1-yl]-8-(ethylamino)-6-fluoro-9H-pyrido[2,3-b]indol-3-yl]pyridine-3-carbonitrile. To a solution of *tert*-butyl N-[4-[3-(aminomethyl)pyrazol-1-yl]-3-(5-cyano-3-pyridyl)-6-fluoro-9H-pyrido[2,3-b]indol-8-yl]-N-ethyl-carbamate (68 mg, 0.129 mmol) in DCM (3 mL) was added TFA (1.5 mL), and the resulting reaction mixture was stirred at room temperature for 1 h. Afterwards, the mixture was concentrated *in vacuo* to give a crude product, which was purified by prep-HPLC to afford the title compound (37 mg, 67.2% yield) as a yellow solid. MS obsd (ESI+) [$(M+H)^+$] 427.2. HRMS calcd [$(M+H)^+$] 427.1795, measured [$(M+H)^+$] 427.1794. ^{1}H NMR (400 MHz, DMSO-*d6*) δ ppm 12.13 (s, 1 H), 8.97 (d, 1 H), 8.72 (s, 1 H), 8.53 (d, 1 H), 8.32 (brs, 3 H), 8.18 (t, 1 H), 8.09 (d, 1 H), 6.69 (d, 1 H), 6.49 (dd, 1 H), 6.00 (dd, 1 H), 4.14 (q, 2 H), 3.25 (q, 2 H), 1.32 (t, 3 H).

Synthetic procedure for the synthesis of 1-[3-(5-cyano-3-pyridyl)-8-(ethylamino)-6-fluoro-9H-pyrido[2,3-b]indol-4-yl]-3-(trifluoromethyl)pyrazole-4-carboxamide (15p).

Step (a). Preparation of 1-(8-((*tert*-butoxycarbonyl)(ethyl)amino)-3-chloro-6-fluoro-9H-pyrido[2,3-b]indol-4-yl)-3-(trifluoromethyl)-1H-pyrazole-4-carboxylic acid. To a solution of *tert*-butyl (3,4-dichloro-6-fluoro-9H-pyrido[2,3-b]indol-8-yl)(ethyl)carbamate (440 mg, 1.1 mmol) and K_2CO_3 (610 mg, 4.42 mmol) in DMSO (6 mL) was added ethyl 3-(trifluoromethyl)-1H-pyrazole-4-carboxylate (920 mg, 4.42 mmol), and the resulting reaction mixture was stirred at 120 °C for 12 h. After the mixture was cooled down to room temperature, it was poured into water and extracted by EtOAc. The organic layer was washed with brine, dried with anhy. Na_2SO_4, filtered, and concentrated *in vacuo* to give a crude product, which was purified first by prep-TLC and then by silica gel flash chromatography to afford the title compound (200 mg, 33.4% yield) as a solid. MS obsd (ESI+) [$(\{^{35}Cl\}M+H)^+$] 542.2, [$(\{^{37}Cl\}M+H)^+$] 544.2.

Step (b). Preparation of 1-(8-((*tert*-butoxycarbonyl)(ethyl)amino)-3-(5-cyanopyridin-3-yl)-6-fluoro-9H-pyrido[2,3-b]indol-4-yl)-3-(trifluoromethyl)-1H-pyrazole-4-carboxylic acid. A solution of 1-(8-((*tert*-butoxycarbonyl)(ethyl)amino)-3-chloro-6-fluoro-9H-pyrido[2,3-b]indol-4-yl)-3-(trifluoromethyl)-1H-pyrazole-4-carboxylic acid (200 mg, 0.369 mmol), 5-(4,4,5,5-tetramethyl-1,3,2-

dioxaborolan-2-yl)nicotinonitrile (170 mg, 0.738 mmol), and CsF (224 mg, 1.476 mmol) in 1,4-dioxane/H_2O (6 mL, v/v = 10:1) was degassed with N_2 several times, and then $Pd_2(dba)_3$ (34 mg, 0.037 mmol) and Xantphos (36 mg, 0.074 mmol) were added into the mixture at 0 °C under N_2. The resulting reaction solution was degassed again with N_2 for five times at 20 °C before it was stirred at 110 °C for 12 h. The reaction mixture was cooled down to room temperature and extracted between water and EtOAc. The organic layer was washed with brine, dried with anhy. Na_2SO_4, filtered, and concentrated in vacuo to give a crude product, which was purified by silica gel flash chromatography to afford the title compound (200 mg, 88.9% yield) as a yellow solid. MS obsd (ESI+) [$(M+H)^+$] 610.2.

Step (c). Preparation of *tert*-butyl (4-(4-carbamoyl-3-(trifluoromethyl)-1H-pyrazol-1-yl)-3-(5-cyanopyridin-3-yl)-6-fluoro-9H-pyrido[2,3-b]indol-8-yl)(ethyl)carbamate. To a solution of 1-(8-((*tert*-butoxycarbonyl)(ethyl)amino)-3-(5-cyanopyridin-3-yl)-6-fluoro-9H-pyrido[2,3-b]indol-4-yl)-3-(trifluoromethyl)-1H-pyrazole-4-carboxylic acid (100 mg, 0.16 mmol), NH_4Cl (43 mg, 0.8 mmol), HOBt (65 mg, 0.48 mmol), and PyBOP (250 mg, 0.48 mmol) in DMF (5 mL) was added DIPEA (124 mg, 0.96 mmol) under N_2. The reaction mixture was stirred at 25 °C for 1 h before concentrated *in vacuo* to give a crude product, which was then purified by silica gel flash chromatography to afford the title compound (90 mg, 90.2% yield) as a yellow solid. MS obsd (ESI+) [$(M+H)^+$] 609.3.

Step (d). Preparation of 1-(3-(5-cyanopyridin-3-yl)-8-(ethylamino)-6-fluoro-9H-pyrido[2,3-b]indol-4-yl)-3-(trifluoromethyl)-1H-pyrazole-4-carboxamide. To a solution of *tert*-butyl (4-(4-carbamoyl-3-(trifluoromethyl)-1H-pyrazol-1-yl)-3-(5-cyanopyridin-3-yl)-6-fluoro-9H-pyrido[2,3-b]indol-8-yl)(ethyl)carbamate (80 mg, 0.131 mmol) in DCM (3 mL) was added TFA (1.5 mL), and the resulting mixture was stirred at 25 °C for 1 h. The reaction mixture was concentrated *in vacuo* to give a crude product, which was purified by prep-HPLC to afford the title compound (50 mg, 74.8% yield) as a yellow solid. MS obsd (ESI+) [$(M+H)^+$] 509.2. HRMS calcd [$(M+H)^+$] 509.1461, measured [$(M+H)^+$] 509.1459. ^{1}H NMR (400 MHz, DMSO-*d6*) δ ppm 12.23 (s, 1 H) 9.01 (d, 1 H), 8.77 (s, 1 H), 8.56-8.69 (m, 2 H), 8.24 (t, 1 H), 7.77 (brs, 1 H), 7.42 (brs, 1 H), 6.53 (dd, 1 H), 5.79-6.00 (m, 2 H), 3.27 (q, 2 H), 1.33 (t, 3 H).

Synthetic procedure for the synthesis of 5-[8-(ethylamino)-6-fluoro-4-[4-(hydroxymethyl)-3-(trifluoromethyl)pyrazol-1-yl]-9H-pyrido[2,3-b]indol-3-yl]pyridine-3-carbonitrile (15q).

Step (a). Preparation of ethyl 1-[8-[*tert*-butoxycarbonyl(ethyl)amino]-3-chloro-6-fluoro-9H-pyrido[2,3-b]indol-4-yl]-3-(trifluoromethyl)pyrazole-4-carboxylate. To a solution of *tert*-butyl N-(3,4-dichloro-6-fluoro-9H-pyrido[2,3-b]indol-8-yl)-N-ethyl-carbamate (440 mg, 1.1 mmol) and K_2CO_3 (610 mg, 4.42 mmol) in DMSO (6 mL) was added ethyl 3-(trifluoromethyl)-1H-pyrazole-4-carboxylate (920 mg, 4.42 mmol), and the reaction solution was stirred at 120 ^oC for 12 h. The mixture was poured into water (50 mL) and extracted by EtOAc (100 mL) twice. Combined organics were washed with brine (50 mL x 2), dried with anhy. Na_2SO_4, filtered, and concentrated *in vacuo* to give a crude product, which was purified by prep-TLC (petroleum ether: EtOAc = 3:1) and then silica gel flash chromatography to afford the title compound (330 mg, 52.4% yield) as a solid. MS obsd (ESI+) [({^{35}Cl}M+H)$^+$] 570.1, [({^{37}Cl}M+H)$^+$] 572.2.

Step (b). Preparation of *tert*-butyl N-[3-chloro-6-fluoro-4-[4-(hydroxymethyl)-3-(trifluoromethyl)pyrazol-1-yl]-9H-pyrido[2,3-b]indol-8-yl]-N-ethyl-carbamate. To a solution of ethyl 1-[8-[*tert*-butoxycarbonyl(ethyl)amino]-3-(5-cyano-3-pyridyl)-6-fluoro-9H-pyrido[2,3-b]indol-4-yl]-3-(trifluoromethyl)pyrazole-4-carboxylate (180 mg, 0.316 mmol) in THF (0.316 mL) was added LAH (30 mg, 0.790 mmol) at 0 ^oC under N_2, and the reaction mixture was stirred at 0 ^oC for 1 h. The mixture was poured into water (50 mL) and extracted with EtOAc (100 mL x 2). Combined organics were washed with brine (50 mL x 2), dried over anhy. Na_2SO_4, filtered, and concentrated *in vacuo* to give a crude title compound (140 mg, 84% yield) as a yellow solid. It was used directly in the next step without further purification. MS obsd (ESI+) [({^{35}Cl}M+H)$^+$] 528.1, [({^{37}Cl}M+H)$^+$] 530.1.

Step (c). Preparation of *tert*-butyl N-[3-(5-cyano-3-pyridyl)-6-fluoro-4-[4-(hydroxymethyl)-3-(trifluoromethyl)pyrazol-1-yl]-9H-pyrido[2,3-b]indol-8-yl]-N-ethyl-carbamate. A solution of *tert*-butyl N-[3-chloro-6-fluoro-4-[4-(hydroxymethyl)-3-(trifluoromethyl)pyrazol-1-yl]-9H-pyrido[2,3-b]indol-8-yl]-N-ethyl-carbamate (130 mg, 0.246 mmol), 5-(4,4,5,5-tetramethyl-1,3,2-dioxaborolan-2-yl)pyridine-3-carbonitrile (113 mg, 0.493 mmol), and CsF (150 mg, 0.986 mmol) in 1,4-dioxane/H_2O (4 mL, v/v=10:1) was degassed with N_2 for five times, and then $Pd_2(dba)_3$ (22.5 mg, 0.0246 mmol) and

Xantphos (23.5 mg, 0.0493 mmol) were added to the mixture at 0 °C under N_2. After the addition, the resulting reaction solution was degassed again with N_2 for five times at 20 °C before it was stirred at 110 °C for 12 h. The reaction mixture was cooled down to room temperature and extracted between water (20 mL) and EtOAc (150 mL x 2). Combined organics were washed with brine (30 mL), dried over anhy. Na_2SO_4, filtered, and concentrated *in vacuo* to give a crude product, which was purified by prep-TLC (DCM:MeOH = 30:1) to afford the title compound (120 mg, 81.8% yield) as a pale yellow solid. MS obsd (ESI+) [$(M+H)^+$] 596.3.

Step (d). Preparation of 5-[8-(ethylamino)-6-fluoro-4-[4-(hydroxymethyl)-3-(trifluoromethyl)pyrazol-1-yl]-9H-pyrido[2,3-b]indol-3-yl]pyridine-3-carbonitrile. To a solution of *tert*-butyl N-[3-(5-cyano-3-pyridyl)-6-fluoro-4-[4-(hydroxymethyl)-3-(trifluoromethyl)pyrazol-1-yl]-9H-pyrido[2,3-b]indol-8-yl]-N-ethyl-carbamate (110 mg, 0.185 mmol) in DCM (3 mL) was added TFA (1.5 mL) and the resulting mixture solution was stirred at 25° C for 1 h. Afterwards, the mixture was concentrated in vacuo to give a crude product, which was purified by prep-HPLC (0.5% TFA in water) to afford the title compound (77 mg, 84.2 % yield) as a yellow solid. MS obsd (ESI+) [$(M+H)^+$] 496.2. HRMS calcd [$(M+H)^+$] 496.1509, measured [$(M+H)^+$] 496.1509. ^{1}H NMR (400 MHz, DMSO-*d6)* δ ppm 12.16 (s, 1 H), 8.99 (d, 1 H), 8.74 (s, 1 H), 8.59 (d, 1 H), 8.08-8.24 (m, 2 H), 6.51 (d, 1 H), 5.92 (d, 1 H), 4.51 (s, 4 H), 3.26 (q, 2 H), 1.32 (t, 3 H). ^{13}C NMR (101 MHz, DMSO-*d6)* δ ppm 160.3, 158.0, 153.2, 153.0, 151.5, 148.4, 140.3, 140.2, 140.0, 138.4, 136.8, 136.7, 134.7, 131.9, 123.9, 123.3, 120.7, 120.6, 117.1, 117.0, 116.8, 111.9, 109.3, 95.6, 93.8, 53.3, 38.1, 14.5.

Synthetic procedure for the synthesis of 5-[4-[4-(Aminomethyl)-3-(trifluoromethyl)pyrazol-1-yl]-8-(ethylamino)-6-fluoro-9H-pyrido[2,3-b]indol-3-yl]pyridine-3-carbonitrile (15r).

Step (a). Preparation of *tert*-butyl N-[4-[4-carbamoyl-3-(trifluoromethyl)pyrazol-1-yl]-3-chloro-6-fluoro-9H-pyrido[2,3-b]indol-8-yl]-N-ethyl-carbamate. To a solution of 1-(8-((*tert*-butoxycarbonyl)(ethyl)amino)-3-chloro-6-fluoro-9H-pyrido[2,3-b]indol-4-yl)-3-(trifluoromethyl)-1H-pyrazole-4-carboxylic acid (520 mg, 0.960 mmol), NH_4Cl (257 mg, 4.8 mmol), HOBt (389 mg, 2.88 mmol), and PyBOP (1.5 g, 2.88 mmol) in DMF (12 mL) was added DIPEA (745 mg, 5.76 mmol) under

N_2. The reaction mixture was stirred at 30 °C for 1 h before concentrated *in vacuo* to give a crude product, which was purified by silica gel flash chromatography to afford the title compound (500 mg, 96.3% yield) as a yellow solid. MS obsd (ESI+) [({^{35}Cl}M+H)$^+$] 541.1, [({^{37}Cl}M+H)$^+$] 543.0.

Step (b). Preparation of *tert*-butyl N-[4-[4-(aminomethyl)-3-(trifluoromethyl)pyrazol-1-yl]-3-chloro-6-fluoro-9H-pyrido[2,3-b]indol-8-yl]-N-ethyl-carbamate. To a solution of BH_3/THF (1N, 10 mL, 10 mmol) was added *tert*-butyl N-[4-[4-carbamoyl-3-(trifluoromethyl)pyrazol-1-yl]-3-chloro-6-fluoro-9H-pyrido[2,3-b]indol-8-yl]-N-ethyl-carbamate (100 mg, 0.185 mmol) at 0 °C under N_2, then the resulting reaction mixture was stirred at 80 °C for 0.5 h. Afterwards, the mixture was cooled down to room temperature and poured into MeOH (150 mL) at 0 °C. The mixture was then concentrated *in vacuo* to give a crude product, which was purified by prep-TLC (DCM:MeOH = 10:1) to afford the title compound (80 mg, 27.4% yield) as a yellow solid. MS obsd (ESI+) [({^{35}Cl}M+H)$^+$] 527.2, [({^{37}Cl}M+H)$^+$] 529.3.

Step (c). Preparation of *tert*-butyl N-[4-[4-(aminomethyl)-3-(trifluoromethyl)pyrazol-1-yl]-3-(5-cyano-3-pyridyl)-6-fluoro-9H-pyrido[2,3-b]indol-8-yl]-N-ethyl-carbamate. A solution of *tert*-butyl N-[4-[4-(aminomethyl)-3-(trifluoromethyl)pyrazol-1-yl]-3-chloro-6-fluoro-9H-pyrido[2,3-b]indol-8-yl]-N-ethyl-carbamate (35 mg, 0.066 mmol), 5-(4,4,5,5-tetramethyl-1,3,2-dioxaborolan-2-yl)nicotinonitrile (31 mg, 0.133 mmol) and CsF (40 mg, 0.264 mmol) in 1,4-dioxane/H_2O (2 mL, v/v = 10:1) was degassed with N_2 several times, and then $Pd_2(dba)_3$ (18.2 mg, 0.0198 mmol) and Xantphos (12.6 mg, 0.0264 mmol) were added to the mixture at 0 °C under N_2. After the addition, the resulting reaction solution was degassed again with N_2 for five times at 20 °C before it was stirred at 100 °C for 12 h. The reaction mixture was cooled down to room temperature and extracted between water (40 mL) and EtOAc (100 mL) twice. Combined organics were washed with brine (50 mL), dried over anhy. Na_2SO_4, filtered, and concentrated *in vacuo* to give a crude product, which was purified by prep-TLC (DCM:MeOH = 10:1) to afford the title compound (30 mg, 76% yield) as a yellow solid. MS obsd (ESI+) [(M+H)$^+$] 595.2.

Step (d). Preparation of 5-(4-(4-(Aminomethyl)-3-(trifluoromethyl)-1H-pyrazol-1-yl)-8-(ethylamino)-6-fluoro-9H-pyrido[2,3-b]indol-3-yl)nicotinonitrile 2,2,2-trifluoroacetate. To a solution of *tert*-butyl N-

[4-[4-(aminomethyl)-3-(trifluoromethyl)pyrazol-1-yl]-3-(5-cyano-3-pyridyl)-6-fluoro-9H-pyrido[2,3-b]indol-8-yl]-N-ethyl-carbamate (25 mg, 0.042 mmol) in DCM (2 mL) was added TFA (1 mL), and the resulting reaction mixture was stirred at 30 ^{o}C for 1 h. Afterwards, the reaction mixture was concentrated *in vacuo* to give a crude product, which was purified by prep-HPLC to afford the title compound (13.5 mg, 67.5% yield) as a yellow solid. MS obsd (ESI+) [(M+H)$^{+}$] 495.3. HRMS calcd [(M+H)$^{+}$] 495.1669, measured [(M+H)$^{+}$] 495.1669. ^{1}H NMR (400 MHz, DMSO-*d*6) δ ppm 12.28 (s, 1 H), 9.00 (d, 1 H), 8.74 (s, 1 H), 8.55 (d, 1 H), 8.36 (br. s., 3 H), 8.30 (s, 1 H), 8.19 (s, 1 H), 6.51 (dd, 1.76 Hz, 1 H), 6.02 (dd, 1.76 Hz, 1 H), 4.09 (br. s., 2 H), 3.26 (q, 2 H), 1.32 (t, 3 H). ^{13}C NMR (101 MHz, DMSO-*d6*) δ ppm 160.2, 157.9, 153.1, 151.5, 148.3, 140.1, 138.4, 136.7, 134.5, 131.9, 125.8, 125.1, 123.4, 120.6, 117.1, 117.0, 116.9, 111.7, 109.3, 95.6, 93.9, 38.1, 35.3, 14.5.

4-[4-(Aminomethyl)-3-(trifluoromethyl)pyrazol-1-yl]-N-ethyl-6-fluoro-3-(2-methoxypyrimidin-5-yl)-9H-pyrido[2,3-b]indol-8-amine (17r).

The title compound was prepared by a similar procedure to that described for compound **15r**. MS obsd (ESI+) [(M+H)$^{+}$] 501.1. HRMS calcd [(M+H)$^{+}$] 501.1774, measured [(M+H)$^{+}$] 501.1775. ^{1}H NMR (400 MHz, DMSO-*d6*) δ ppm 12.23 (s, 1H), 8.71 (s, 1H), 8.31-8.40 (m, 6H), 6.48 (m, 1H), 5.94 (m, 1H), 4.12 (s, 2H), 3.94 (s, 3H), 3.25 (q, 2H), 1.32 (t, 3H). ^{13}C NMR (101 MHz, DMSO-*d6*) δ 164.7, 160.2, 159.1, 157.9, 153.0, 148.1, 139.8, 138.3, 136.7, 134.2, 125.6, 125.1, 123.5, 123.5, 119.2, 116.8, 112.1, 95.4, 93.7, 55.2, 38.1, 35.3, 14.5.

***In Vitro* Assay for the Determination of GyrB and ParE Inhibition (*Ki*).** The *E. coli* GyrB, ParE and ParC proteins were purified from *E. coli* cells overexpressing the respective genes individually. *Ki* for the respective enzymes was determined by ATPase coupled reaction assay modified from previously published method.[15] All chemicals were purchased from Sigma Chemicals. The reaction volume was 60 uL. For the GyrB reaction, the reaction mixture contained final concentrations of 40 mM Tris.HCl (pH 8.0), 25 mM KCl, 2.5 mM Spermidine, 4 mM $MgCl_2$, 0.4 mM phosphoenolpyruvate monopotassium, 0.5 mM NADH (B-NAD reduced form dipotassium), 0.4 uM pyruvate kinase (Sigma P1506), 0.4 uM L-lactic dehydrogenase (Sigma L3916), 20-60 nM GyrB (depending on the desired assay window) and 600 uM ATP. The reaction was started with the addition of ATP substrate and the

initial OD340 of the reaction in 384 microtiter well was measured and recorded in a plate reader (Envision 2103, Perkin Elmer). After desired time (120-180 min) of incubation at room temperature, the OD340 of the reaction mixture was measured again. The change in the OD340 was used as the extent of ATP to ADP conversion during the reaction. To test compound inhibition, a 18 point 2-fold titration was done for each compound, including a no compound (100% reaction) control. After the reaction, the fractional reaction velocity at each compound concentration was obtained and data points were plotted against the linear concentration. The *Ki* value was obtained through a Morrison curve-fit with either GraphPad or XcelFit softwares, setting ATP Km at 600 uM.

For the ParE reaction, the condition was the same as for the GyrB except 50 nM ParE and 50 nM ParC proteins were mixed with DNA (Sigma D1626) and added instead of the GyrB protein. The ATP Km for the ParC/ParE was also previously determined to be 800 uM. Unlike GyrB, ParE protein alone contained very low level ATPase activity, therefore, ParC protein was needed for efficient reaction to occur.

Minimal Inhibitory Concentration (MIC) Measurement. The MIC of antibacterial compounds against multiple species and strains was determined using the broth microdilution method according to M07-A10 Clinical and Laboratory Standards Institute (CLSI) guidelines (CLSI (2015) Methods for dilution antimicrobial susceptibility tests for bacteria that grow aerobically; Approved Standard, Tenth Edition. CLSI Document M7-A10 (ISBN 1-56238-987-4). Wayne, PA: Clinical and Laboratory Standards Institute, 19087, USA). In short, bacterial strain preparation was performed on Day1 and Day 2. The bacterial strains were revived from storage frozen two days before the MIC screening and streaked onto the surface of agar plates, incubated in an ambient-air incubator with humidity for 20-24 hr at 35±2 °C. 5-10 well-isolated colonies of similar morphology were selected and re-streaked onto fresh agar plates using sterile loops and incubated for 20-24 hr at 35±2 °C. Bacterial strains were sub-cultured two times to ensure fresh inoculums for MIC screening. On the day of MIC assay (Day 3), colonies were transferred from fresh culture plates into 5 mL of saline with sterile loops and mixed well, which was measured and adjusted turbidity to 0.5 McFarland barium sulfate standard ($1\text{-}2\times10^8$

Colony Forming Units (CFU)/mL) using a turbidity meter. Alternatively, 1-2 colonies were transferred into 500 µL of saline, and OD600 was adjusted to ~0.1 using an OD meter. Bacterial inoculum was diluted by 1:280 for Gram-positive strains and 1:400 for Gram-negative strains into corresponding medium broth (CAMHB) (e.g. 35.6 µL of inoculum into 10 mL of CAMHB or 25 µL of inoculum into 10 mL of CAMHB). For the compound plate, the compound stock solutions were prepared in 100% DMSO on the day of MIC screening and used immediately. Compound stock concentration = [(highest testing concentration) × 100 µL / 2 µL] (e.g. if the required highest testing concentration is 16 µg/mL in assay plates, stock concentration = 16 µg/mL ×100 µL / 2 µL =3.2 mg/mL). The compound plates were prepared by dispensing 100 µL of each stock solution in the first well of a 96 well microtiter plate (MTP) at a concentration 100-fold higher than the final concentration desired in broth. Eleven serial 2-fold dilutions of the highest concentration were made in DMSO for new compounds and for reference compounds (GP-6 and ciprofloxacin). 1 µL of each well was transferred in a new MTP, which served as the test plate by subsequent inoculation. The bacterial suspension prepared above is dispensed at 98 µL/well within 15 minutes after preparation. Negative controls (lack of bacterial cells) and growth control wells (lack of compound) were included in all plates. MTPs were incubated for 18-24 hours at 35±2 ^{o}C in ambient air. The MIC was recorded and CFUs were calculated on Day 4. The assay plate was placed on top of the MIC reader, and the magnification mirror was adjusted to read each well, recording growth status as raw data. Photo images of each assay plates were recorded using Q Count 530 (Spiral Biotech). The MIC value of each compound, expressed as µg/mL, was determined as the lowest concentration required for complete growth inhibition (no visible growth).

pKa Determination. Acid dissociation constant (ionization constant) pKa is determined in a high-throughput assay based on photometric titration. This technique allows relating the UV-spectral changes of a molecule upon addition of acid or base to its degree of ionization. In the ProfilerSGA (Sirius Analytical Instruments Ltd.), an aqueous solution of sample compound (solubility up to 10^{-6} M) is injected at constant flow rate into a flowing pH gradient. Changes in UV absorbance are monitored as a function of the pH gradient. The pKa valuess are found and determined where the rate of change of

absorbance is at a maximum. The pH gradient is established by proportionally mixing two flowing buffer solutions containing 10%/volume methanol. The buffer solutions contain a mixture of weak acids and bases that do not absorb significantly in the UV above 240 nm.

logD Determination. The distribution coefficient of compounds was determined in a carrier-mediated distribution system (CAMDIS, EP2005102211A) assay, as previously reported.[25]

Solubility. The solubility of compounds was determined in a lyophilization solubility assay (LYSA). The test samples were prepared in duplicate from 10 mM DMSO stock solution. After the evaporation of DMSO with a centrifugal vacuum evaporator, the compounds were redissolved in a phosphate buffer (0.05 M, pH 6.5). The mixture was stirred for 1 hr, shaken for 2 hr, and then allowed to stand overnight and filtered through a microtiter filter plate. The filtrate and its 1/10 dilution were analyzed by HPLC-UV. Solubility determination was determined from a four-point calibration curve; the percentage of the sample measured in solution after evaporation divided by the calculated maximum of sample amount was bigger than 80%; and the solubility data were reported as bigger than this value, with a unit of μg/mL.

Liver Microsomal Stability (LM). Each test compound was preincubated in an incubation mixture consisted of 0.5 mg of microsomal protein/mL mouse liver microsomes, 1 mM NADP, 3 mM glucose 6-phosphate, 3 mM $MgCl_2$, and 0.05 mg/mL glucose 6-phosphate dehydrogenase in a total volume of 400 μL of potassium phosphate buffer (100 mM, pH 7.4) for 10 min at 37 ^{o}C. The reactions were initiated by the addition of NADPH regenerating system. At different time points (0, 3, 6, 9, 15, and 30 min), an aliquot (50 μL) sample was taken and quenched with 150 μL of acetonitrile containing an internal standard. Following precipitation and centrifugation, the supernatants were analyzed by LC/MS-MS.

Hepatocyte Stability (Hepa Cl). Metabolic stability of compounds in mouse liver hepatocyte was determined in screening mode using hepatocyte suspension culture. Incubations of a test compound at different concentrations are performed in 96 well plates containing liver cells (5% CO_2 atmosphere and 37 °C). At defined time points, either cell medium is taken, or the whole well is quenched with acetonitrile containing an internal standard. Samples are then cooled and centrifuged before analysis by LC-MS/MS. Log peak area ratios (test compound peak area / internal standard peak area) or concentrations are plotted against incubation time, and a linear fit made to the data with emphasis upon the initial rate of compound disappearance. The slope of the fit is then used to calculate the intrinsic clearance: Cl_{int} (μL/min/1x10^6 cells) = -slope (min^{-1}) * 1000 / [1x10^6 cells].

Plasma Protein Binding (fu). The percentage of unbound compound was determined using a 96-well Micro-Equilibrium dialysis device (HTDialysis, Gales Ferry, CT, USA) with a molecular weight cutoff membrane of 12-14 kDa (HTDialysis, Gales Ferry, CT, USA) and using Diazepam as a positive control. Pooled rat and cynomolgus monkey plasma were purchased from Biopredic (Rennes, France). Compounds were measured in a cassette of 2-5 with an initial total concentration of 1 μM, and one of the cassette compounds is the positive control. The integrity of membranes was validated by confirming the unbound fraction values of the positive control. Equal volumes of blank dialysis buffer (Soerensen buffer at pH 7.4) and matrix samples containing substances were loaded into the acceptor and donor compartment, respectively. The HTD dialysis block was then sealed and kept in an incubator at 37 °C for 5 hr under 5% CO_2 environment. At the end of dialysis, the plasma and buffer samples were retrieved and the drug concentrations were quantified by LC/MS-MS.

Single dose Intravenous PK study in Female CD-1 mouse. The single-dose PK in female CD-1 mouse was performed to assess the compound's pharmacokinetic properties. One group of animals were dosed via bolus intravenous (IV) of the respective compound. Blood samples (approximately 30 μL) were collected via saphenous vein at 5 mins, 15 min, 30 min, 1hr, 2hr, 4hr, and 7hr. For the last time point (24hr), samples were collected via cardiac puncture while the mouse was under anesthesia. Blood

samples were placed into tubes containing EDTA-K2 anticoagulant (2 μL of 0.5M per tube) and centrifuged at 3000 rpm for 10 minutes at 4°C within half an hour to separate plasma from the samples. Following centrifugation, plasma samples were stored in polypropylene tubes, quick-frozen over dry ice, and kept at −70±10 °C until LC-MS/MS analysis. The pharmacokinetic parameters were calculated using a non-compartmental module of WinNonlin® Professional 6.4.

Experimental Details for Protein Generation and Crystallization of *P. aeruginosa* GyrB with Compounds 12o and 12x. ATP-binding domain of *P. aeruginosa* GyrB was cloned into vector pET30 (Novagen) with a C terminal 6xHis tag and overexpressed in *E. coli* strain BL21 (DE3) at 16 ^{0}C overnight. Cell pellets were lysed and purified with nickel affinity, ion exchange, and size exclusion chromatography. The purified protein was concentrated and stored in a buffer solution containing 20 mM Tris (pH 8.0) and 200 mM NaCl. The protein-ligand complex was co-crystallized by sitting drop vapor diffusion method with reservoir solution: 38% w/v PEG3350, 200mM Lithium sulfate, and 100 mM sodium citrate (pH 5.6). Cocrystals appeared within two weeks and were flash-frozen with the addition of 20% glycerol. X-ray diffraction images were collected at 100 K at the beamline BL17U of the Shanghai Synchrotron Radiation Facility (SSRF).

Experimental Details for *in vivo* Neutropenic Mouse Thigh Infection Experiments. Female ICR mice weighing 23-25 g were purchased from Beijing Vital River Laboratory Animal Technology Co. Ltd. The animals were housed at 20-25 °C and 40-70% relative humidity, with food and water available ad libitum throughout the study. The study protocol was approved by the Institutional Animal Care and Use Committee (IACUC) of Roche Pharma Research and Early Development China. Mice were rendered neutropenic (neutrophils, less than 100/mm^3) by injection of cyclophosphamide (Shanxi Pude Pharmaceuticals, Co. Ltd) intraperitoneally 4 days (150 mg/kg body weight) and 1 day (100 mg/kg) before thigh infection. Thigh infection in mice was carried out by intramuscular injection of 0.1 mL inoculum into right posterior thigh muscle, with about an inoculum size of 10^6 CFU/thigh (inoculum was prepared by inoculating single colony into fresh MHB media the day prior to thigh infection and

cultured at 150 rpm and 35 °C for 15 hr. The overnight culture (the bacterial suspension) was further diluted to a concentration of 10^7 CFU/mL in fresh MHB media prior to use). 2 hours post thigh infection, mice were dosed with compound via intravenous tail injection. Blood samples were collected -5 min, 30 min, 55 min, 1.5 h, 2 h, 3 h, 5 h, 7 h, and 24 h after compound or vehicle application. The mice were sacrificed by euthanasia after 12 or 24 hr of therapy, and the thighs were removed. Thigh muscles were transferred into 5 mL sterile EP tubes and homogenized in 2 mL saline for subsequent CFU determination.

ASSOCIATED CONTENT

Supporting Information

^{1}H NMR, ^{13}C NMR and LC-MS spectra of compounds **15r**, **17r**, and **17x**; PK/PD correlation of compound **17r** in neutropenic mouse thigh infection model; molecular formula strings of compounds **10**, **12**, **15**, and **17**. This material is available free of charge via the Internet at http://pubs.acs.org.

Accession Codes

The PDB codes for **12o** and **12x** are 6M1S and 6M1J, respectively. Authors will release the atomic coordinates and experimental data upon article publication.

AUTHOR INFORMATION

Corresponding Author

*Phone: +86 21 28946746. E-mail: xuefei.tan@roche.com.

Author Contributions

All authors have given approval to the final version of the manuscript.

Notes

The authors declare no competing financial interest.

ACKNOWLEDGMENT

We acknowledge Liqin Chen, Leimin Wang, Xiaojie Xia, Qingshan Gao, Yujuan Gao, and Dr. Jin Ge for technical assistance in the purification of final compounds and analytical analysis. We thank Yi Zhang, Hongxia Qiu, Yuxia Zhang, and Sheng Zhong for the support of DMPK profiling. This work was supported exclusively by F. Hoffmann-La Roche Ltd.

ABBREVIATIONS

PDB, protein data bank; PK, pharmacokinetics; PD, pharmacodynamics; SDPK, single dose pharmacokinetics; HPLC, high-performance liquid chromatography; SFC, supercritical fluid chromatography; UV, ultraviolet spectrometry; CFU, colony forming units; BINAP, 2,2′-bis(diphenylphosphino)-1,1′-binaphthyl; MCPBA, meta-chloroperoxybenzoic acid; X-phos, 2-dicyclohexylphosphino-2′,4′,6′-triisopropylbiphenyl; DBU, 1,8-diazabicyclo[5.4. 0]undec-7-ene; DMA, dimethylacetamide; HOBt, 1-Hydroxybenzotriazole; PyBOP, benzotriazol-1-yl-oxytripyrrolidinophosphonium hexafluorophosphate; Xantphos, 4,5-Bis(diphenylphosphino)-9,9-dimethylxanthene.

REFERENCES

(1) Pendleton, J. N.; Gorman, S. P.; Gilmore, B. F. Clinical relevance of the ESKAPE pathogens. *Expert Rev. Anti-Infect. Ther.* **2013**, *11*, 297-308.

(2) Santajit, S.; Indrawattana, N. Mechanisms of antimicrobial resistance in ESKAPE pathogens. *Biomed. Res. Int.* **2016**, *2016*, 2475067.

(3) Kim, W.; Prosen, K. R.; Lepore, C. J.; Coukell, A. On the road to discovering urgently needed antibiotics: so close yet so far away. *ACS Infect. Dis.* **2020**, *6*, 1292-1294.

(4) Silver, L. L. A gestalt approach to gram-negative entry. *Bioorg. Med. Chem.* **2016**, *24*, 6379-6389.

(5) Nabriva Therapeutics Receives U.S. FDA Approval of Xenleta™ (lefamulin) to Treat Community-Acquired Bacteria Pneumonia (CABP) [news release]. http://investors.nabriva.com (accessed August 19, 2019).

(6) Silver, L. L. Challenges of antibacterial discovery. *Clin. Microbio. Rev.* **2011**, *24*, 71-109.

(7) Schillaci, D.; Spanò, V.; Parrino, B.; Carbone, A.; Montalbano, A.; Barraja, P.; Diana, P.; Cirrincione, G.; Cascioferro, S. Pharmaceutical approached to target antiobiotic resistance mechanisms. *J. Med. Chem.* **2017**, *60*, 8268-8297.

(8) Champoux, J. J. DNA topoisomerases: structure, function, and mechanism. *Annu. Rev. Biochem.* **2001**, *70*, 369-413.

(9) Azam, M. A.; Thathan, J.; Jubie, S. Dual targeting DNA gyrase B (GyrB) and topoisomerse IV (ParE) inhibitors: a review. *Bioorg Chem.* **2015**, *62*, 41-63.

(10) Dalhoff, A. Global fluoroquinolone resistance epidemiology and implictions for clinical use. *Interdiscip. Perspect. Infec. Dis.* **2012**, *2012*, 976273.

(11) Redgrave, L. S.; Sutton, S. B.; Webber, M. A.; Piddock, L. J.V. Fluoroquinolone resistance: mechanisms, impact on bacteria, and role in evolutionary success. *Trends Microbiol.* **2014**, *22*, 438-445.

(12) Shirude, P. S.; Hameed, S. Nonfluoroquinolone-based inhibitors of mycobacterial type II topoisomerase as potential therapeutic agents for TB. *Annu. Rep. Med Chem.* **2012,** *47,* 319-330.

(13) Bisacchi, G. S.; Manchester, J. I. A new-class antibacterial-almost. Lessons in drug discovery and development: a critical analysis of more than 50 years of effort toward ATPase inhibitors of DNA gyrase and topoisomerase IV. *ACS Infect. Dis.* **2015**, *1*, 4-41.

(14) Tiz, D. B.; Kikelj D.; Zidar, N. Overcoming problems of poor drug penetration into bacteria: challenges and strategies for medicinal chemists. *Expert Opin. Drug Discov.* **2018**, *13*, 497-507.

(15) Durcik, M.; Tomašič, T.; Zidar, N.; Zega, A.; Kikelj, D.; Mašič, L. P.; Ilaš, J. ATP competitive DNA gyrase and topoisomerase IV inhibitors as antibacterial agents, *Expert Opin. Thera. Pat.* **2019**, *29*, 171-180.

(16) Tari, L. W., Li, X., Trzoss, M., Bensen, D. C., Chen, Z.; Lam, T., Zhang, J., Lee, S. J., Hough, G., Phillipson, D., Akers-Rodriguez, S., Cunningham, M. L., Kwan, B. P.; Nelson, K. L.; Castellano, A., Locke, J. B., Brown-Driver, V., Murphy, T. M., Ong, V. S., Pillar, C. M.; Shinabarger, D. L.; Nix J.; Lightstone, F. C., Wong, S. E., Nguyen, T. B., Shaw, K. J., and Finn, J. Tricyclic GyrB/ParE

(TriBE) inhibitors: a new class of broad-spectrum dual-targeting antibacterial agents. *PLoS One* **2013**, *8*, e84409.

(17) Tari, L. W., Li, X., Trzoss, M., Bensen, D. C., Li, X.; Chen, Z.; Lam, T., Zhang, J., Creighton, C. J.; Cunningham, M. L., Kwan, B.; Stidham, M.; Shaw, K. J.; Lightstone, F. C., Wong, S. E.; Nguyen, T. B.; Nix, J.; Finn, J. Pyrrolopyrimidine inhibitors of DNA gyrase B (GyrB) and topoisomerase IV (ParE). Part I: Structural guided discovery and optimization of dual targeting agents with potent, broad-spectrum enzymatic acticity. *Bioorg. Med. Chem. Lett.* **2013**, *23*, 1529-1536.

(18) Trzoss, M.; Bensen, D. C., Li, X.; Chen, Z.; Lam, T., Zhang, J., Creighton, C. J.; Cunningham, M. L., Kwan, B.; Stidham, M.; Nelson, K.; Brown-Driver, V.; Castellano, A.; Shaw, K. J.; Lightstone, F. C., Wong, S. E.; Nguyen, T. B.; Nix, J.; Finn, J.; Tari, L. W. Pyrrolopyrimidine inhibitors of DNA gyrase B (GyrB) and topoisomerase IV (ParE). Part II: Development of inhibitors with broad-spectrum, Gram-negative antibacterial activity. *Bioorg. Med. Chem. Lett.* **2013**, *23*, 1537-1543.

(19) Ho, S. Y.; Wang, W.; Ng, F. M.; Wong, Y. X.; Poh, Z. Y.; Tan, S. W. W.; Ang, S. H., Liew, S. S.; Wong, Y. S. J.; Tan, Y.; Poulsen, A.; Pendharkar, V.; Sangthongpitag, K.; Manchester, J.; Basarab, G.; Hill, J.; Keller, T. H.; Cherian, J. Discovery of dual GyrB/ParE inhibitors active against gram-negative bacteria. *Eur. J. Med. Chem.* **2018**, *157*, 610-621.

(20) Rosemarie O'Shea, R.; Heinz E. Moser, H. E. Physicochemical properties of antibacterial compounds: implications for drug discovery. *J. Med. Chem.* **2008**, *51*, 2871-2878.

(21) Brown, D. G.; May-Dracka, T. L.; Gagnon, M. M.; Tommasi, R. Trends and exceptions of physical properties on antibacterial activity for gram-positive and gram-negative pathogens. *J. Med. Chem.* **2014**, *57*, 10144-10161.

(22) Manchester, J. I.; Dussault, D. D.; Rose, J. A.; Boriack-Sjodin, P. A.; Uria-Nickelsen, M.; Ioannidis, G. Bist, S.; Fleming, P.; Hull, K. G. Discovery of a novel azaindole class of antibacterial agents targeting the ATPase domains of DNA gyrase and Topoisomerase IV. *Bioorg. Med. Chem. Lett.* **2012**, *22*, 5150-5156.

(23) Richter, M. F.; Hergenrother, P. J. The challenge of converting Gram-positive-only compounds into broad-spectrum antibiotics. *Ann. NY Acad. Sci.* **2019**, *1435*, 18-38.

(24) Richter, M. F.; Drown, B. S.; Riley, A. P.; Garcia, A.; Shirai, T.; Svec, R. L.; Hergenrother, P. J. Predictive compound accumulation rules yield a broad-spectrum antibiotic. *Nature*, **2017**, 545, 299-304.

(25) Wagner, B.; Fischer, H.; Kansy, M.; Seelig, A.; Assmus, F. Carrier mediated distribution system (CAMDIS): a new approach for the measurement of octanol/water distribution coefficients. *Eur. J. Pharm. Sci.* **2015**, *68*, 68-77.

(26) Kadri, S. S.; Adjemian, J.; Lai, Y. L.; Spaulding, A.; B.; Ricotta, E.; Prevots, D. R.; Palmore, T. N.; Rhee, C.; Klompas, M.; Dekker, J. P.; Powers III, J. H.; Suffredini, A. F.; Hooper, D. C.; Fridkin, S.; Danner, R. L. Difficult-to-treat resistance in gram-negative bacteremia at 173 US hospitials: retrospective cohort analysis of prevalence, predictors, and outcome of resistnace to all first-line agents. *Clin. Infect. Dis.* **2018**, *67*, 1803-1814.

Table of Contents Graphic